

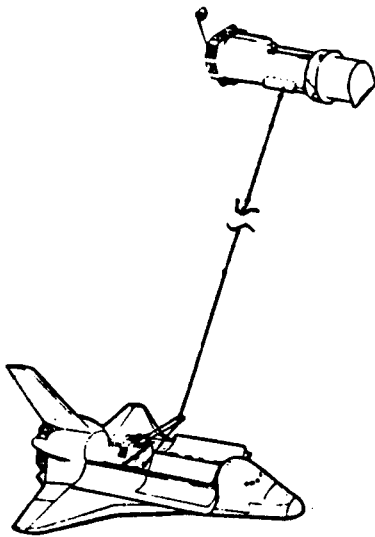


# Phase III Study of Selected Tether Applications In Space

Contract: NAS8 - 36617

DPD 665 DR - 4

## Final Report Volume II - Study Results December 1986

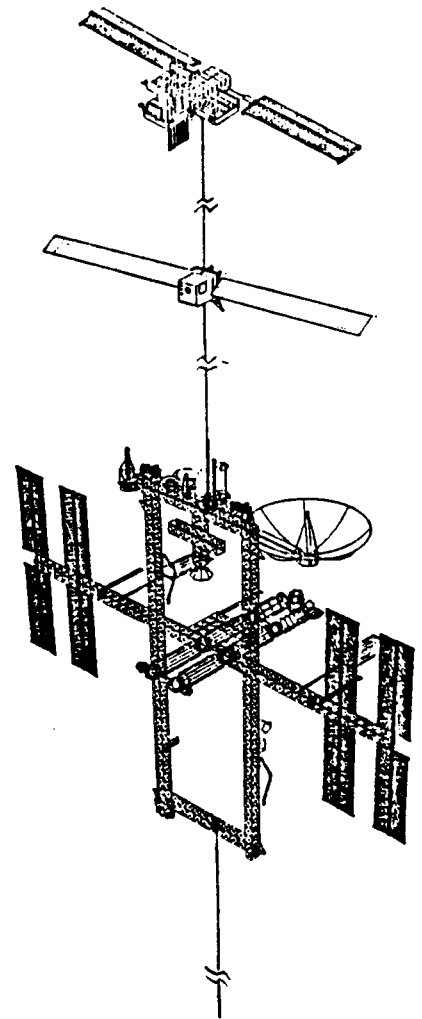


Prepared for:

George C. Marshall Space Flight Center  
National Aeronautics and Space Administration  
Marshall Space Flight Center, Alabama 35812

By:

Ball Aerospace Systems Division  
P.O. Box 1062  
Boulder, Colorado 80306



## Introduction and Overview

This report covers the results from study Phase III of a five phase NASA program to discover, understand, and develop applications for tethers in two general categories: (1) Tether Transportation Applications (TETRA) and (2) Tether Spacecraft Constellations (TESCON). In this report Item (1) addresses a tethered launch assist from the Shuttle for payloads with up to 10,000 kg mass for the mission model. Item (2) addresses the tethering of a 15,000 kg science platform from the Space Station. It also encompasses the design and cost analysis for a variable "g" device that could be placed on the tether and allow ultra-low "g" or other types of experiments to be conducted. This device would move up and down the tether as required to accomplish the experiments.

In the first two phases of the NASA program numerous tether applications were examined and their theoretical feasibility and technology requirements assessed. In this phase engineering designs are developed relative to (1) and (2) and these are used as the basis for a cost benefit analysis which assesses the feasibility of using such systems as a practical alternative to what would otherwise be accomplished by conventional means. The term "conventional" as related to both these applications is intended to apply to the use of some form(s) of chemical propulsion system.

## TABLE OF CONTENTS

1.0	TETHERED PLATFORM AND CRAWLER STUDY .....	1-1
1.1	TETHERED PLATFORM RESULTS .....	1-1
1.1.1	COST/DESIGN DRIVERS .....	1-2
1.1.1.1	Space Station AND SCIENCE PLATFORM IMPACTS - GENERAL .....	1-2
	<u>Tension Loading of Truss Structure</u> .....	1-2
	<u>Attitude Control Subsystem</u> .....	1-4
	<u>"g" Levels</u> .....	1-4
	<u>Safety and Docking</u> .....	1-4
	<u>Pointing and Fields of View</u> .....	1-5
	<u>Impacts On Space Station Subsystems</u> .....	1-8
	<u>Propellant Savings</u> .....	1-8
1.1.1.2	STATIONKEEPING PROPELLANT COSTS .....	1-9
	<u>Propulsion Subsystem</u> .....	1-9
	<u>Propellant Usage-Analyses Parameters, Requirements,</u> <u>and Assumptions</u> .....	1-10
	<u>Stationkeeping Fuel Estimates</u> .....	1-10
1.1.1.3	MICROGRAVITY CONSIDERATIONS FOR TETHERED PLATFORMS .....	1-18
	<u>Experimenter Requirements</u> .....	1-18
	<u>Gravity Map of the Space Station</u> .....	1-21
	<u>Single Tether Configurations</u> .....	1-29
	<u>Dual Platform Concept</u> .....	1-33
1.1.1.4	COMMUNICATIONS TETHER TRADE .....	1-36
1.1.1.5	POWER TETHER VS SOLAR ARRAY POWER SYSTEM .....	1-39
	<u>General Description of Science Platform Power Options</u> .....	1-43
	<u>Autonomous Powered Science Platform</u> .....	1-43
	<u>Platform Powered from the Space Station Tether</u> .....	1-45
	<u>Conducting Tether Power Concerns</u> .....	1-46
	<u>Tether EMF</u> .....	1-46
	<u>Powered Tether Efficiency</u> .....	1-47
	<u>Power Tether Weight and Cost Trade</u> .....	1-55
1.1.2	TETHER DEPLOYER DESIGN .....	1-60
1.1.2.1	CARRIER .....	1-61
1.1.2.2	REEL DRIVE COMPONENTS .....	1-61
1.1.2.3	TAPPS MECHANISM .....	1-66
1.1.2.4	POWER, C&DH, AND THERMAL .....	1-66
1.1.3	MISSION OPERATIONS .....	1-67
1.1.4	TETHERED PLATFORM COST ANALYSIS SUMMARY .....	1-70
1.2	TETHER CRAWLER RESULTS .....	1-72
1.2.1	CRAWLER DESIGN COST DRIVERS .....	1-74
1.2.2	CRAWLER DESIGN AND DYNAMICS .....	1-75
1.2.3	CRAWLER SUBSYSTEM DESCRIPTIONS .....	1-79
1.2.3.1	POWER SUBSYSTEM .....	1-79
	<u>Transfer Phase Expressions</u> .....	1-80
	<u>Solar Array Sizing</u> .....	1-80
	<u>Battery Selection</u> .....	1-83
1.2.3.2	MOMENTUM WHEEL SIZING .....	1-84
1.2.3.3	NITROGEN RCS SIZING .....	1-86
1.2.4	CRAWLER DEPLOYMENT AND RETRIEVAL DYNAMICS ANALYSIS .....	1-87
1.2.5	CRAWLER OPERATIONS TIMELINES .....	1-88
1.2.6	CRAWLER STUDY COST ANALYSIS SUMMARY .....	1-88

2.0	STS TETHER TRANSPORTATION STUDY .....	2-1
2.1	INTRODUCTION .....	2-1
2.1.1	TETHER SYSTEM SIZING .....	2-2
	<u>Weight of Fuel Needed to Boost a Payload to a Higher Orbit ...</u>	2-8
	<u>Ratio of Tether Mass to Fuel Mass for a Given Orbit Transfer .</u>	2-10
	<u>Estimate Tether Deployment System Weight .....</u>	2-12
2.1.2	DESIGN ASSUMPTIONS/GUIDELINES .....	2-15
2.1.3	MOMV VERSES OMV TRADE RATIONALE .....	2-16
2.2	MINI-OMV DESIGN .....	2-18
2.2.1	REQUIREMENTS .....	2-18
2.2.2	CONFIGURATION .....	2-19
2.2.3	STS INTERFACE .....	2-21
2.2.4	SUBSYSTEM DESCRIPTIONS .....	2-21
2.2.4.1	ATTITUDE CONTROL .....	2-21
2.2.4.2	THERMAL CONTROL .....	2-23
2.2.4.3	COMMUNICATIONS .....	2-25
2.2.4.4	POWER .....	2-28
2.2.4.5	PROPULSION .....	2-31
2.2.5	OPERATIONAL TIMELINE .....	2-36
2.2.6	MOMV COST ANALYSIS SUMMARY.....	2-40
2.3	SHUTTLE TETHER DEPLOYMENT SYSTEM (STEDS) .....	2-42
2.3.1	REQUIREMENTS .....	2-43
2.3.2	CONFIGURATION .....	2-44
2.3.3	STS INTERFACE .....	2-48
2.3.4	SUBSYSTEM DESCRIPTIONS .....	2-52
2.3.4.1	STRUCTURE .....	2-52
2.3.4.2	STEDS TENSION CONTROL .....	2-54
2.3.4.3	THERMAL CONTROL .....	2-59
2.3.5	TETHER DESIGN TRADE .....	2-66
	<u>Mass of Tapered Tether .....</u>	2-66
	<u>Mass of Constant Diameter Tether .....</u>	2-68
	<u>Ratio of Constant Cross-Section to Optimum Cross-Section</u> <u>Tether Mass .....</u>	2-69
2.3.6	TENSION CONTROL LAW AND SIMULATIONS .....	2-71
2.3.7	OPERATIONAL TIMELINES .....	2-76
2.3.8	STEDS COST ANALYSIS SUMMARY .....	2-84
3.0	CONCLUSIONS OF TETHER APPLICATIONS IN SPACE STUDY .....	3-1
3.1	TETHER TRANSPORTATION MISSIONS FROM SHUTTLE .....	3-1
3.2	TETHERED PLATFORM .....	3-2
3.3	COMMUNICATION TETHER .....	3-4
3.4	POWER TETHER .....	3-5
3.5	CRAWLER SYSTEM .....	3-6
4.0	RECOMMENDED FUTURE EFFORT.....	4-1
	<u>Crawler as a Variable "g" Lab and Mass Balancer.....</u>	4-1
	<u>Investigation of SEDS Deployment Technique.....</u>	4-2
	<u>Use of a Tether for Plasma Measurements.....</u>	4-2
	<u>Further Investigation of Space Station Tethered Platforms.....</u>	4-3
	<u>Dynamic Model Verification.....</u>	4-4

## FIGURES

Figure 1.1 Tethered Platform System Elements.....	1-3
Figure 1.1.1.2-1 Co-Orbiting Science Platform Characteristics.....	1-11
Figure 1.1.1.2-2 Error Sources Contributing to Fuel Usage for Stationkeeping Platforms.....	1-12
Figure 1.1.1.2-3 Additional Fuel to Offset Tether Drag.....	1-14
Figure 1.1.1.2-4 Days to Drift 10km From Nominal Separation Distance..	1-15
Figure 1.1.1.2-5 Annual Fuel Required to Maintain Platform Within 10 km Deadband Centered at Nominal Distance.....	1-16
Figure 1.1.1.3-1 Typical Materials Processing Acceleration Requirements	1-20
Figure 1.1.1.3-2 Acceleration Duration Requirements.....	1-22
Figure 1.1.1.3-3 Recent Space Station Change Request to Allowable Acceleration Levels.....	1-23
Figure 1.1.1.3-4 Space Station Attached Payload "g" Requirements.....	1-24
Figure 1.1.1.3-5 Space Station Gravity Map With Single Platform.....	1-26
Figure 1.1.1.3-6 Tethered Platform Mass Restrictions to Meet Acceleration Limits.....	1-27
Figure 1.1.1.3-7 Space Station Gravity Map for Dual Platforms.....	1-28
Figure 1.1.1.4-1 Cost Comparison For 50 Mbps Optical Tether at 1, 5, and 10 km Lengths.....	1-38
Figure 1.1.1.4-2 Cost Comparison For 1 Mbps Optical Tether at 1, 5, and 10 km Lengths.....	1-40
Figure 1.1.1.5-1 Solar Array Size and Weight Vs. Power Output.....	1-44
Figure 1.1.1.5-2 Tether Power System.....	1-48
Figure 1.1.1.5-3 Load Resistance vs Wire Size for Efficiency.....	1-49
Figure 1.1.1.5-4 Voltage vs Wire Size for Efficiency.....	1-50
Figure 1.1.1.5-5 Two Wire Line - Wire Spacing vs $Z_0$ .....	1-53
Figure 1.1.1.5-6 System Voltage vs Characteristic Impedance.....	1-54
Figure 1.1.1.5-7 Efficiency vs Wire Size (100 to 700 ohms).....	1-56
Figure 1.1.1.5-8 Tether Weight vs Wire Size (1 wire to 10 km dist.)...	1-57
Figure 1.1.2-1 Tether Deployer - Top View.....	1-62
Figure 1.1.2-2 Tether Deployer - Side View.....	1-63
Figure 1.1.2-3 Tether Deployer - Front View.....	1-64
Figure 1.1.2-4 Tether Deployer and TAPPS - Perspective View.....	1-65
Figure 1.1.3-1 Installation and Operational Sequence for Tether Deployer System.....	1-68
Figure 1.1.3-2 Installation and Operational Timeline for Tether Deployer System.....	1-69
Figure 1.2.2-1 Crawler Design.....	1-77
Figure 1.2.3.1-1 Crawler Array Trade-offs.....	1-82
Figure 1.2.5-1 Crawler Operational Sequence.....	1-89
Figure 1.2.5-2 Crawler Operations Timeline.....	1-90
Figure 2.1.1-1 Ratio of Tether Mass to Payload Mass for Constant Cross-.....	2-9
Figure 2.1.1-2 Ratio of Fuel Mass to Payload Mass to Achieve Same Orbit as a Hanging Tether Release.....	2-11
Figure 2.1.1-3 Ratio of tether to Fuel Mass to Accomplish the Same Orbit Transfer.....	2-11
Figure 2.1.1-4 Ratio of Tether System Mass to Fuel System Mass for Design.....	2-14
Figure 2.2.2-1 Mini-OMV Layout .....	2-20
Figure 2.2.3-1 MOMV/STS Electrical Interface .....	2-22

Figure 2.2.4.3-1 Communications Concept for MOMV .....	2-27
Figure 2.2.4.4-1 MOMV Electrical Power System Concept .....	2-29
Figure 2.2.4.5-1 MOMV Propulsion Subsystem .....	2-32
Figure 2.2.4.5-2 MOMV Propellant Manifest Sizing .....	2-35
Figure 2.2.5-1 MOMV Operational Sequence .....	2-37
Figure 2.2.5-2 MOMV Deployment Timeline .....	2-38
Figure 2.3.2-1 Shuttle Tether Deployment System (STEDS) .....	2-46
Figure 2.3.2-2 STEDS Side View .....	2-47
Figure 2.3.2-3 Alternative STEDS Tether Deployment Control Concept ...	2-49
Figure 2.3.2-4 STEDS Remotely Mateable Tether End-Effector Concept ...	2-50
Figure 2.3.3-1 STEDS/STS Electrical Interface .....	2-51
Figure 2.3.4.2-1 STEDS Optimally Positioned in STS Bay .....	2-56
Figure 2.3.4.2-2 STEDS Positioned for Maximum Payload Length .....	2-57
Figure 2.3.4.3-1 STEDS Thermal Control Concept .....	2-60
Figure 2.3.4.3-2 Power Generation vs Deployment Time .....	2-62
Figure 2.3.5-1 Mass Ratio Between Constant and Optimum Cross-Section .	2-70
Figure 2.3.6-1 Tension Control Law .....	2-73
Figure 2.3.6-2 Deployment Scenario .....	2-74
Figure 2.3.6-3 Tether Length vs Time (8 hr deployment) .....	2-77
Figure 2.3.6-4 Tether Velocity vs Time (8 hr Deployment) .....	2-78
Figure 2.3.6-5 Tether In-Plane Angle vs Time (8 hr deployment) .....	2-79
Figure 2.3.6-6 Tether Tension vs Time (8 hr deployment) .....	2-80
Figure 2.3.6-7 Tether Power vs Time (8 hr deployment) .....	2-81
Figure 2.3.7-1 STEDS Operational Sequence .....	2-82
Figure 2.3.7-2 STEDS Deployment Timeline .....	2-83

## TABLES

TABLE 1.1.1.4-1 Cost Comparison for 50 Mbps Optical Tether.....	1-38
at 1, 5, and 10 km lengths.	
TABLE 1.1.4-2 Cost Comparison for 1 Mbps Optical.....	1-40
at 1, 5, and 10 km lengths	
TABLE 1.1.1.5-1 Tether Power Subsystem Options.....	1-42
TABLE 1.1.1.5-2 Power Tether Weight and Cost Deltas .....	1-58
TABLE 1.1.4.1 Tether Deployer System Costs.....	1-70
TABLE 1.2.6-1 Crawler Costs.....	1-88
TABLE 2.2.4-1 MOMV AC&D Subsystem Components List .....	2-23
TABLE 2.2.4.2-1 MOMV Thermal Analysis Results .....	2-26
TABLE 2.2.4.3-1 C&DH Component List .....	2-28
TABLE 2.2.4.4-1 MOMV Power Subsystem Requirements .....	2-30
TABLE 2.2.4.4-2 MOMV Power Subsystem Component List .....	2-31
TABLE 2.2.4.5-1 MOMV Propulsion Subsystem Component List .....	2-33
TABLE 2.2.6-1 Mini-OMV Costs.....	2-40
TABLE 2.3.4.1-1 STEDS Structural Components List .....	2-54
TABLE 2.3.4.2-1 STEDS Tension Control Components .....	2-59
TABLE 2.3.4.3-1 STEDS Thermal Control Components .....	2-65
TABLE 2.3.8-1 STEDS Costs.....	2-85

## ACRONYMS LIST

AC&D - Attitude Control and Determination  
 AKA - Active Keel Assembly  
 ATCS - Active Thermal Control System  
 AXAF - Advanced X-ray Astronomical Facility  
 BASD - Ball Aerospace Systems Division  
 bps - bits per second  
 C&DH - Communications and Data Handling  
 CDU - Command Decoder Unit  
 CG - Center of Gravity  
 CM - Center of Mass  
 CRRES - Combined Release and Radiation Effects Satellite  
 DOD - Department of Defense  
 DTU - Digital Telemetry Unit  
 EMF - Electro Motive Force  
 ERBS - Earth Radiation Budget Satellite  
 EVA - Extra Vehicular Activity  
 FOV - Field of view  
 FSS - Flight Support System  
 GPS - Global Positioning System  
 IOC - Initial Orbital Configuration  
 JSC - Johnson Spacecraft Center  
 KITE - Kinetic Isolation Tether Experiment  
 LCC - Life Cycle Cost  
 Mbps - Mega bits per second  
 MLI - Multi Layer Insulation  
 MMC - Martin Marietta Corp.  
 MMS - Multi Mission Spacecraft  
 MOMV - Mini Orbital Maneuvering Vehicle  
 MRD - Mission Requirements Database  
 MRMS - Mobile Remote Manipulator System  
 MSFC - Marshall Space Flight Center  
 NASA - National Aeronautics and Space Administration  
 OMV - Orbital Maneuvering Vehicle  
 PIA - Payload Interface Adaptor  
 POCC - Payload Operations Control Center  
 PRICE - Programmed Review of Information for Costing and Evaluation  
 PRLA - Payload Retention Latch Actuator  
 RCS - Reaction Control System  
 RF - Radio Frequency  
 RMS - Remote Manipulator System  
 RSS - Root Sum Square  
 SEDS - Small Expendable Deployer System  
 SIRTf - Shuttle Infrared Telescope Facility  
 SMM - Solar Max Mission  
 SOW - Statement of Work  
 SS - Space Station  
 SSP - Standard Switch Panel  
 STEDS - Shuttle Tether Deployment System  
 STS - Space Transportation System  
 TAPPS - Tether Alignment and Platform Positioning System  
 TCS - Thermal Control System  
 TDM - Telemetry Distribution Unit  
 +Z-LV - +Z-Local Vertical



1.0 TETHERED PLATFORM AND CRAWLER STUDY

1.1 TETHERED PLATFORM RESULTS

A tether can be used as an alternative to a propulsion system for stationkeeping of certain co-orbiting experiments and payloads, which, because of their special nature or operating characteristics, cannot be located on the Space Station. Isolation may be needed with respect to Space Station contaminating effluents and energy fields as well as from Space Station vibrations and imposed course pointing capabilities. Alternately, certain Space Station payloads and elements may have to be isolated from the effects of certain contaminating experiments such as the one presently being proposed to characterize the effects of thruster plume plasmas on solar arrays. These "co-orbiting" payloads will rendezvous with the Space Station, perhaps every few months, for servicing.

The a tether can also, serve as a conductor for communications and electrical power, and a guideway for other special purpose payloads via a Crawler vehicle.

This part of the study examines the implications of tethering such payloads to the Space Station as compared to using the propulsion system method from the standpoints of achieving primary payload performance objectives.

The baseline tethered platform weights 15,000 kg and is deployed 10 km upwards. A 15,000 kg balance mass is deployed downwards the same 10 km in order to preserve microgravity conditions aboard the Space Station. A Tether Deployer design is presented to serve as a baseline for the cost comparison. Separate trade studies and a relative cost analysis are also conducted with respect to using modified forms of the tether as both communications and electrical power conduits as opposed to using separate integral systems. A final trade study examines the design and cost of implementation for a variable g Crawler vehicle. Here the baseline design consists of a 2000 kg

Crawler/Payload vehicle which can be deployed/retrieved to a distance of up to 100 km under its own power in approximately one eight hour shift. The Crawler, which is designed for up to one year of operation between servicing, produces an orbital average power of 2 kw. Figure 1.1 illustrates the tethered platform/Crawler concept.

#### 1.1.1 COST/DESIGN DRIVERS

##### 1.1.1.1 Space Station AND SCIENCE PLATFORM IMPACTS - GENERAL

In this section we discuss the impacts of a tethered platform system on the Space Station. The subjects covered are those related to tension loading on the Space Station truss structure, g-levels, safety and STS docking, fields of view and pointing, and subsystems.

##### Tension Loading of Space Station Truss Structure

Standard NASTRAN runs were made based upon a tether tension load of 3200 N (720 lbf) or 6 times that expected for a 15,000 kg platform deployed to 10 km. Five centimeter (2 in.) O.D. AL6061-T6 aluminum tubes were used as typical Space Station structural members. Buckling was found to first occur in the long diagonal member of a truss cube when the tube wall thickness was reduced to .31 cm (0.122 in.). At this time the compression force was 1805 N (406 lbf). Members in tension saw loads of relatively small magnitudes compared to critical levels. As the above thickness represents the optimum stress condition design the tether impacts the Space Station's design to the extent that the thickness of the tubes in the vicinity of the deployer must be increased in accordance with the above. Since the Space Station is currently undergoing a major redesign it is not possible to quantify the extent of such an impact at the present time.

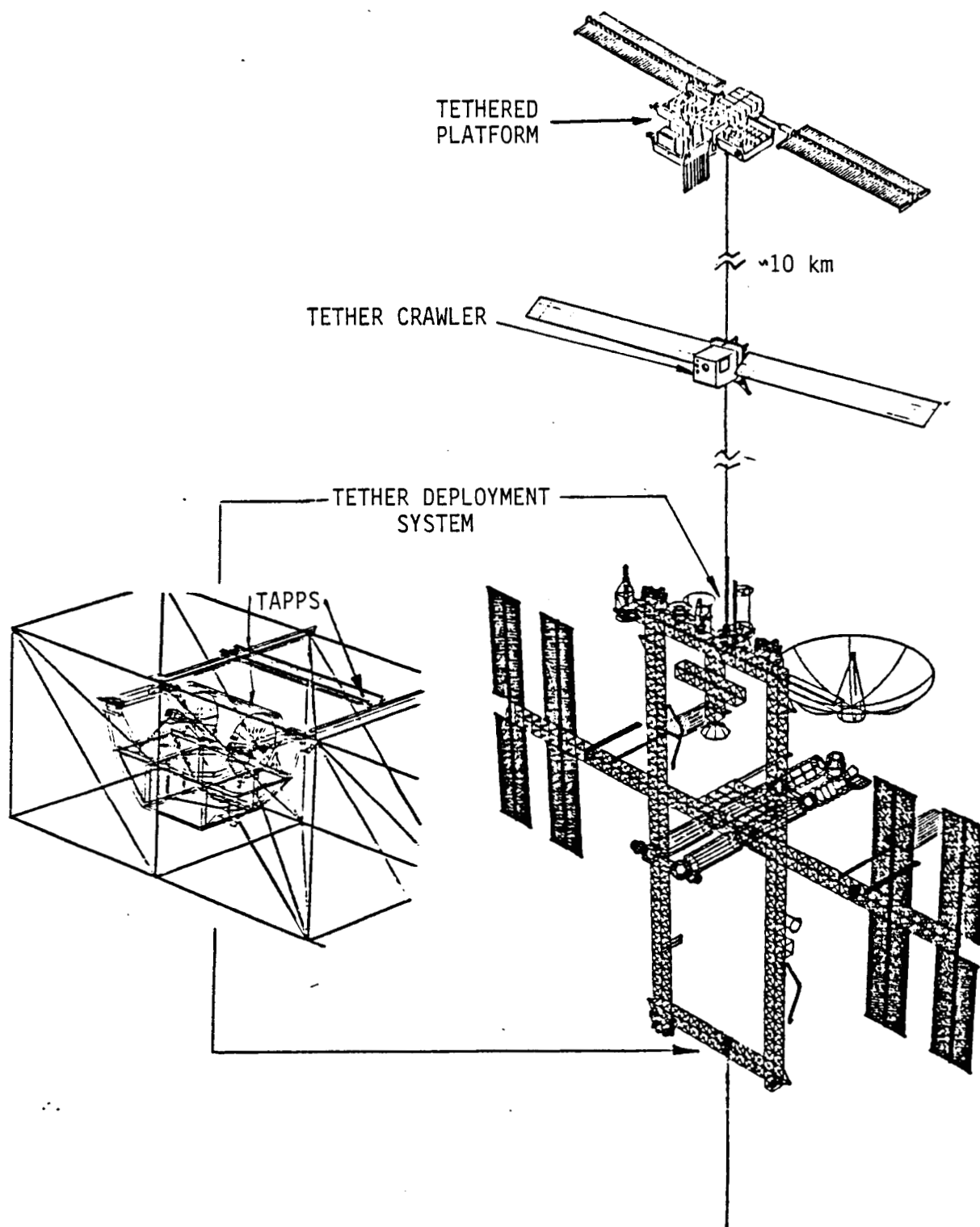


FIGURE 1.1 TETHERED PLATFORM SYSTEM ELEMENTS

### Attitude Control Subsystem

Both the tethered and free flying platforms must have virtually identical sensing systems if they are to achieve the same equally precise pointing performance. Although the free-flying platform would require a propulsion system, the tethered platform would also require a propulsion system to provide attitude stabilization in the event of a tether failure as previously noted. It is also anticipated that there will be a cost equivalence between the Kinetic Isolation Tether Experiment (KITE)<sup>1</sup> actuation system on the tethered platform and the momentum exchange actuation system aboard the free flyer. Thus it appears that neither system offers a cost advantage from the standpoint of attitude control implementation.

### "g" Levels

The attachment of tethers to the Space Station has a large impact upon g levels. If a single tether is used the zero-g point may be moved outbound by as much as a kilometer. If dual tethers are used, the zero-g point can be maintained near its original inboard location or it can be moved to any point within a region of approximately plus or minus one km centered about the stand-alone Space Station CM. This is the principal reason why the two tether system has been adopted as the baseline design. For a complete description of the impact of tethering on g levels refer to Section .

### Safety and Docking

The tether obviously occupies a volume along the local vertical which could otherwise be used for shuttle rendezvous corridors. This consideration would seem to rule-out the set of shuttle proximity operations known as R-bar

-----

<sup>1</sup>Lemke, L. G.; "A Concept for Attitude Control of a Tethered Astrophysical Observatory Platform", NASA Ames Research Center, Moffett Field, CA, revised 4/86.

rendezvous, leaving only V-bar rendezvous as the standard technique. Though this represents some loss of mission flexibility, there should be no significant implications relative to safety and docking.

If a single tether is used some additional orbiter fuel may have to be used to accomplished rendezvous, however. This is because the system center of mass (center of motion) of the Space Station/Platform combination may be shifted outwards from the Space Station by as much as one kilometer, thus upsetting conventional free-flight minimum energy trajectory dynamics.

#### Pointing and Fields of View

The presence of a tether will apparently not impact either pointing or field-of-view capabilities for Space Station experiments. This is because, though attitude knowledge must be determined to 0.01 degrees, attitude control capability i.e., the ability to point, only has to be controlled to 5.0 degrees.<sup>2</sup> Further, except perhaps for certain long wavelength instruments with cooled optics which would be especially sensitive to tether photon emissions, most instruments could probably "work around" a tether being within or near their field of views.

For instruments and experiments located on platforms, however, a tether system imposes a significant disturbance to vehicle dynamics when compared to a free-flyer. Table 1.1.1.1 gives the required platform attitude control conditions.

-----

<sup>2</sup>"Space Station Program Definition and Requirements", JSC-30000, NASA, Lyndon B. Johnson Space Center, Houston, TX, October 15, 1985.

## Final Report - Volume II - Study Results

TABLE 1.1.1.1 REQUIRED ATTITUDE CONTROL FOR SPACE STATION PLATFORM

Attitude Control	0.03 degs	(108 arcsec)
Attitude Determination	0.01 degs	( 36 arcsec)
Maximum Jitter	0.0003 degs	( 1 arcsec)

It is understood that the KITE system is being designed to achieve such control accuracies. The utility of a tethered platform hinges on the successful operation of some system like the KITE. This is due to the adverse effect of tethering on platform "g" levels, which would probably dictate that such platforms house only astrodynamic or possibly earth pointing experiments as opposed to materials processing experiments.

Three broad areas of free-flyer capabilities are being exploited over and above the obvious advantages of isolation from environment disturbances and the FOV enhancement associated with a highly elevated platform. These include a long term accessibility to a very low-g environment, the availability of long term highly-accurate pointing and pointing stability, and the utility associated with the concept of a Space Station transportation node. The latter relates to use as a staging area for assembly and check-out of payload and booster elements prior to injection into geo-synchronous, lunar, or heliocentric transfer orbits.

A close inspection of the payloads contained in the Space Station Mission Requirements Database (MRDB)<sup>3</sup> reveals that just about every platform payload has a tight requirement in at least one of the three aforementioned categories of exploitation. Thus if such payloads were to be considered

-----

3"Space Station Program Definition and Requirements", JSC-30000, Section 5: Mission Integration Requirements, NASA, Lyndon B. Johnson Space Center, Houston, TX, October 15, 1985.

candidates for a tethered application then the effects of the tether would have to be addressed in almost every individual payload case.

In reviewing the data it was noteworthy that although micro-gravity is an important driver, the requirements associated with pointing capability appear to dominate the platform payloads. Since a tether system is an inherently earth oriented configuration, it is difficult to comprehend how the presence of a tether could lead to anything but detrimental performance characteristics in the cases where accurate long-term inertial and solar pointing and pointing stability is required unless KITE development is successful. It should be noted that even if the KITE system can produce pointing performance consistent with astrodynamic payload requirements inertial pointing can only be achieved for approximately half an orbit before a reacquisition sequence would have to be initiated, limiting viewing time to this maximum value.

Even in the case of free-flyers, some sort of compensation will in fact be required in certain cases for instruments which require mechanical scanning and/or rapid reconfigurations. This is typically handled by incorporating into the design a counterrotating reaction mass system. Such features are already shown incorporated into many of the data base payload design descriptions.

The third utility, that of a transportation node staging area for assembly and check-out of large systems prior to injection into higher energy trajectories really has no applicability to the present analysis relative to tethering Science Platform Payloads. However, they are included here for completeness. Typically, such transportation payloads might involve the deployment of a very large antenna system, for example, prior to injection into geo-synchronous orbit where they would otherwise be inaccessible if problems developed relative to a deployment there.

An interesting and distinctly different tether application in this case might involve a tether system as a temporary station-keeping aid during assembly of the various components of any such large system or space structures.

The typical eventual payload manifest for the Science Platform is viewed as consisting of inertially oriented telescope-like instrumentation and an additional complement of payloads, not yet identified in the MRDB that could take advantage of the environment offered by a tethered platform.

In summary, it would appear that most low micro-g experiments would have to be excluded from a tethered platform but high accuracy pointers could be conditionally included depending upon the success of KITE development.

#### Impacts On Space Station Subsystems

The principal Space Station Subsystems impacted by a tethered platform are Power and Thermal as related to deployment and retrieval operations. Related effects should be of little significance, however, since such operations are transitory. In addition, they can be carried out slowly, thus obviating the need for both high power consumptions and thermal dissipations.

A 10 km, 15,000 kg platform retrieval conducted over one 8-hour shift, for example, requires an average electrical power of less than 100 watts. Assuming that the reel-in motor is at least 85% efficient then the thermal dissipation is only say 10 to 20 watts which is insignificant. During deployment, the full 100 watts would have to be dissipated, but this, too, would be insignificant.

#### Propellant Savings

The biggest cost benefit of a tethered platform is in the propellant that can be saved verses a free-flying platform attempting to stationkeep using



conventional propellant systems. This is discussed in detail in the next section of the report.

#### 1.1.1.2 STATIONKEEPING PROPELLANT COSTS

This section provides a comparative description of the costs associated with stationkeeping propellant consumption. The free-flying platform will require a significant amount of propellant to remain in the vicinity of the Space Station. The tether approach automatically keeps the platform positioned with only a minimal propellant requirement due to the increased drag on the tether.

#### Propulsion Subsystem

The Platform propulsion Subsystem design specified by the General Electric Space Station Work Package 3 - Definition and Preliminary Design Document dated 14 June 1985, is used as a reference point in this study. This design incorporates the capability for three axis attitude control and low thrust reboost functions needed for stationkeeping operations.

The hardware elements consist of the various components needed to support a blowdown type of hot gas monopropellant hydrazine system. These elements include propellant tanks, latching isolation valves, fill and drain valves, filter, low-force thrusters, heaters, and pressure and temperature transducers. The arrangement of thrusters is such that torque free motion can be induced in each of the principal radial, tangential, and orbit normal directions. Minimum impulse bits and thrust levels afford the capability of inducing an incremental delta velocity of as little as one millimeter per second in each of these three directions.

Propellant usage in the case of the free flyer was found to be dependent upon both the drag differential between the platform and the Space Station, and

the ability to accurately re-establish the Platform state vector at the start of each unattended drift cycle. In the case of the tethered concept, relative Space Station fuel consumption increases slightly due to the additional drag on the tether. This is itself very slightly offset by the decreased drag of the platform due to the latter's slightly higher altitude above the Space Station.

#### Propellant Usage-Analyses Parameters, Requirements, and Assumptions

This section summarizes the assumptions related to derived requirements, types and magnitudes of error sources, and resulting fuel consumption estimates. Our assumptions concerning the design and operation of the platform are summarized in Figures 1.1.1.2-1 and 1.1.1.2-2. The decision to base the principal error source magnitudes on expected GPS performance was based upon discussions with JSC Space Station Program office personnel. Although the free-flying platform would require a propulsion system, the tethered platform would also probably require a propulsion system to provide attitude stabilization in the event of a tether failure. It also seems likely that one would be desired so that the platform could free-fly during periods when a tether could not conveniently be deployed due to other Space Station activities. These activities might include orbiter dockings, OTV launches, major Space Station altitude raising maneuvers, periods when other tethered payloads needed to be deployed, periods when ultra micro-g conditions on the Space Station were needed, etc... Thus we assume a cost equivalence between propulsion system implementation costs for the two platform systems.

#### Stationkeeping Fuel Estimates

Our estimates of the relative fuel savings between the tethered and non-tethered Science Platform schemes are summarized by Figures 1.1.1.2-3 through 1.1.1.2-5.

## Coorbiting Science Platform Characteristics

Mass ~ 15,000 KG

Power ~ 5 KW

Minimum Standoff Distance ~ 10 KM

Return to SS for Servicing Every Few Months

Number of Payloads ~ 23

Reasons For Desiring Location Away From Space Station  
Isolation From Contaminating Effluents and Energy Fields  
Isolation From Vibrations – Improved Pointing Stability  
Variable G Capability

Typical Payloads  
Material Processing  
Deep Space Astronomical Research

No Radar Is Currently Planned For The Space Station

All Objects Within 37 KM are Assumed To Be Within The Close – In Traffic Pattern Of The Space Station And Will Be Equipped With GPS Receivers

Figure 1.1.1.2 -- 1

Figure 1.1.1.2 – 2

**Error Sources Contributing to Fuel Usage  
For Stationkeeping Platforms**

Ballistic Coef Differential (3 $\sigma$ )	GPS Radial Position Error (3 $\sigma$ ,m)	GPS Tangential Velocity Error (3 $\sigma$ ,m/sec)
50 %	21 <sup>(1)</sup>	0.3 <sup>(2)</sup>

(1) RSS of 15m, 3  $\sigma$  Each for Individual Space Station and Platform Determinations

(1) RSS of 0.2 m/sec, 3  $\sigma$  Each for Individual Space Station and Platform Determinations

Figure 1.1.1.2-3 illustrates the annual supplemental fuel needed to compensate for tether drag less the slight effect of a drag reduction due to the Platform flying 10 km higher than the Space Station. For a 2 1/2 mm diameter tether required fuel make-up relative to just the tether was found to vary between 3.2 and 44.5 kg/year when the exospheric temperature ranged between 800°K and 1300°K, respectively. At the same time the intervehicle altitude delta afforded a savings of 2.2 and 21.7 kg/year, respectively. Thus the net annual supplemental fuel requirement is 1.0 and 22.8 kg, respectively.

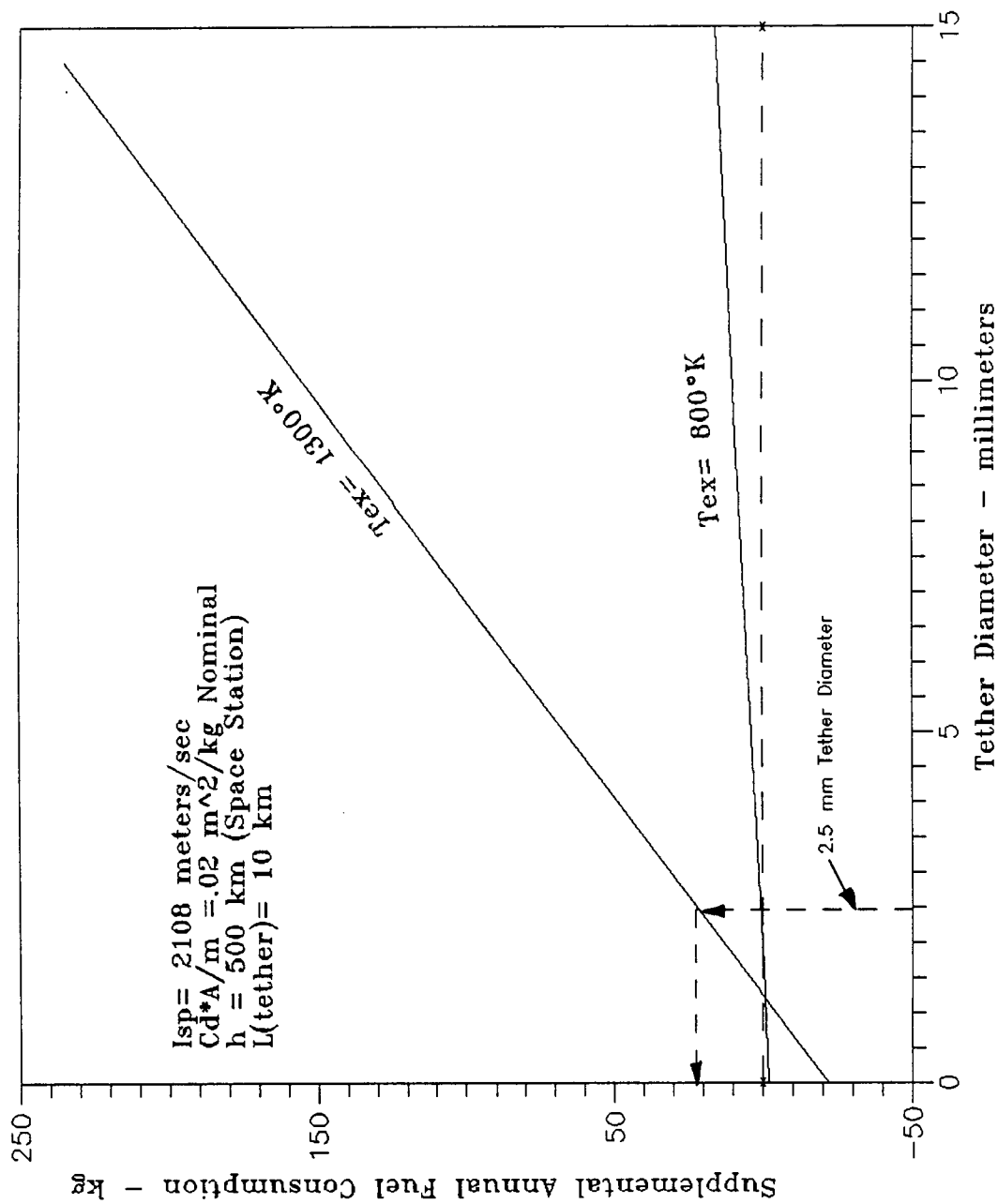
For the free-flyer concept we found that the additional fuel requirement was associated with the differential ballistic coefficient between the two vehicles plus the magnitude of the state vector initialization errors which give rise to secular drifts. The latter include the radial position error and the tangential velocity error components of the state vector only; the other components give rise to only periodic displacements.

We have taken the largest credible ballistic coefficient differential to be 50% and have further based our initialization errors on the GPS performance values summarized in Figure 1.1.1.2-2. In the case of the latter we decided to use 1.5 sigma values as being most representative, which gives initialization errors of 11.5 meters and 0.15 meters per second, respectively.

Referring to Figure 1.1.1.2-4, we note that the above error sources give rise to 10 km displacements in time periods ranging between about one quarter day to several weeks. Here the driving error source is associated with initial differential tangential velocity, with differential ballistic coefficient having little effect by comparison.

In Figure 1.1.1.2-5, the annual fuel consumption required to compensate for the foregoing is presented. It is assumed that a typical drift cycle

Figure 1.1.1.2-3  
 Additional Fuel to Offset Tether Drag Less  
 Savings Due to 10 km Higher Platform Altitude



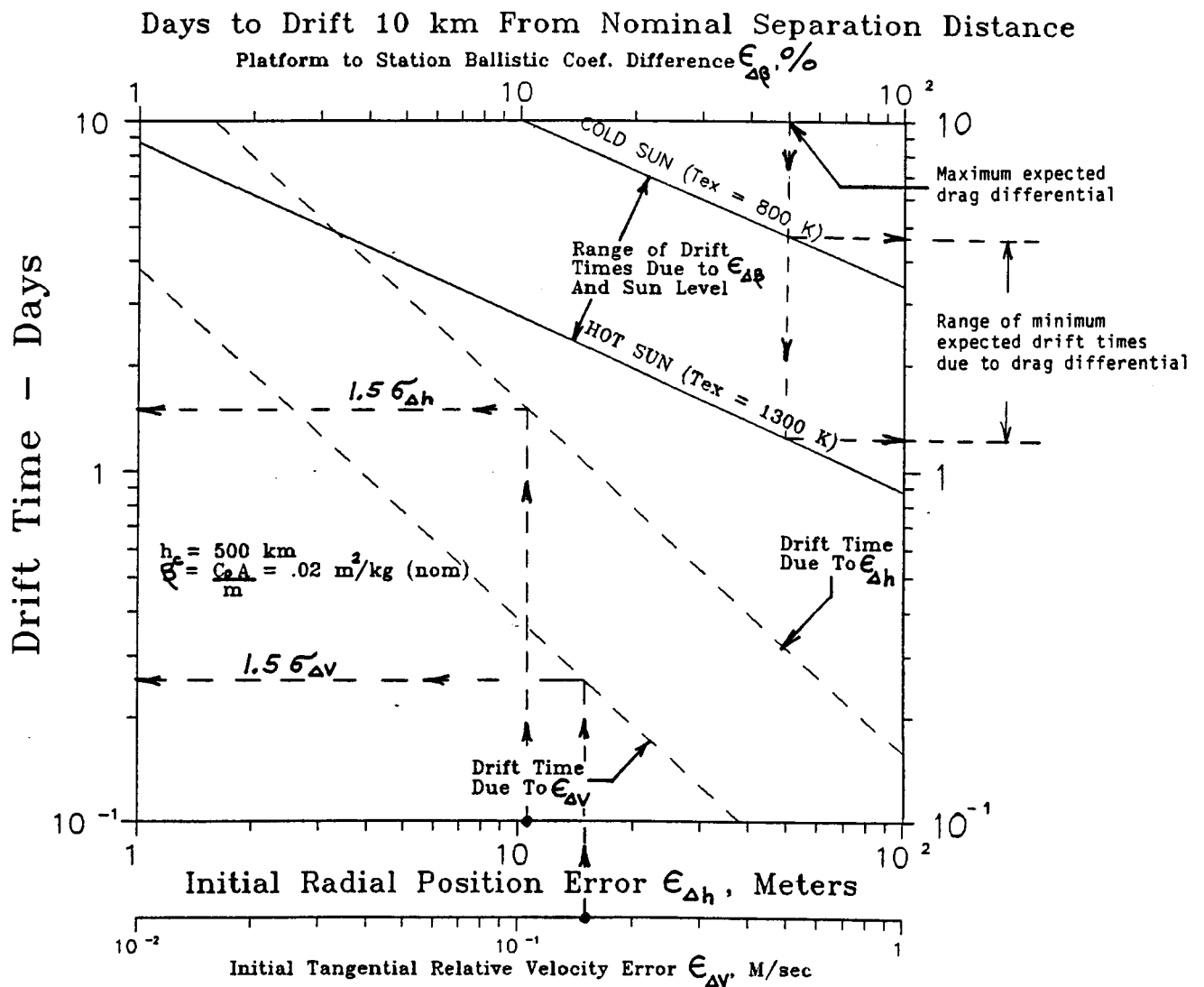


Figure 1.1.1.2-4

Annual Fuel Required to Maintain Platform  
Within  $\pm 10$  km Deadband Centered at  
Nominal Distance

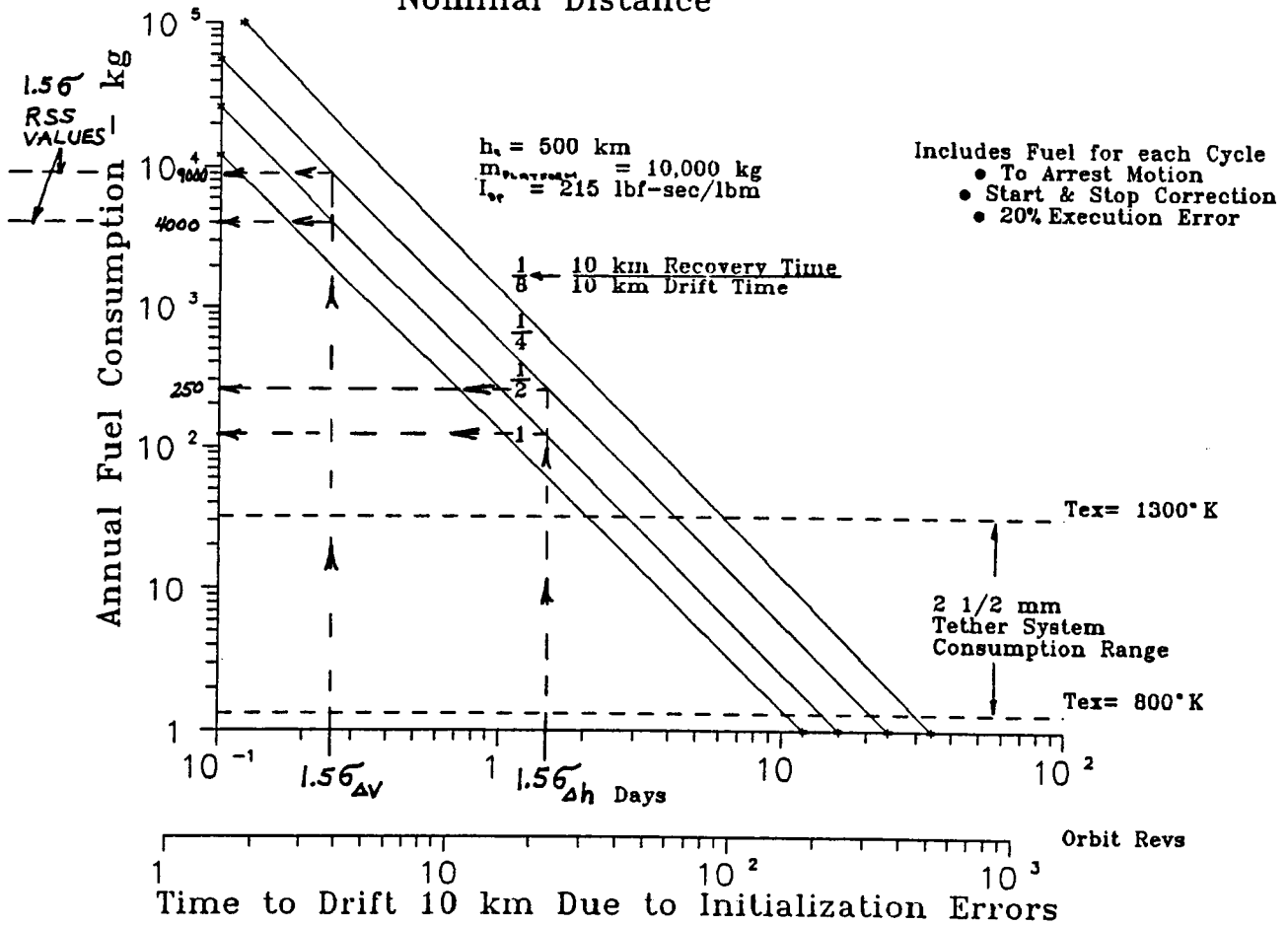


Figure 1.1.1.2-5



includes fuel to arrest motion once 10 km of drift referenced to the nominal stationkeeping point has been noted, and then fuel to both initiate and arrest a compensating drift in the opposite direction. Obviously the speed at which a return to the nominal stationkeeping point is accomplished is directly related to fuel consumption rate. Finally, the chart incorporates an additional amount of fuel equal to 20% of the basic consumption rate to account for execution errors. The latter is also intended to account for corrective thrusting which is in a non-optimal direction during the maneuvers. This comes about because thrusters would be geometrically arranged to fire only along the principle radial and tangential directions.

Finally it should be noted that the results shown in Figure 1.1.1.2-5 were prepared relative to a nominal 10,000 kg platform scaling mass for convenience. To obtain the annual fuel consumption for other platform masses, one merely scales linearly from those values shown.

For example, we note that for a mass of 10,000 kg, the annual fuel consumption attributable to the largest error source, a tangential velocity initialization error of 0.15 m/sec, would range between 4000 and 9000 kg of propellant depending upon whether the return to the stationkeeping point during each cycle was conducted in 1/2 day or 1/4 day, respectively (the effect of errors effectively RSS out). For the 15,000 kg baseline Platform the annual consumptions would be 6000 kg and 13,500 kg, respectively. Compared to these figures, the additional fuel consumption associated with the tether system are insignificant.

We believe the 6000 kg and 13,500 kg annual consumptions relative to our 15,000 kg baseline Platform to be representative of nominal and maximum cases, respectively. A minimum consumption case would probably correspond to 3000 kg. Based upon the Shuttle pricing guide which includes a 4/3 reimbursement factor, together with the current estimate of \$111M per flight for a 29,550 kg (65,000 lbm) payload, the annual cost savings in fuel using a tether system are computed to be \$15M/yr, \$30M/yr, and \$68M/yr, respectively.

1.1.1.3 MICROGRAVITY CONSIDERATIONS FOR TETHERED PLATFORMS

Tethering a single platform to the Space Station will adversely affect the micro-gravity environment on both the Platform and the Space Station while simultaneously creating a region of very low microgravity along the tether between the two vehicles. Materials processing and other experiments which were planned to be flown aboard one or the other of the vehicles specifically to take advantage of the micro-g free-flyer environment would, in the presence of the tether, necessarily have to be transferred to the shifted micro-g region to re-establish parity. The best procedure would be to include such payloads aboard a Crawler Vehicle which could then seek-out the low-g region. The same vehicle could also function as a variable-g lab of modest capability. Unfortunately, due to the sheer volume constraints associated with the design of such a crawler, only a small number of such payloads could be simultaneously accommodated in this fashion at any one time. This would surely drive up the expense of gaining access to a microgravity environment. Thus, in terms of being able to provide adequate micro-g operations time for experiments, it appears that the single tether method is impractical as compared to the free-flyer concept.

However, it appears that the application of a dual tether system circumvents the shifted micro-g problem by maintaining the micro-g region aboard the Space Station. It also allows for vernier control of the position of the system center of gravity. Here a dummy mass, comparable to the Science Platform, is deployed by a second tether on the opposite end of the Space Station. The dual tether concept is our tethered Science Platform baseline and is shown in Figure 1.1.

Experimenter Requirements

A survey was conducted relative to the needs of experimenter requirements on-board both the Space Station and the Science Platform. At present, the

micro-g spec requirement for the Space Station is  $1 \times 10^{-5}$  g. Currently, there appears to be a tendency towards desiring lower and lower micro-g level requirements approaching the level of background drag ( $1 \times 10^{-6}$  g to  $1 \times 10^{-8}$  g). In this regard the current  $1 \times 10^{-5}$  g Space Station Specification level appears about to change to a  $1 \times 10^{-6}$  g to  $1 \times 10^{-7}$  g level. The background leading to this change in philosophy can be summarized as follows.

Recent studies<sup>4</sup> seem to indicate that most forms of low micro-g materials processing have a relatively high tolerance for high frequency disturbances, but have a quite low tolerance for low frequency disturbances. This is demonstrated in Figure 1.1.1.3-1 which shows frequency dependency for a number of different experiment types. Apparently, the importance of being able to maintain an ultra-low acceleration background at the lowest frequencies had not previously been realized. This accounts for the current spec limit of  $1 \times 10^{-5}$  g which is independent of frequency.

It is believed that the introduction of a tether system would unfortunately aggravate this situation because tethers were originally envisioned to provide low micro-g payloads attached to platforms with isolation from high frequency disturbances. Little regard was paid relative to the considerably high levels of very low frequency disturbances naturally characteristic of tethers (including steady-state). Unfortunately, as noted above, most forms of low micro-g materials processing have a relatively high tolerance for high frequency disturbances, but have quite low tolerance for low frequency disturbances. Tethers therefore provide a inverted micro-g level environment with respect to frequency from what is needed as depicted by the dashed curve in the figure.

-----

<sup>4</sup>"Low Acceleration Characterization of Space Station Environment", SP85-MSFC-2928, Rev. B, Final Report, Teledyne Brown Engineering, Huntsville, AL, October, 1985.

\*Teledyne Brown SS Low Acceleration Final Report, October, 1985.

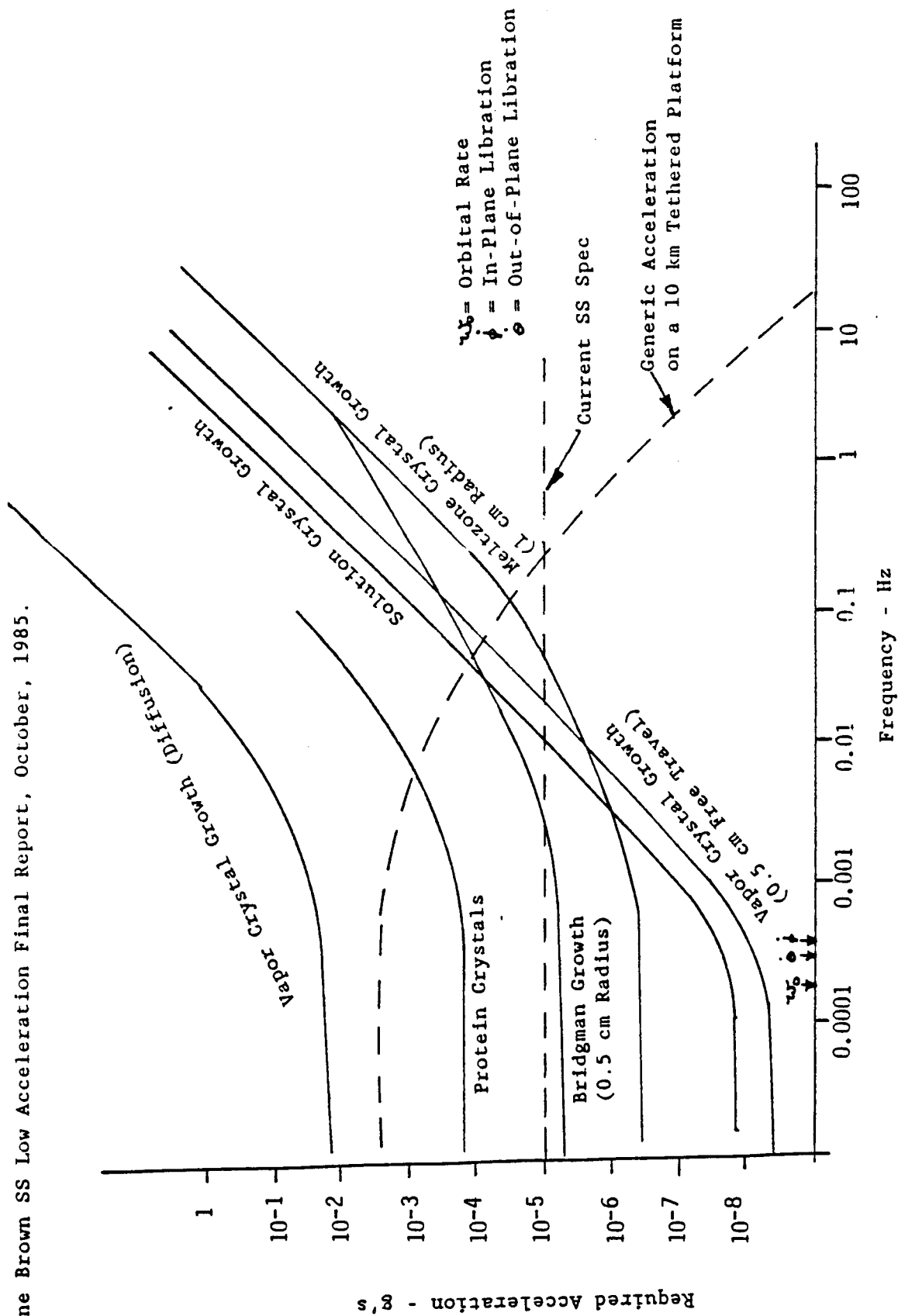


Figure 1.1.1.3-1 Typical Materials Processing Acceleration Requirements

In addition to a strong low frequency dependency, most of such experiments also have requirements for sustained low micro-g operation. Typical examples are summarized in Figure 1.1.1.3-2.

As a result of the above a Space Station change board request is currently under study which would make acceleration levels both more stringent and frequency dependent. The new spec levels are summarized in Figure 1.1.1.3-3. The outcome of this request is unknown at the time of this writing.

#### Gravity Map of the Space Station

This section quantifies the impact of a tethered Science Platform on g-level, CM shift, design, etc., on the Space Station vehicle itself. The study provides an assessment based upon the current Space Station Top System Spec acceleration limit of  $1 \times 10^{-5}$  g. Thus the previous discussion relative to the desire for lower micro-g levels is treated only as reference material here since a formal change is still pending.

A thorough investigation was made relative to the micro-g requirements of the numerous research and manufacturing entities which are currently designated as "Attached" Space Station payloads. This information was assembled from data supplied by on-going Space Station WP-3 activities of which BASD is a key participant in the preparation of Space Station Requirements.

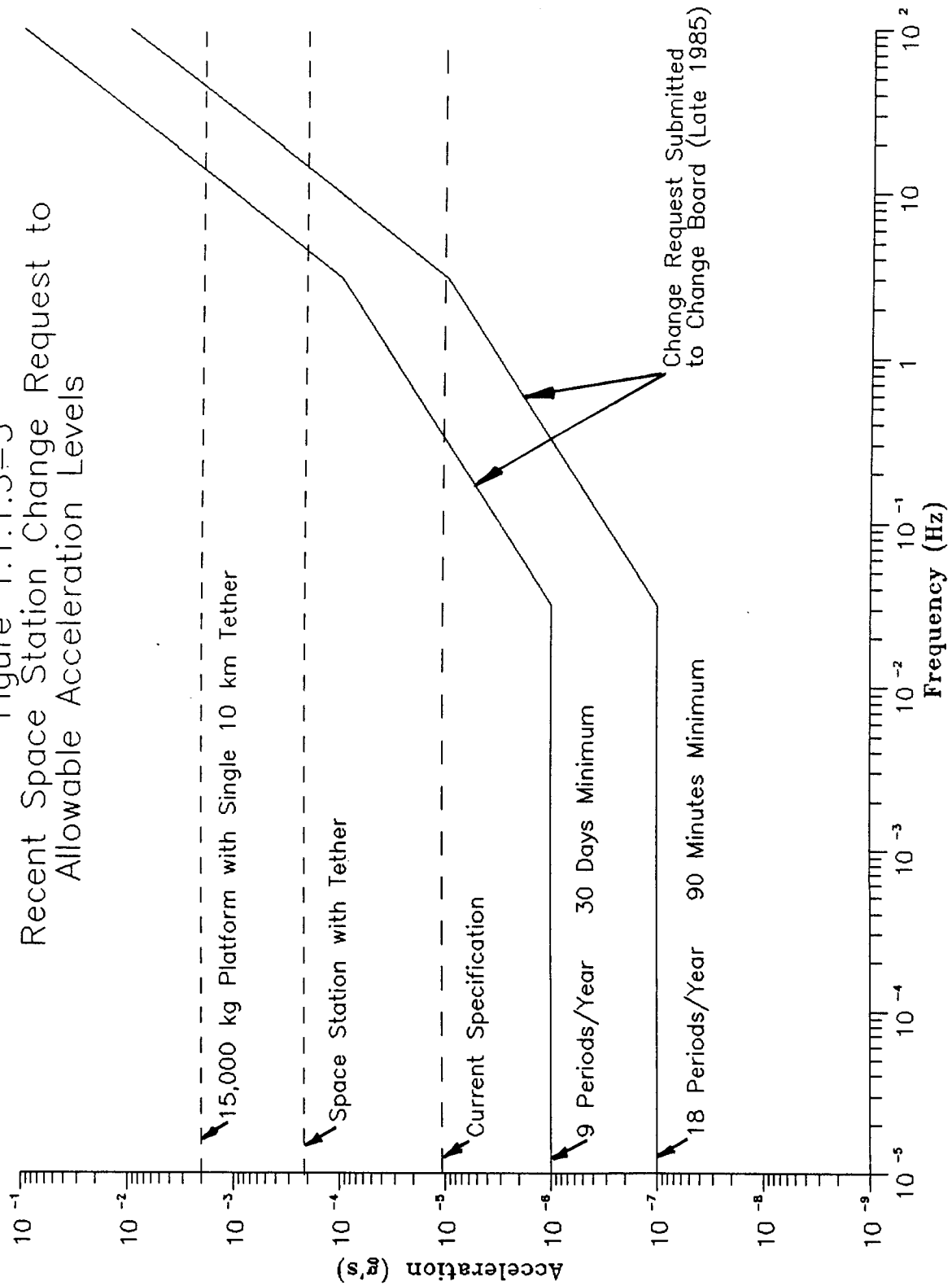
For the numerous payloads (of which at least six, incidentally, are identified as requiring long tethers, representing therefore, separate and complete tether systems over and above the present Science Platform tether application), at least 79 have been identified as requiring low-g acceleration levels as illustrated in Figure 1.1.1.3-4. Of these, 51 payloads require  $1 \times 10^{-5}$  steady-state g level environments while two additional payloads require a g level of  $1 \times 10^{-6}$ . These data are further broken down as to external or internal attachments as well as with respect to pressurization requirements in Figure 1.1.1.3-4.

Process	Maximum Usable Acceleration	Desired Acceleration
Alloy Formation	$10^{-5} g_0$ for several days	$10^{-6} g_0$ for several days
Electroepitaxy	$10^{-5} g_0$ for several days	$10^{-8} g_0$ for several weeks
Crystal Growth from Melt	$10^{-6} g_0$ for several days	$10^{-8} g_0$ for many days
Crystal Growth from Solution	$10^{-6} g_0$ for several days	$10^{-8} g_0$ for several weeks
Vapor Crystal Growth	$10^{-3} g_0$ for several days	$10^{-6} g_0$ for several months
Protein Crystal Growth	$10^{-5} g_0$ for one days	$10^{-7} g_0$ for one month
Particle Suspension	$10^{-4} g_0$ for several days	$10^{-8} g_0$ for several weeks
Commercial Production	$10^{-6} g_0$ for many days	$10^{-8} g_0$ for months

\*TELEDYNE BROWN FINAL REPORT

Figure 1.1.1.3-2 Acceleration Duration Requirements

Figure 1.1.1.3-3  
Recent Space Station Change Request to Allowable Acceleration Levels



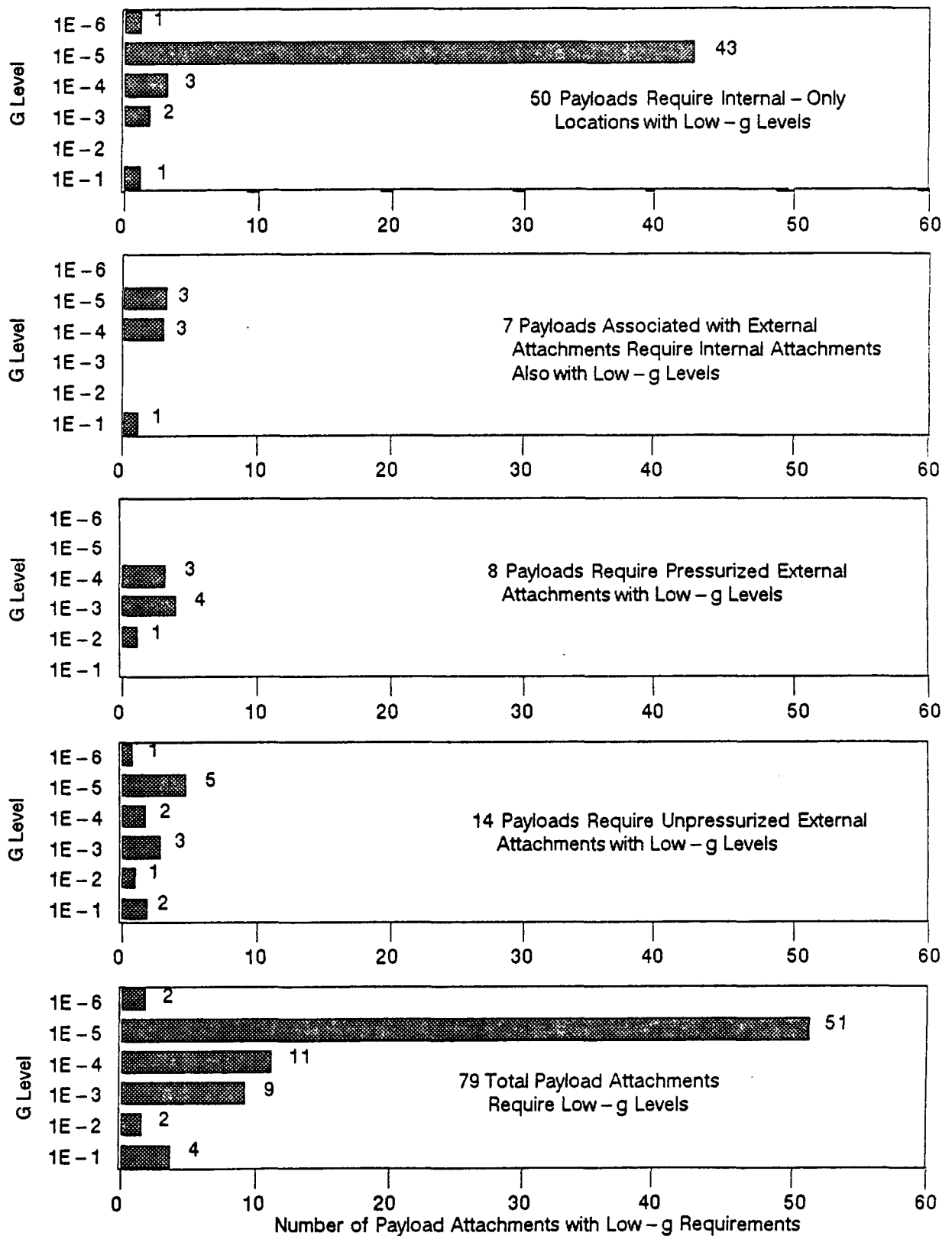


Figure 1.1.1.3 - 4 Space Station Attached Payload "g" Requirements



These requirements have recently had a great influence on the overall design of the Space Station, the latest version of which appears to reflect the broadened realization that one of the Station's greatest utilities will be in the steady-state simultaneous accommodation of a large number of very low-g payloads. This would appear to be related, in no small part, to the potential for such a large humanitarian as well as financial payback by accommodating the largest possible number of profit making manufacturing processes and customers. It is important to point out that many such payloads are identified as requiring at least some daily operations time on a 365 days per year schedule.

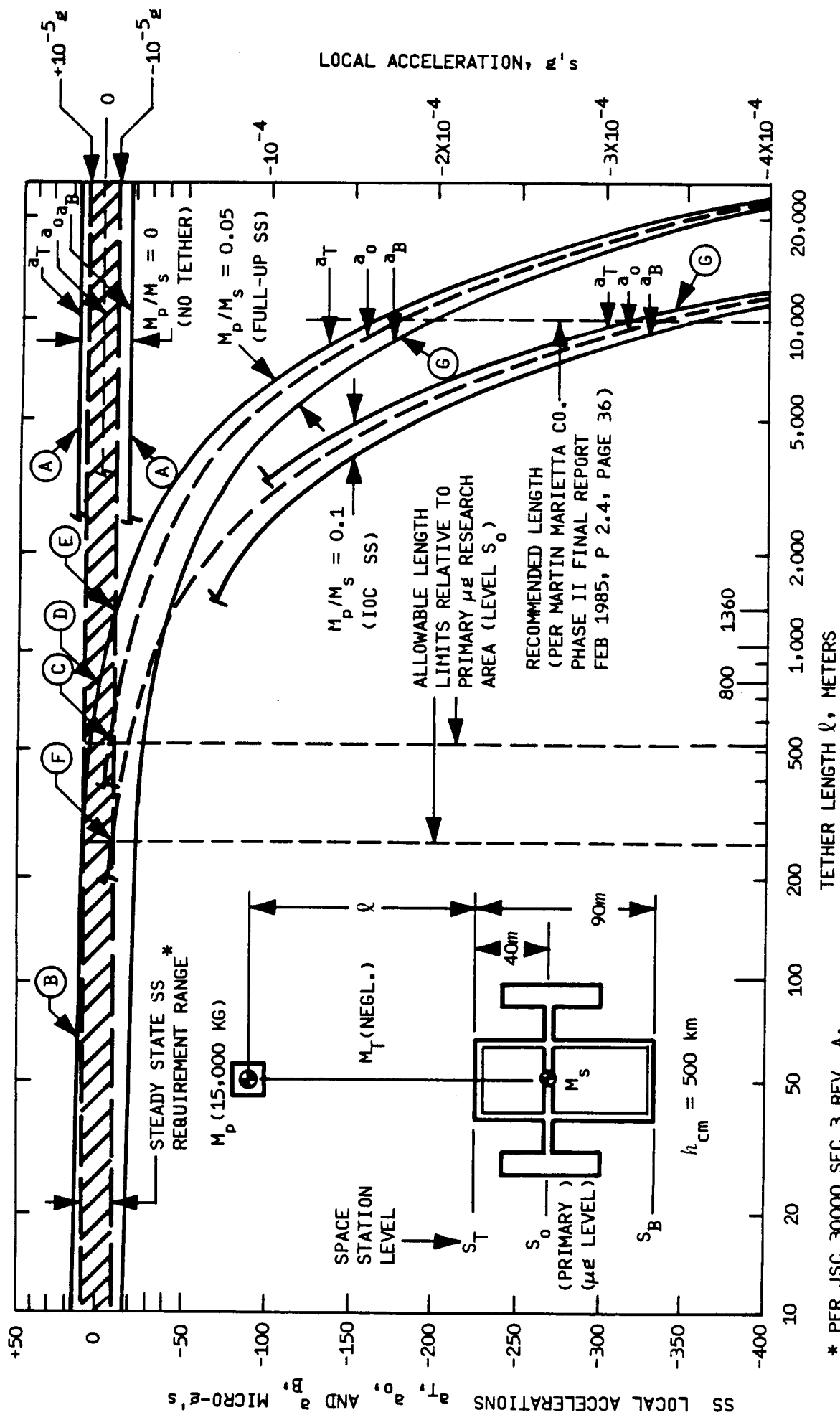
The desire for lower micro-g levels, has lead to considerable discussion about a "Man Tended" Space Station Concept. This would avoid the shock loads and accelerations induced by a "live-in" crew.

Figures 1.1.1.3-5, 1.1.1.3-6 and 1.1.1.3-7 provide a quantitative assessment of the effects of a tethered Science Platform on the acceleration environment at the Space Station relative to the above system requirement. The Science Platform is assumed to have a mass of 15,000 kg and to be tethered at a constant distance of 10 KM.<sup>5</sup> The mass is representative of the Platform descriptions in the GE/TRW and RCA Space Station Work Package 03 documents.

The results in the foregoing figures are driven by two fundamental properties of static earth pointed gravity gradient systems. The first is that for a particular combination of any number of differing masses strung out at arbitrary distances along a local vertical, only one point very near the center of mass (CM) of the system, can provide a g level which is identically equal to zero. The second property is that if a length segment is defined within which the g level is to be less than  $\pm$  a particular value, then such a

-----

<sup>5</sup>Martin Marietta Phase II, Final Report, "Selected Tether Applications in Space", February 1985.



\* PER JSC 30000 SEC 3 REV. A, 16 SEPT 1985, PARA. 2.2.7.2.3 ACCELERATIONS (SPACE STATION PROGRAM - SYSTEMS REQUIREMENTS)

Figure 1.1.1.3-5 Space Station Gravity Map with Single Platform

A/N 7218

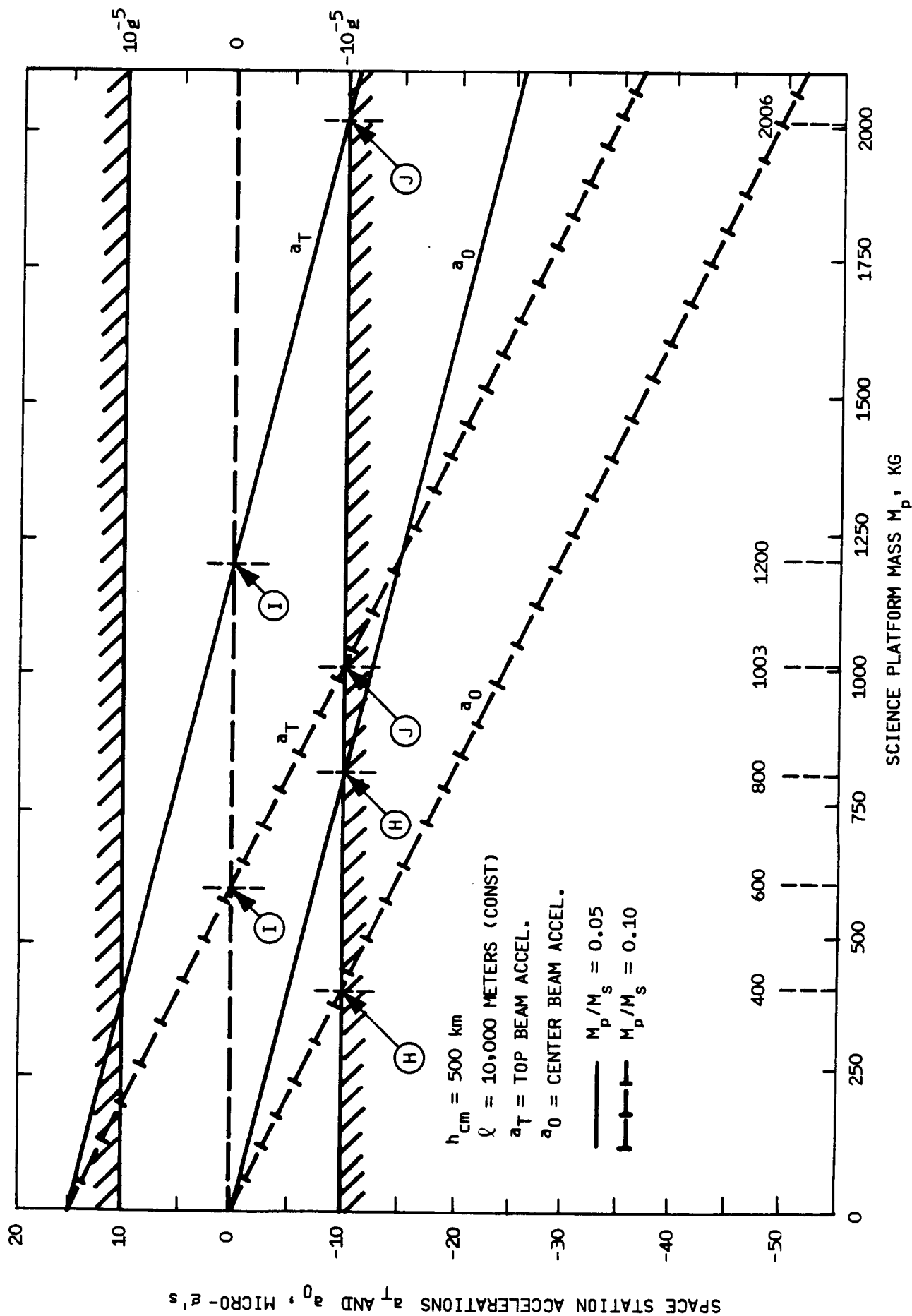
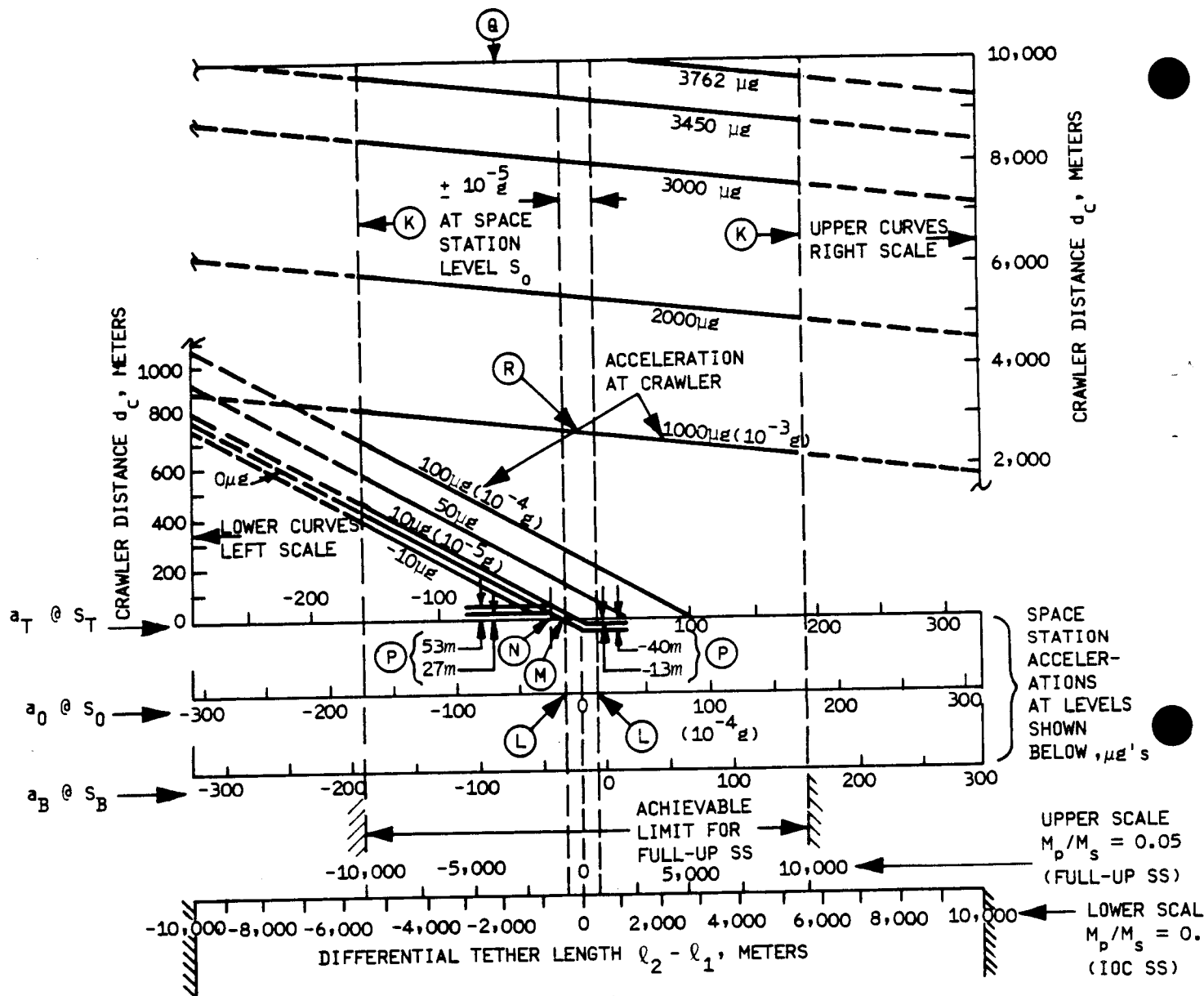
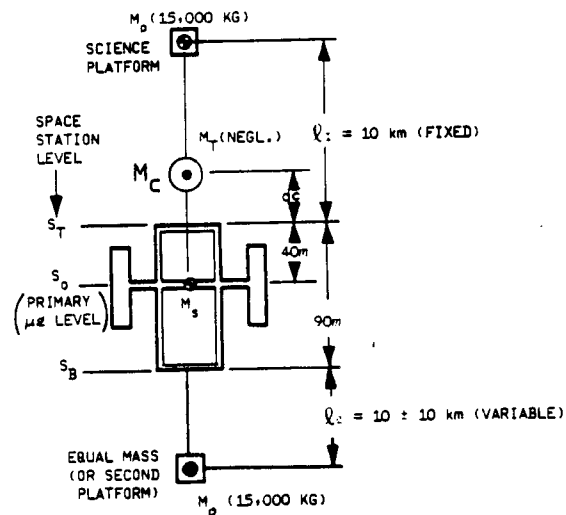


Figure 1.1.1.3-6 Tethered Platform Mass Restrictions to Meet Space Station Acceleration Limits



- TETHER AND CRAWLER MASSES  $M_T$  &  $M_C$  ASSUMED NEGLIGIBLE
- $h_{cm} = 500$  km



A/N 7218

Figure 1.1.1.3-7 Space Station Gravity Map for Dual Platforms

segment will always be centered about this single point. Furthermore, the length of the segment will be fixed and related only in a very weak manner to the center of mass altitude (with respect to low earth orbiters taken as a class). This will be true irrespective of the number, size, combination, or separation distances between individual masses (which govern only the location of the CM, per property number one).

For a Space Station altitude of 500 km and a  $\pm 1 \times 10^{-5}$  g environment, this second property translates into a fixed length segment of about 53 meters, which is considerably less than the length of the Space Station by itself, at just over 90 meters. For  $\pm 1 \times 10^{-4}$  g's the fixed segment would be 10 times larger or 530 meters, due to the linear dependence of acceleration on length. For  $1 \times 10^{-6}$  g and  $1 \times 10^{-7}$  g the segment length is only 5.3 meters and 0.53 meters, respectively. Here the g level is always zero at the segment center, increasing to  $\pm$  the selected limits at the segment extremities.

As discussed above, the only degree of freedom available is the ability to control the position of the centroid of any such fixed length segment by controlling, through mass additions and separation distance variations, the location of the overall center of mass.

#### Single Tether Configurations

Figure 1.1.1.3-5 illustrates how these properties translate into changes in the micro-g environment on the Space Station as a result of a single tether Science Platform deployment to various distances. The chart shows how acceleration varies at the three main payload station levels, which correspond to the top and bottom payload booms as well as the principal micro-g payload region near the habitable modules along the central transverse boom.

Three ratios of Platform to Space Station mass are considered: 0.10 (a 150K kg IOC Space Station), 0.05 (a 300,000 kg Full-Up Space Station), and 0 (a

massless Science Platform). Tether mass effects are assumed to be negligible in each case. A crosshatched horizontal bar representing the currently allowable frequency independent steady-state g level of  $\pm 10$  micro-g's ( $\pm 1 \times 10^{-5}$  g's) per the Space Station System Specification is shown at the top of the chart.

(Note that we use the nomenclature  $1 \times 10^{-5}$  g's = 10 micro g's,  $1 \times 10^{-4}$  g's = 100 micro g's, etc. interchangeably, as needed throughout this text in order to relate conventionally named Space Station payloads to the micro g system, which is more revealing relative to analysis results.)

Several items of interest are apparent from the figure. First, if no tether is present and the CM of the free-flying Space Station is nominally near the primary micro-g boom, then the accelerations (refer to values at points A) experienced at both the upper and lower booms, at 15 and -19 micro-g's, respectively already exceed the requirement by 50% and 90%, respectively. This corresponds to the fact that the CM and the  $\pm 10$  micro g segment of 53 meters lies wholly within the 90 meter Space Station. Secondly, for very short tethers, of say up to about 75 meters (point B), this situation is not materially altered, in agreement with logic.

Next, considering the full-up Space Station, it can be seen (point C) that for a central boom in which the local acceleration was initially zero with no tether, the acceleration would fall to -10 micro-g's with a tether length of 520 meters. At 800 meters length (point D) the top boom decreases to zero g's, decreasing further to the lower spec limit of -10 micro g's (point E) when the length is increased to 1360 meters. The latter represents the maximum tether length for which there would be at least one area of the Space Station, i.e., along the upper boom, where  $1 \times 10^{-5}$  g payloads could be operated within their specification acceleration levels. For the IOC Space Station the above tether length limits are corresponding roughly halved,

being 254 meters for -10 micro g's at the center boom (point F) and 400 and 694 micro g's for the zero and -10 micro g crossings of the top beam, respectively (the latter not shown for clarity).

At a standoff distance of 10 km (point G) it can be seen that all levels of the Space Station would be subjected to acceleration levels ranging between about 175 to 350 micro-g's depending upon the mass status of the Space Station. Such levels would exceed the specification value by an average of about 260 times!

Figure 1.1.1.3-5 also implies that the only way to achieve a single tethered standoff distance of 10 km while simultaneously maintaining specified micro gravity requirements on the Space Station is to use a very light weight Science Platform. This is pursued further in Figure 1.1.1.3-6, which identifies 10 km Science Platform mass limits required to maintain the Space Station center boom at -10 micro g's and the top boom at either zero or -10 micro g's. This chart illustrates that the center boom acceleration can be kept within 10 micro g's (points H) so long as platform mass does not exceed 400 to 800 kg (depending upon Space Station mass). Similarly, the top beam can be held at zero acceleration (points I) for 600 to 1200 kg platforms, and at -10 micro-g's (points J) for 1000 to 2000 kg platforms. For each of the top boom cases the acceleration at the center would be greater than 10 micro g's as discussed previously.

Thus in summary, if a 15,000 kg free flyer platform is tethered 10 km from the Space Station the allowable accelerations on the Space Station are grossly exceeded (Figure 1.1.1.3-5). If platform mass is maintained but the tether is shortened to a length which would permit less than 10 micro g accelerations, then the platform will be so near the Space Station that most of the desired isolation parameter values will surely be violated (also Figure 1.1.1.3-5). Similarly, if the platform is afforded the desired degree of isolation at 10 km distance, then platform mass is limited to only about three to ten percent of the free-flyer mass, the latter range being dependent

upon Space Station mass and the linear dimension of the 10 micro g or less in-board region which is acceptable (Figure 1.1.1.3-6). More stringent considerations would of course have to be applied were the specification lowered into the  $1 \times 10^{-7}$  to  $1 \times 10^{-6}$  g range.

In order to see where a micro g crawler might be located relative to the above, we invoke the use of the 53 meter,  $\pm 1 \times 10^{-5}$  g ( $\pm 10$  micro-g) segment property noted earlier. (Here we exclude the effect of the crawler mass addition which is negligible when near the system center of mass and quite small level at remote locations.)

If the g level aboard the crawler is to be no greater than, say, the present  $\pm 10$  micro g's required at the Space Station, then the crawler must be located within the 53 meter segment centered about the system center of mass. For the range of variable values covered by Figures 1.1.1.3-5 and 1.1.1.3-6 above, such a center of mass could be located anywhere between the Station center boom (for a zero platform mass) and 873 meters outboard of the top boom (for  $M_p/M_s = 0.1$  and a tether length of 10 km).

But from a practical standpoint, relative to the previous discussion, it seems apparent that almost the entire outer range of CM distances must be excluded on the basis of Space Station acceleration violations caused by the presence of the tethered platform itself.

In fact, the furthest outboard that the crawler could be practically located (relative to a possibly acceptable Space Station acceleration situation) is 53 meters. This corresponds to a platform mass and distance combination that yields -10 micro g's at the top boom, in which case crawler acceleration is +10 micro g's and the CM is halfway between at 26.5 meters outboard. (A crawler situated at this latter point would, of course, experience no acceleration.) Further, if the center boom were at -10 micro g's, then a +10 micro-g crawler would be only 13 meters outboard. If crawler acceleration was to be zero under these same conditions, then the crawler would actually



have to be located inboard by 13 meters. Clearly a micro-g crawler would lack any special utility if it were required to be operated over this small close-in range of possible CM distances.

In summary, no clear or useful role for a crawler, when used as a micro-gravity laboratory, can be identified if such a vehicle is employed in conjunction with the tethering of a single free-flyer Science Platform and the 10 micro-G main Space Station requirements are to be simultaneously obeyed.

#### Dual Platform Concept

In light of the foregoing conclusions a dual tether platform system has been adopted and analyzed. It was found that such a system could, in fact, satisfy simultaneously, the dual requirements of both a near-zero-g Space Station and a completely isolated 15,000 kg Science platform tethered at a distance of 10 km, though platform accelerations would still be very high. Unfortunately, it was also determined again that no utility could be found for a crawler used specifically as a micro-gravity laboratory, for reasons very similar to those discussed previously relative to the single tether system.

The data leading to these conclusions are summarized in Figure 1.1.1.3-7. This chart can be used as a vertical nomograph to relate an independent variable equal to dual tether differential length shown horizontally at the bottom of the chart, to acceleration at the three Space Station boom levels, to crawler acceleration as a function of outboard distance, and finally to acceleration aboard a 15,000 kg fixed-mass Science Platform which is also assumed fixed at a distance of 10 km (at the top of the chart). Here the second tethered 15,000 kg mass, deployed in the opposite direction, which could of course consist of a duplicate Science Platform, is allowed to vary between  $10 \pm 10$  km to provide the range of values shown. One takes vertical

"slices" through the figure to relate pertinent data. Thus the vertical "slice" taken at the extreme left-side of the chart corresponds approximately to a zero length second tether and therefore to the conditions described relative to single tether usage as described in the previous section. (Actually, although the values indicated at this position are very similar to those shown in Figure 1.1.1.3-5 closer inspection will reveal that they are not exactly equal. This is because even though second tether length is assumed to be zero in Figure 1.1.1.3-7, the small effect of the second 15,000 kg mass is still included).

The chart also incorporates values for both the IOC and Growth Space Station versions through mass ratio parameter  $M_p/M_s$ . Thus the complete range of values extending between left and right extremes of the chart are actually accessible only for the lightweight IOC version, whereas values accessible relative to the full-up version are contained only within the outermost set of vertical dashed lines (points K) as shown.

Figure 1.1.1.3-7 illustrates how a Science Platform can be tethered at 10 km while providing simultaneous fine position control of the 53 meter micro gravity region aboard the Space Station through small variations in the length of the second tether. For a 300,000 kg Space Station, the center boom for example, can be kept between  $\pm 10$  micro g's by controlling differential length in the range between -597 and +577 meters (points L). Alternately, top boom acceleration can be brought to zero (point M) or to -10 micro g's (point N) by using length differentials of -890 meters and -1477 meters, respectively. Further when needed, such a system would additionally permit the entire Space Station to be highly accelerated for short periods up to the horizontal limits indicated, to transfer fluids, settle fuel tanks, precipitate chemical products, aid in dockings, etc.

The diagonal lines in Figure 1.1.1.3-7 (Note scale change) are contours of constant outboard acceleration, meaning that for a particular tether length differential, an object such as a crawler placed at the distance indicated

would experience that level of acceleration. Thus the diagonal line marked zero micro-g's corresponds to the system center of mass. As before, the 53 meter rule applies, so that the arguments and conclusions reached with respect to the utility of a crawler as a microgravity laboratory for the single tether application are unfortunately, identical to those for a dual tether system. (Note that the same close-in crawler distances are required (points P) if the Space Station is to remain near zero-g's.) The crawler could, of course, operate further from the Station, perhaps as a transfer vehicle, but not as a micro-g laboratory, as indicated by diagonal contours which very quickly increase into the 100 and 1000 micro-g range with increasing distance.

Figure 1.1.1.3-7 can also be used to predict the range of accelerations aboard the Science Platform. Such values correspond to a horizontal line at a crawler distance of 10 km, that is to the top of the chart, point Q. It is noted that there is very little difference between platform accelerations for a single tether system (at the left side of the chart) and the platform accelerations that could be produced by the complete range of dual tether length differentials.

Lastly, since Figure 1.1.1.3-7 is plotted as a function of length differential, it can readily be used to determine acceleration values for shorter length dual tether systems as well. For example, an acceleration of 1000 micro-g's would exist on a platform attached to a tether of length 2628 meters (point R), assuming, of course, the existence of an equal length tether and mass on the other end. The accessible horizontal range of the chart is reduced accordingly in such a case.

In summary, a dual tether system can, in fact, satisfy simultaneously, the dual requirements of both a near-zero-g Space Station and a completely isolated 15,000 kg Science Platform tethered to a distance of 10 km, plus provide a micro-g vernier control for the Space Station as well. However, the high acceleration levels that would be present on the Science Platform

for either a single or dual tether system would appear to represent a serious technical drawback and cost disadvantage as compared to the original free-flyer concept.

#### 1.1.1.4 COMMUNICATIONS TETHER TRADE

The tether used to hold the Science Platform in place could also be used as a communications link. This could be accomplished using fiber optics, metal wires woven into the tether, or possibly metallized Kevlar strands like those being produced under another NASA contract<sup>6</sup>. The purpose of this section is to address the cost benefits associated with this concept.

The cost of a communications tether will be compared with the cost of a conventional RF system to accomplish the same task. This data will give a measurement of the cost benefit associated with this approach. However, it should be noted that there may be some "benefits" associated with a communications tether that are not easy to quantify in terms of cost and these may make the communications tether very desirable in some applications. These "benefits" are increased data security, reduced RF noise, and frequency crowding in the vicinity of the Space Station. These could become very important considerations as the use of the Space Station increases and the demands for frequency allocation and data security (both by DOD and commercial activities) grow.

-----

<sup>6</sup>Orban, R.F.: "Metallized Kevlar Space Tether System," NASA SBIR 0906-5785, Contract NAS8-35268, presented at the NASA Tether Applications in Space Program Review, General Research Corporation, McLean, VA, July 1985

## Final Report - Volume II - Study Results

These two communication approaches make use of the following assumptions:

- Platform-to-Space Station data rate of 1 Mbps and 50 Mbps
- Space Station-to-Platform data rate of 100 kbps
- \$2k/watt cost penalty for solar array procurement and integration
- \$1k/watt cost penalty for increased battery size
- 0.2 kg/watt weight penalty for added solar array size
- 0.49 kg/watt weight penalty for added battery capacity
- \$4.4k/kg launch cost penalty for added system weight
- tether lengths of 1 to 10 km

Note that two different data system requirements will be looked at and that the tether length will be varied from 1 to 10 km to determine what effect this might have on the system costs. Penalties in terms of system cost and weight are assessed for increased power usage, and a penalty is charged for increased launch weight.

A Ku band 2 watt solid state transmitter was used to accommodate the very high data rate (50 Mbps) requirement and an S-band system for the lower (1 Mbps) data rate. The Ku band solid state transmitter is very inefficient therefore a 90 watt input is estimated to obtain the required 2 watt of output power.

Table 1.1.1.4-1 (50 Mbps data rate) shows the resulting cost elements and cost benefits for an RF vs fiber optic communications system. The last column indicates the overall comparison between the two approaches. The summary on row 6 of the table indicates that the fiber optic cable has a \$70k cost benefit before the launch weight and power penalties are accounted for. Lines 7 and 8 of the table show the weight and power penalty costs for the two systems. Note that the launch costs (line 7) of the tether based system drive

TABLE 1.1.1.4-1 Cost Comparison for 50 Mbps Optical Tether at 1,5, and 10 km lengths.

COST COMPARISON FOR 50 MBPS DATA RATE CAPABILITY (100 KBPS REVERSE)

#	ITEM COMPARED CABLE LENGTH=====	R.F. AT KU-BAND (~ 15 GHz)	FIBER OPTICS AT 850 nm	DIFFERENCE (FO'S - RF'S)
		10 KM 5 KM 1 KM	10 KM 5 KM 1 KM	10KM 5KM 1KM
1	SOURCE TRANSMITTER			
		2 WATTS 1 WATT 100 mW 1 mW 500 uW 100 uW		
		<== \$450K FOR DEV. & B.P.==>	\$ 250 K DEV. + B.P.==>	
		<== \$260K FOR 2 XMTRS ==>	\$ 100 K FOR 2 XMTRS ==>	
		\$ 710 K TOTAL ==>	\$ 350 K TOTAL ==>	\$ - 360K \$ - 360K \$ - 360K
2	ANTENNAS			
		B ELEMENT SME TYPE MEDIUM GAIN; NOT APPLICABLE		
		\$ 100 K FOR B.P.		
		\$ 10 K FOR 2 ANT'S.		
		\$ 110 K TOTAL		\$ -110K \$ -110K \$ -110K
3	TETHER CABLE SYSTEM			
		KEVLAR STRESS ONLY	STRESS + FIBER OPTICS	
		\$ 200 K DEV. + B.P.	\$ 500 K DEV. + B.P.	
		\$ 100 K BUILD	\$ 200 K BUILD	
		\$ 300 K TOTAL	\$ 700 K TOTAL	\$ 400 K \$ 400 K \$ 400 K
4	RECEIVER SYSTEM			
		\$ 100 K DEV. + B.P.	\$ 250 K DEV. + B.P.	
		\$ 250 K FOR 2 RCVR'S	\$ 100 K FOR 2 RCVR'S	
		\$ 350 K TOTAL	\$ 350 K TOTAL	"PUSH" "PUSH" "PUSH"
5	ALL OTHER COMPONENTS			
		\$ 100 K FOR B.P.	\$ 100 K FOR B.P.	
		\$ 50 K FOR HARDWARE	\$ 50 K FOR HARDWARE	
		\$ 150 K TOTAL	\$ 150 K TOTAL	"PUSH" "PUSH" "PUSH"
6	RESULTS<WT & PMR ANALYSIS>	\$1,620K \$1,620K \$1,620K	\$ 1,550 K \$ 1,550 K \$ 1,550 K	\$ - 70 K \$ - 70 K \$ - 70 K
7	WEIGHT PENALTY AT \$4410/KG. OR \$2K/LB.	25 KG. 12.5 KG. 2.5 KG. \$55.1K \$11.0K	510 KG. 255 KG. 51 KG. \$2,249K \$1,125K \$224.9K	\$2,139K \$1,070K \$ 214K
8	D.C. POWER PENALTY AT \$6,000 / WATT (5% CYCLE)	100 W 55 W 19 W \$ 16.5K \$ 5.7K	20 W 20 W 20 W \$ 6K \$ 6K	\$-24K \$-10.5K \$ 0.3K
9	OVERALL COST COMPARISON	\$1,760K \$1,692K \$1,637K	\$3,805K \$2,681K \$1,781K	\$2,045K \$ 989K \$ 144K
RFVFOCAD.WRK--R. S. 6/2/1986				

the overall cost benefit results. Line 9 of the table shows the overall results. The fiber optic tether is more expensive in all cases, although for shorter tethers ( $l > \text{km}$ ) the two systems are practically equivalent.

Table 1.1.1.4-2 presents the same type of data for the low data rate (1 Mbps) scenario. Again line 9 indicates that the fiber optic tether approach is more costly than all of the S-band systems.

So the results show that communications tethers are not cost competitive with conventional RF systems. However, they do offer the unique "benefits" referred to earlier which may make them desirable regardless of the cost benefits.

#### 1.1.1.5 POWER TETHER VS SOLAR ARRAY POWER SYSTEM

A study to evaluate the cost effectiveness of using a conductive tether to power the science platform using Space Station power was accomplished. The conclusions are presented in terms of a marginal cost summary for each of the concepts. The feasibility of a power tether has been addressed by several authors<sup>7</sup> and the results of their studies are included where applicable.

The two basic methods that could be used to provide electrical power to the science platform are

- 1) a completely autonomous, spacecraft-type, electrical power subsystem or
- 2) a science platform powered from the Space Station via a conducting tether.

-----

<sup>7</sup>"Science and Applications Tethered Platform Definition Study - Mid-Term Report", Aeritalia, TA-RP-AI-002, March 21, 1986.

TABLE 1.1.1.4-2 Cost Comparison for 1 Mbps Optical Tether at 1, 5, and 10 km lengths.

COST COMPARISON FOR 1 MBPS DATA RATE CAPABILITY (100 KBPS REVERSE)										
#	ITEM COMPARED	R.F. AT 5-BAND		1 KM	FIBER OPTICS AT 850 nm		DIFFERENCE (FO\$'S - RF\$'S)			
		10 KM	5 KM		10 KM	5 KM	1 KM	10KM	5KM	1KM
1	SOURCE TRANSMITTER	25 mW	15mW	5 mW	25 uW	15 uW	5 uW			
		<=== \$ 140 K FOR B.P. =====>			\$ 250 K DEV. + B.P. =====>					
		<=== \$ 20 K FOR 2 XMTRS =====>			\$ 100 K FOR 2 XMTRS =====>					
		\$ 160 K TOTAL =====>			\$ 350 K TOTAL =====>			\$ 190 K	\$ 190 K	\$ 190 K
2	ANTENNAS	SINGLE PATCH WIDE BEAM			NOT APPLICABLE					
		\$ 16 K FOR B.P.								
		\$ 4 K FOR 2 ANT'S.								
		\$ 20 K TOTAL						\$ - 20 K	\$ - 20 K	\$ - 20 K
3	TETHER CABLE SYSTEM	KEVLAR STRESS ONLY			STRESS + FIBER OPTICS					
		\$ 200 K DEV. + B.P.			\$ 500 K DEV. + B.P.					
		\$ 100 K BUILD			\$ 200 K BUILD					
		\$ 300 K TOTAL			\$ 700 K TOTAL			\$ 400 K	\$ 400 K	\$ 400 K
4	RECEIVER SYSTEM	\$ 100 K DEV. + B.P.			\$ 250 K DEV. + B.P.					
		\$ 250 K FOR 2 RCVR'S			\$ 100 K FOR 2 RCVR'S					
		\$ 350 K TOTAL			\$ 350 K TOTAL			"PUSH"	"PUSH"	"PUSH"
5	ALL OTHER COMPONENTS	\$ 100 K FOR B.P.			\$ 100 K FOR B.P.					
		\$ 50 K FOR HARDWARE			\$ 50 K FOR HARDWARE					
		\$ 150 K TOTAL			\$ 150 K TOTAL			"PUSH"	"PUSH"	"PUSH"
6	RESULTS < WT. ANALYSIS	\$ 980 K	\$ 980 K	\$ 980 K	\$ 1,550 K	\$ 1,550 K	\$ 1,550 K	\$ 570 K	\$ 570 K	\$ 570 K
7	WEIGHT PENALTY AT \$4410/KG. OR \$2K/LB.	25 KG.	12.5 KG.	2.5 KG.	510 KG.	255 KG.	51 KG.	\$2,139K	\$1,070K	\$ 214K
		\$110.2K	\$ 55.1K	\$11.0K	\$2,249K	\$1,125K	\$224.9K			
8	OVERALL COST COMPARISON	\$1,090K	\$1035K	\$ 991K	\$3,799K	\$2,675K	\$1,775K	\$2,709K	\$1,640K	\$ 784K
RFVFOCAC.WRK==R.S. 6/										



Table 1.1.1.5-1 lists the advantages and disadvantages of both approaches. The decision as to which approach provides the optimum cost/performance depends upon the power requirements of the payload. The desired power capability could be between 1 and 20 KW. This analysis is based upon a 10 Km tether. If the length of the tether is changed the efficiency of the system will be changed. The basic trade-off necessary is the weight and efficiency of a tether power system versus the complexity and pointing requirements of a autonomous science platform.

The following sections will discuss the advantages/disadvantages described in Table 1.1.1.5-1 and then attempt to analyze the properties of the tether pertinent to the electrical power subsystem. This analysis is the first step in the study of the feasibility of powering the science platform from the Space Station from a conducting tether. The first section will provide a general discussion of the Table 1.1.1.5-1 parameters. The next section will discuss the problems of tether generated EMF and a possible method of solution using A.C. power and the efficiency of such a conducting tether power system. Finally, the last section will discuss the actual cost trades relative to a power tether.

TABLE 1.1.1.5-1  
TETHER POWER SUBSYSTEM OPTIONS

Three design options were identified for the tether power subsystem:

- 1) science platform is powered by a separate power system with batteries and solar array
- 2) science platform is powered via a tether from the Space Station
- 3) science platform has batteries for peak demand but the battery charge and control is provided by the Space Station

OPTION 1

SEPARATE POWERED SCIENCE PLATFORM

ADVANTAGES

AUTONOMOUS PLATFORM  
SIMPLE TETHER  
SIMPLE SS INTERFACE

DISADVANTAGES

PLATFORM COST  
SOLAR ARRAY POINTING  
PLATFORM THERMAL  
PLATFORM WEIGHT

OPTION 2A

PLATFORM POWERED BY SPACE STATION TETHER

ADVANTAGES

PLATFORM WEIGHT  
PLATFORM COMPLEXITY  
PLATFORM COST  
PLATFORM RELIABILITY  
SIMPLER PLATFORM CONTROL

DISADVANTAGES

CONDUCTIVE TETHER  
TETHER WEIGHT  
SS INTERFACE COMPLEXITY  
TETHER COST  
INDUCED VOLTAGE  
POWER EFFICIENCY  
PLATFORM FREE-FLYING

OPTION 2B

SPACE STATION PROVIDES POWER FOR PLATFORM BATTERY CHARGE

ADVANTAGES

SS INTERFACE  
POWER EFFICIENCY

DISADVANTAGES

PLATFORM WEIGHT  
PLATFORM COST

### General Description of Science Platform Power Options

While some of the trade-off parameters in Table 1.1.1.5-1 are obvious, and some are not, a brief discussion of each will assure completeness of the analysis.

#### Autonomous Powered Science Platform

The greatest advantage of a separate powered science platform is that an autonomous platform has no interfaces with the Space Station except for the tether, which is common to either power system approach. The disadvantages of the autonomous platform are mainly concerned with the cost of implementing solar arrays. The array cost, and the associated thermal system, weight and array pointing requirements will increase dramatically with the size of the solar array or the power requirement of the science platform. Based upon 12 Watts per square foot (full sun) and .05 kg per watt, Figure 1.1.1.5-1 shows the size and weight of the required solar array versus the power required by the platform. Actually, the curve of Figure 1.1.1.5-1 is optimistic because the efficiency of the solar array will decrease for larger solar arrays.

The size of the solar array must be defined before deployment such that structure, solar array mechanism, thermal and other requirements can be defined. The large 20 kW power system would be prohibitive and costly. If the science requirements are too small, the solar array would not be cost effective. However, a power system of 1 kW would limit the growth capability of the science platform. Also, the science platform must be a modular design which can be easily serviced and experiments changed. Since the solar arrays and batteries are items always considered to be critical elements of the electrical power subsystem, extra design effort will be required to assure their easy replacement capability.

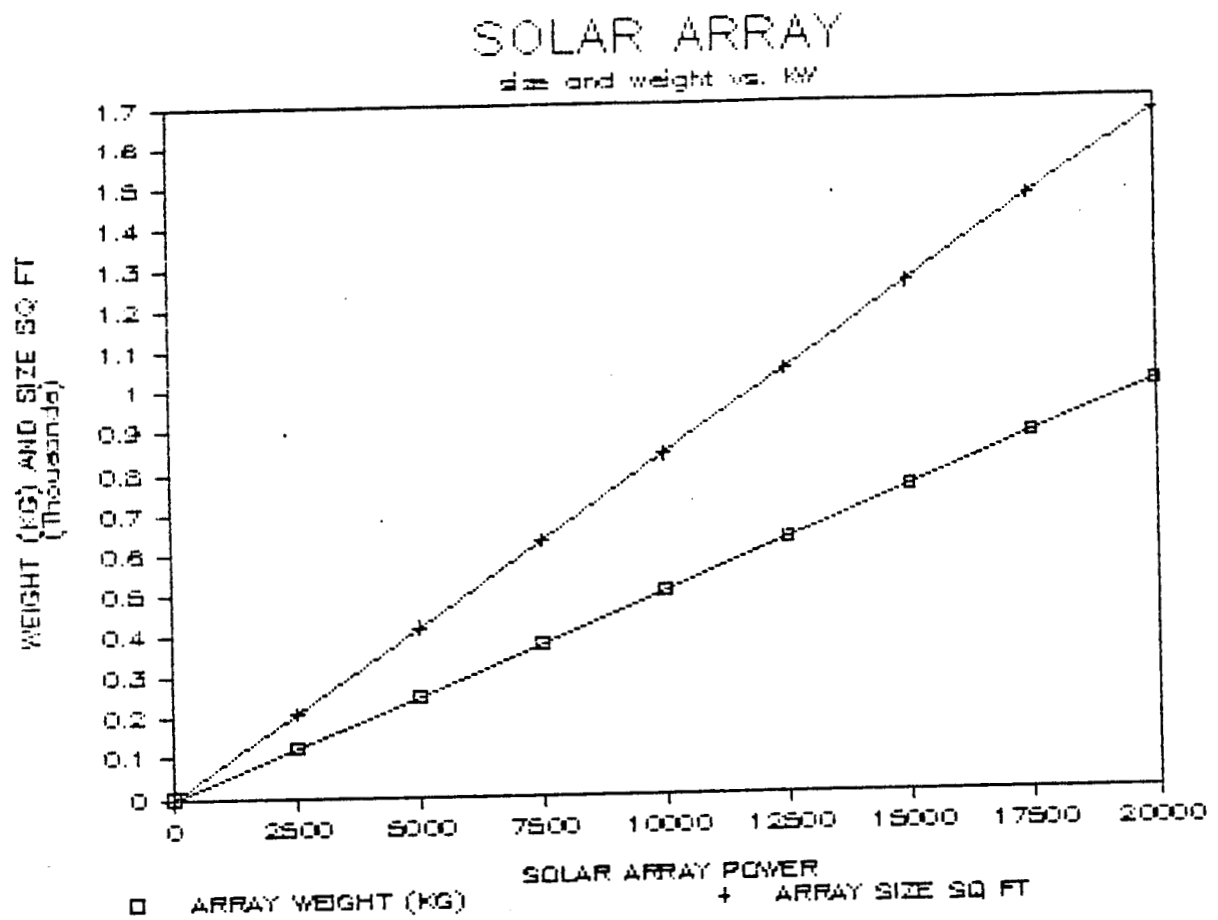


Figure 1.1.1.5-1  
Solar Array Size and Weight Versus Power Output

Platform Powered from the Space Station Tether

The advantages of a tethered powered platform are the reduction of the platform cost and complexity. If the science platform is powered via a conducting tether, the power generation cost of the science platform would be transferred to the Space Station. The required additional power is greater than one-half of a Space Station solar panel. If the powered tether were considered to be an attached payload, this cost would already exist in the Space Station. At present, a tethered science platform is not be considered to be an attached payload however, thus greatly impacting the cost of the Space Station. Here the pointing of the solar arrays is considered to be part of the complexity transferred to the Space Station. On the other hand, the science platform attitude control and science pointing control systems will be simplified if they do not have to compensate for torques developed by a science platform solar array pointing. The reliability of the science platform will also be enhanced simply because of the removal of several components such as batteries, and solar array controls. However, the reliability of the tether itself will have to be determined before any overall reliability observation can be made.

The disadvantages of the conducting tether are not trivial. The weight of the tether will increase because of the metallic wires. There will also be a need for micrometeoroid protection, which will further add to the system weight. The tether deployer mechanism will be more complicated with some form of slip ring mechanisms (probably high voltage) for the powering of the tether. The science platform, which does not have it's own power, would not be able to be detached from the tether to become a free-flyer for brief periods of time. This includes free-flying periods due to a broken tether.

The two most crucial electrical power subsystem concerns of the conducting tether are the generation of EMF or a voltage potential between the Space

Station and the science platform caused by the motion of the tether through the earth's magnetic field and the efficiency of powering the science platform from the Space Station.

#### Conducting Tether Power Concerns

##### Tether EMF

The voltage potential (EMF) between Space Station and the science platform will be as high as 200 Volts per Km of tether or 2000 Volts (10 Km tether). Tethers of these potentials have been proposed for the generation of power; however, an electron emissions source is required to create the second path of the current loop. When this secondary path is created, current will flow in the tether. These currents will cause heating of the conducting tether and eventually deorbit of the Space Station. Without the electron emission source, the effect of the tether potential will be inconsequential. The science platform will simply be at a higher potential than the Space Station.

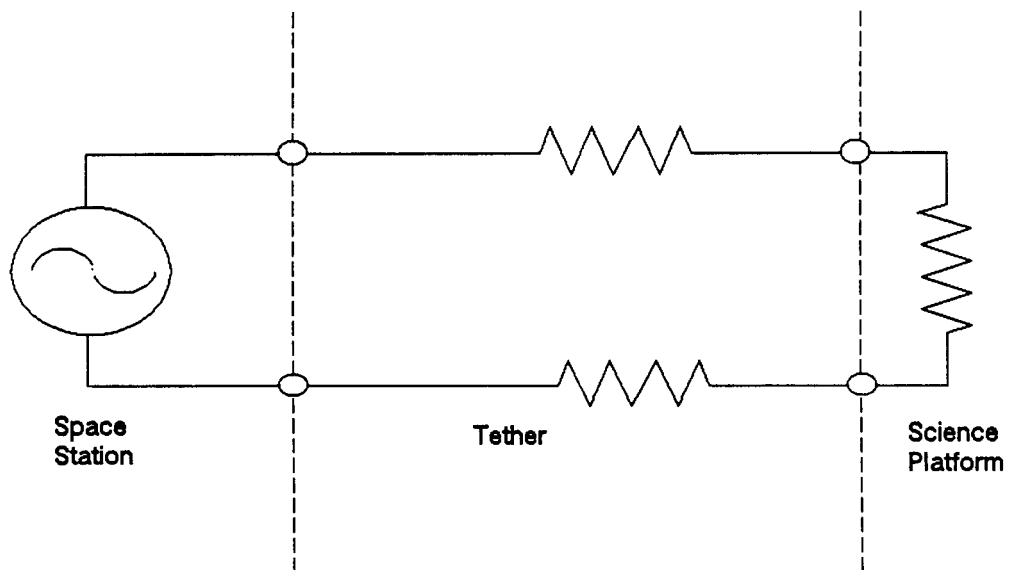
With the science platform at an elevated potential, the operation of any experiments on the science platform or the Space Station will have to be constrained from the use of any type of emissions similar to an electron emission. Also, when the OMV approaches the science platform, a potential will exist between the OMV and the platform. This potential will have to be slowly discharged with a high resistance probe before final contact is made.

A possible solution to the EMF differential is to use A.C. to power the science platform with line capacitors in series with the conducting tether. Since the tether EMF is basically direct or slowly varying current, the in-line capacitors in the tether could provide isolation such that the tether voltage would not be as large a concern.

### Powered Tether Efficiency

The cost of powering the science platform is acutely dependent upon the efficiency of the system. The trade-off is the cost of buying power from the Space Station versus the cost of autonomous generation of power. This efficiency is primarily a function of the size of the tether and the potential of the power system. Figure 1.1.1.5-2 illustrates the tether power system. The two resistances  $R_1$  are the resistance of the tether wire.  $R_L$  is the resistance of the load, or the science platform. This figure logically states that the efficiency increases monotonically with the ratio of the tether wire resistance to that of the science platform load. In other words, the higher the load impedance in proportion to the the wire loss, the greater will be the system efficiency. Figure 1.1.1.5-3 shows the required load resistance versus wire size (AWG) for efficiencies of 70, 80 and 90 percent. The load impedance for a fixed power output to the platform can be increased only if the voltage of the system is increased. Figure 1.1.1.5-4 shows voltage required versus wire size for the same efficiencies. If small wire sizes are desired, the required power system voltages can be thousands of volts. Larger wires would be a simple solution, but would lead to greatly increase launch weight and cost.

The illustration shown in Figure 1.1.1.5-2 is for D.C. power. A.C. power provides many advantages. The main advantage is the ability to simply transform the system voltage. The Space Station can provide attached payloads with 60 Hz, 400 Hz, and 10 KHz A.C. power. Because of the low frequency, the circuit could be analyzed as either a D.C. circuit or as a lossy transmission line with the loss factor being:



$$\text{Efficiency} = n = P(\text{out})/P(\text{in}) = 1/(1 + (2 \cdot R_1/R_2))$$

Figure 1.1.1.5 – 2 Tether Power System



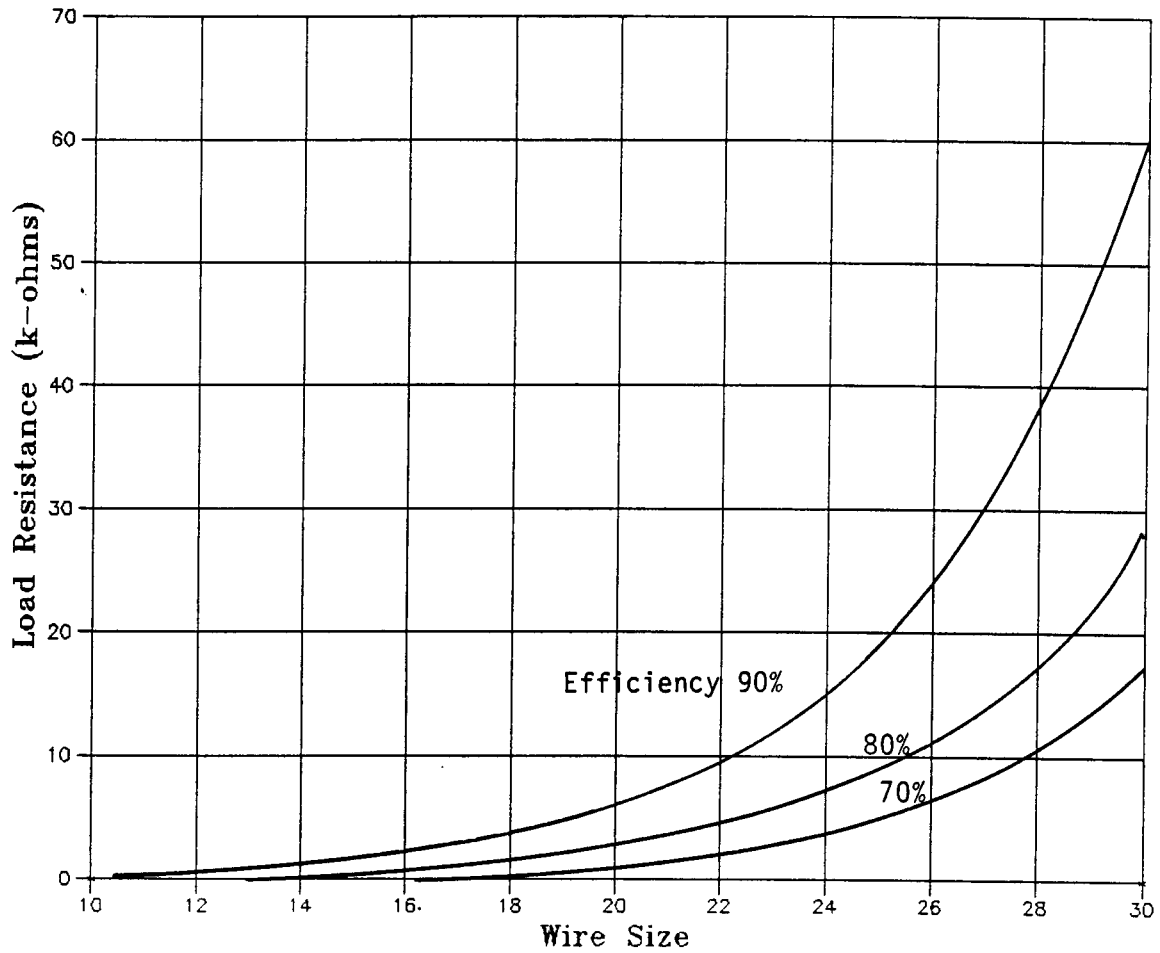


Figure 1.1.1.5-3

Load Resistance Versus Wire Size for Efficiency

$$\text{Efficiency} = \eta = \frac{P_{\text{out}}}{P_{\text{in}}} = \frac{1}{1 + (2 \cdot R_1/R_2)}$$

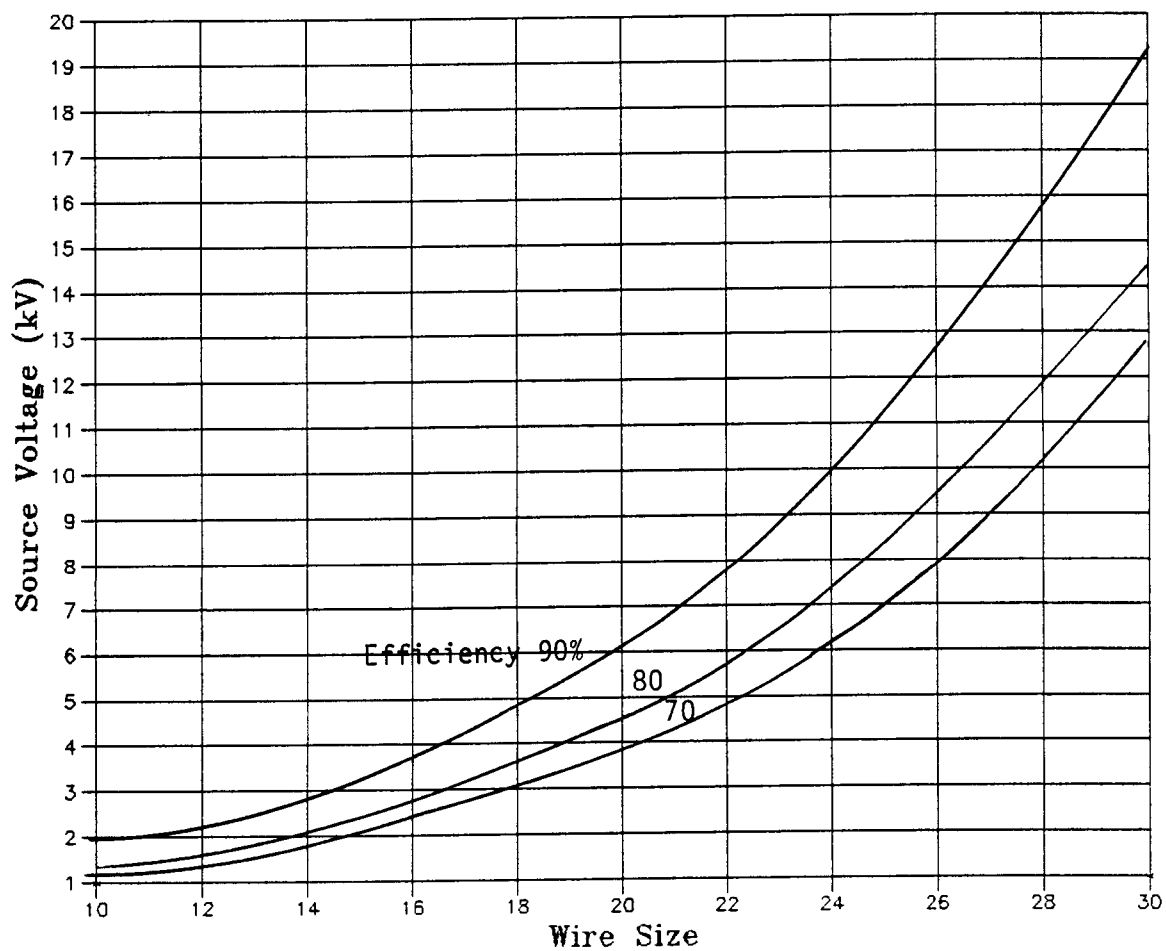


Figure 1.1.1.5-4

Voltage Versus Wire Size for Efficiency

$P_{out} = 5000 \text{ Watts}$

$V = \text{Square Root } (P_{out} \cdot R_1 / n^2)$

## Final Report - Volume II - Study Results

$$\text{loss} = e^{-(R_s/(2 \cdot Z_o)) \times \text{length}}$$

$R_s$  : conductor loss

$Z_o$  : characteristic impedance of power transmission  
line

$$(Z_o = \text{voltage/current})$$

Both analyses yield the same efficiency results. The transmission approach clearly states that the efficiency is proportional to the ratio of the conductor loss and the transmission line characteristic impedance.

The transmission approach, however, identifies another concern with A.C. power: the velocity factor. A 10 Km tether transmission line is 0.01 wavelength long at 400 Hz., but the line would be 0.33 wavelengths at 10 KHz. When the transmission line is greater than 0.1 wavelength several things such as impedance transformation, standing waves, etc., must be considered. If, for example, the transmission line characteristic impedance were 700 ohms and the load impedance were 350 ohms, the actual impedance, because of the transmission line voltage standing wave ratio, seen by the Space Station would be 800 ohms and highly capacitive. The Space Station would be required to match the power factor of the tether. If the load impedance of the science platform varied, the Space Station could be required to compensate for some widely varying power factors. A possible solution to this problem would be to design a power control system which would deliver power to the science platform on an intermittent basis. When power is delivered, the science platform would present a constant impedance which would charge batteries located on the platform. The addition of batteries to the platform would decrease some of the advantages of the tether system; however, it could decrease the total system cost, allow for more flexible platform power requirements, and possibly allow short time autonomous operation with battery only operation.

The use of high frequency A.C. power could have other advantages. The impedance of capacitors in series in the transmission line will be much

lower at 10 KHz and transmission line techniques could be used to "match" these reactances. In-line capacitors could isolate the tether induced EMF. Capacitive coupling of the Space Station power to the tether and from the tether to the science platform would provide high impedance to the slowly varying tether EMF but small impedance for the 10 KHz power. Also, 10 KHz transformers would be smaller and lighter than 60 Hz transformers or dc to dc converters.

Thus far, the primary factor which effects the tether power efficiency has been described as the ratio of the load impedance and the resistance of the tether wires (A.C. or D.C.). Figures 1.1.1.5-2 through 1.1.1.5-4 described how a higher load impedance or a higher system voltage would improve the tether power system efficiency. The higher system voltage (for a fixed power transmission) means that the  $Z_0$  or characteristic impedance of the tether transmission line must be higher. In order to apply the effect of the higher characteristic impedance to our trade-off, a relative perception of the impact of the higher impedance line is needed. Figure 1.1.1.5-5 shows the spacing required between two wires for impedances between 500 and 1200 ohms with 0, 10, or 20 gauge wires. The spacings in Figure 1.1.1.5-5 are given in feet. The actual spacings would be modified somewhat when dielectric spacers are used, but the numbers in the figure are representative. It is obvious that impedances greater than 1000 ohms requiring spacings of tens of feet are not viable. If wire dimension are assumed which would be viable for a proposed tether system: 0.1 inch to 24 inches for two wire line or 0.5 inch to 2 inches for coaxial line, the characteristic impedances would be constrained to 100 to 600 ohms for two wire line and 100 to 250 Ohms for coaxial line.

Figures 1.1.1.5-3 and 1.1.1.5-4 showed the required voltage and load resistances versus wire size for various efficiencies. The range of load impedance has now been limited to 100 to 600 Ohms. Therefore, the data of Figures 1.1.1.5-3 and 1.1.1.5-4 can be presented for a narrower range of impedances. Figure 1.1.1.5-6 shows the voltage required for the

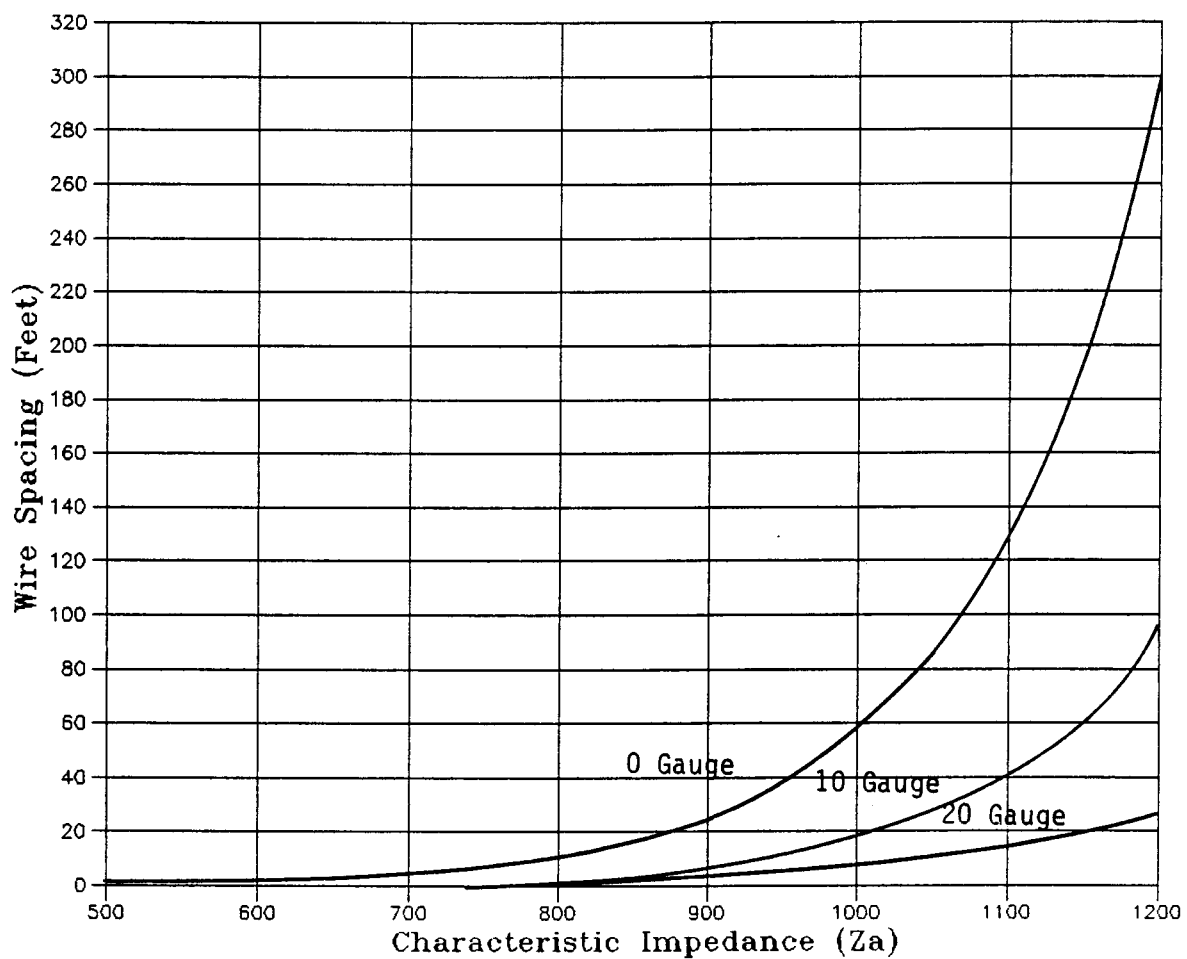


Figure 1.1.1.5-5  
Two Wire Line -- Wire Spacing Versus  $Z_0$

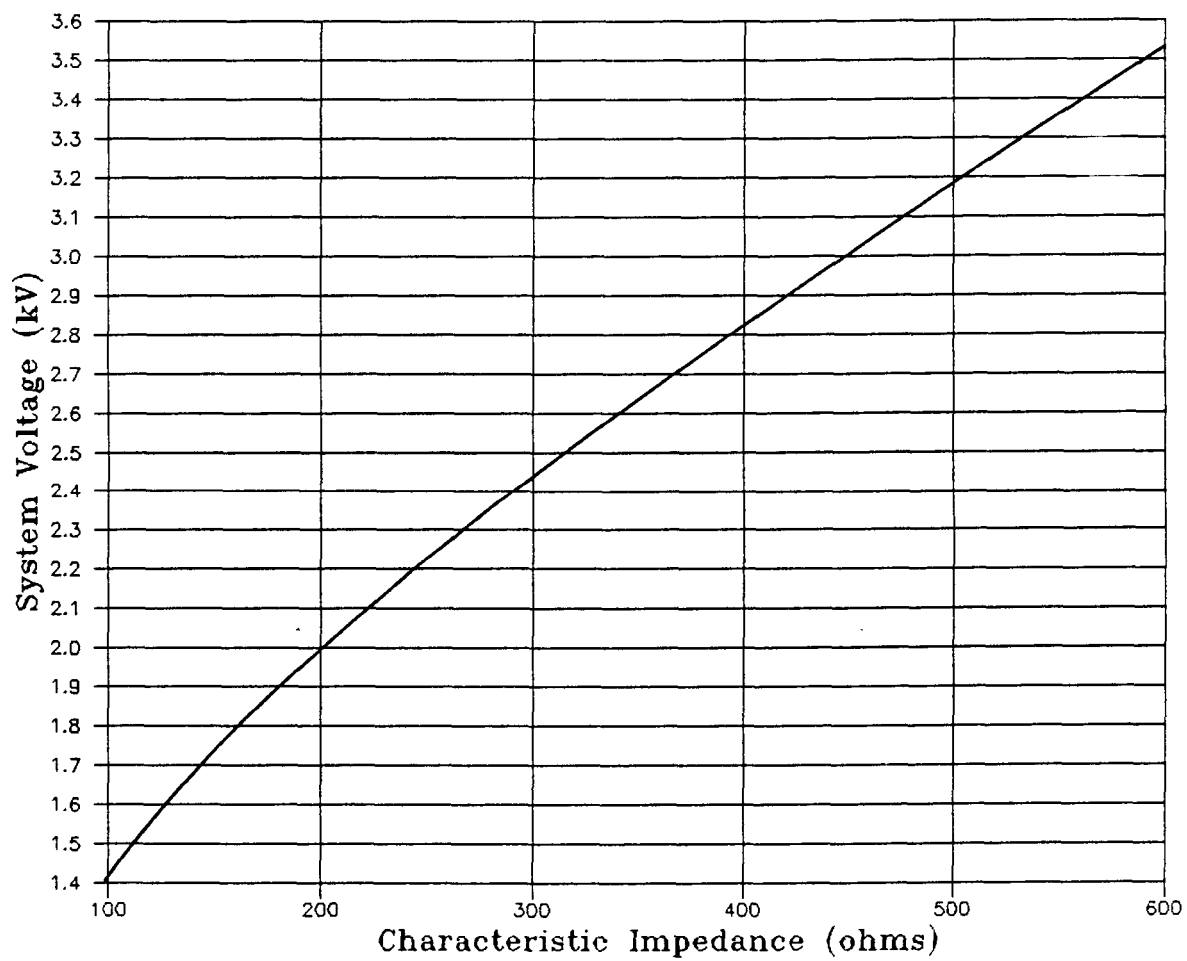


Figure 1.1.1.5-6

System Voltage Versus characteristic Impedance

transmission of 20,000 watts input on transmission lines of 100 to 600 Ohms. With a reasonable system efficiency of at least 70 percent, the output power would be 14,000 Watts and the input voltage required would be less than 3500 volts. These voltage levels are feasible for a tether application. Figure 1.1.1.5-7 is slightly different than Figure 1.1.1.5-3 Figure 1.1.1.5-7 shows a plot of efficiency versus load impedance (100 to 700 Ohms) for various wire sizes. If it is assumed that the reasonable power efficiency is to be at least 70 percent, Figure 1.1.1.5-7 shows that the required wire sizes would be between 0 to 14 AWG. The obvious choice of wire size for electrical efficiency is the 0 gauge wire.

Another important parameter is tether weight. The tether weight is effected dramatically as a function of wire gauge. This is demonstrated in Figure 1.1.1.5-8.

#### Power Tether Weight and Cost Trade

Based on power subsystem design work for the co-orbiting platforms<sup>8</sup> and power tether trade studies published by the<sup>9</sup> the following weight impacts table can be constructed for a 10 kW platform requirement.

-----

8 Space Station Definition and Preliminary Design Work Package 03, EMS Transmittal No. 5, Volume I Platforms, June 14, 1985, RCA Astro-Electronics  
9 Italians Science and Applications Tethered Platform Definition Study- Mid Term Report, Feb. 21, 1986, Aeritalia

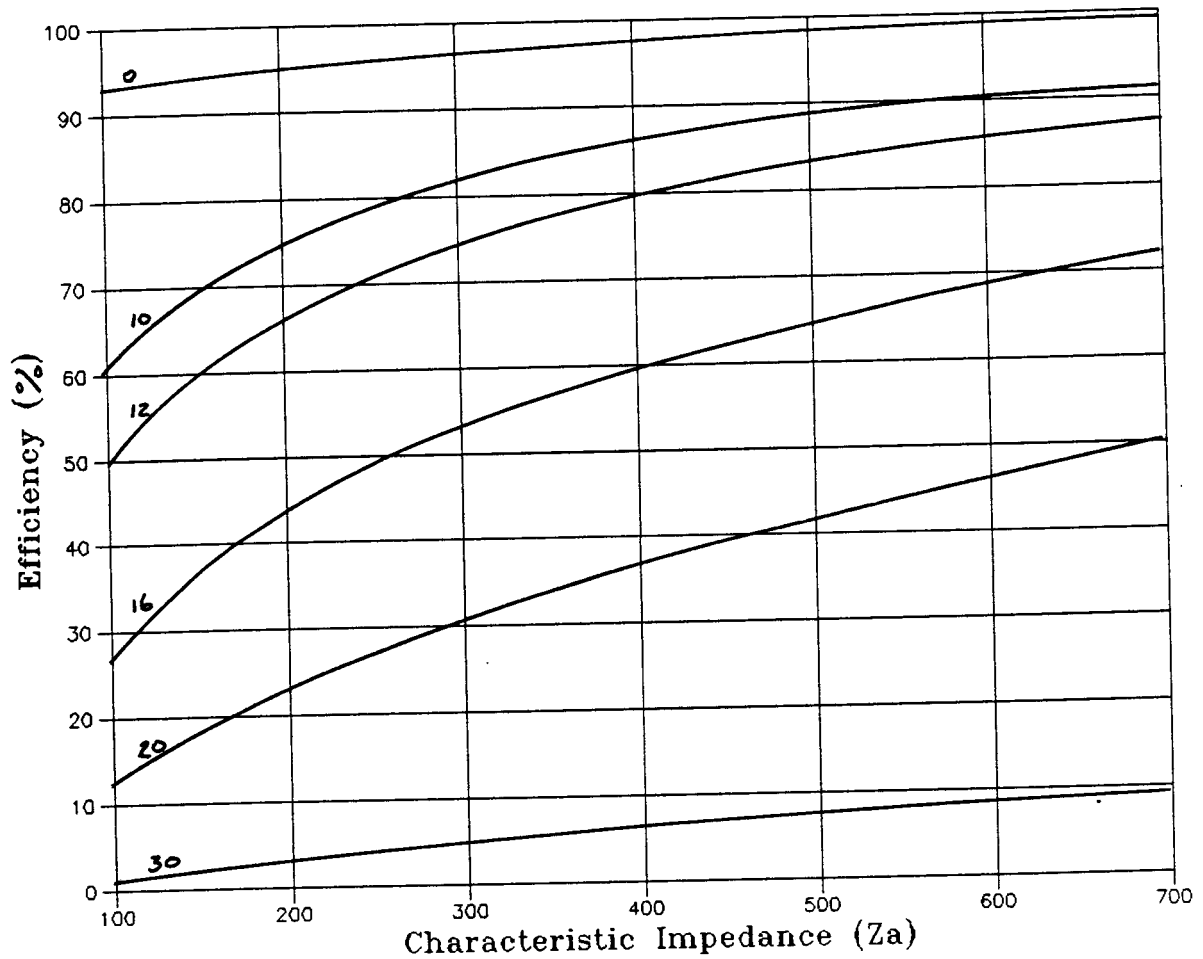


Figure 1.1.1.5-7  
Efficiency Versus Wire Size (100 to 700 Ohms)



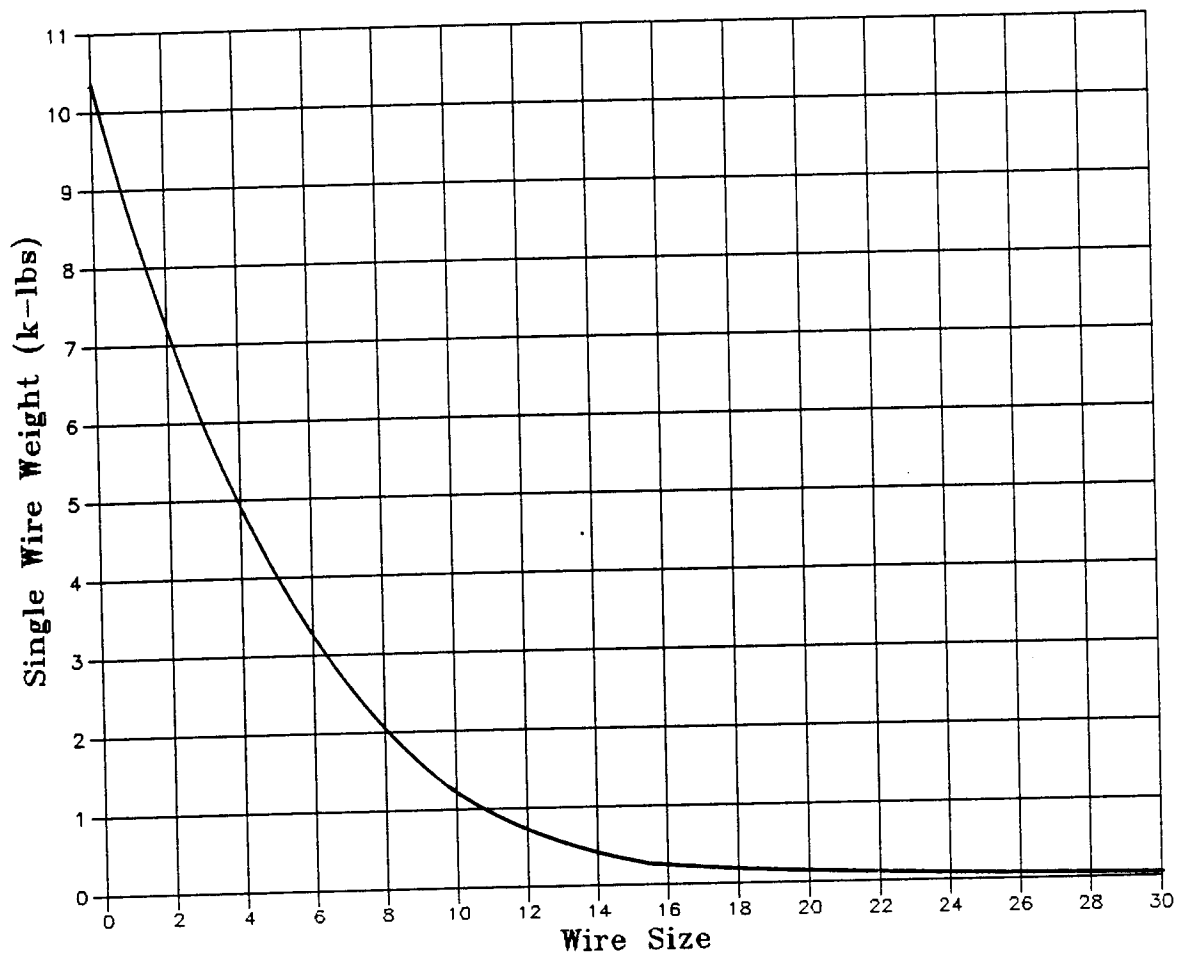


Figure 1.1.1.5-8  
Tether Weight Versus Wire Size (1 Wire 10 Km)

# Final Report - Volume II - Study Results

Component	Weight Penalty (kg)		Cost Delta (\$K)
	Free-flyer	Power Tether	
Solar Arrays	580	0	\$10,274
Power Conditioning	0	100	(\$7,839)
Tether Cable	0	850	( \$708)
Batteries	0*	0*	--
Slip Ring Assemblies	0	68	(\$1,533)
Solar Array Drives	54	0	\$4,180
Power Bus Regulation	0*	0*	--
Thermal Control	0	68	(\$1,280)
	<hr/>	<hr/>	<hr/>
Totals	634	1086	\$3,094
Transportation Wt Penalty		-452 kg	(\$2,262)
Net Savings Using a Power Tether			\$832K

\* indicates items considered equivalent in weight and cost

Table 1.1.1.5-2 Power Tether Weight and Cost Deltas

The above numbers are based on a two conductor tether using high voltage DC (4.5 kV) transmission. Power conditioning devices for the electrical power tether assume electronic implementation of the conversion from Space Station source voltage and frequency to DC and back again at the platform. The batteries are considered equivalent for the two systems since the platform will need survival power in case of a tether break or problems with the Space Station source. Similarly both approaches will need power bus regulation for the payloads and platform subsystems. The solar array drive weights are based

on estimates of the Space Station beta joint, which will be used on the co-orbiting platforms also. Space Station cost estimates are a total of \$4.2M for the two drives required. The power tether approach is penalized in the slip ring area because of the increased complexity of a high voltage slip ring assembly. In the thermal control area additional cold plates and/or radiator area will be required to dissipate the efficiency losses of the tether power transmission system components.

The actual cost benefit of the power tether over solar arrays will depend on the relative costs of producing the solar arrays versus the power tether and the increased transportation cost for lifting the power tether system into orbit. The solar arrays proposed for a co-orbiting platform are the same as those used on the Space Station so only recurring costs have been associated with this cost. The power conditioning equipment assumed for the power tether does not exist in space qualified form so a development program would be necessary for this equipment as well as the tether itself.

The cost estimates above were produced using the PRICE cost modeling program and the given marginal weights listed in Table 1.1.1.5-2 above. Note that these costs do not represent the total cost of the components, but only the marginal costs associated with increased requirements of the particular approach. For instance, both systems will need slip ring assemblies, but the power tether is assessed a marginal weight because of the increased complexity of high voltage slip ring assemblies. In some cases the weight indicates the total estimated weight (i.e. solar arrays) if the component is unique to one of the approaches.

The cost advantage of using a power tether is quite small (\$832k) when compared to the uncertainties and risks associated with developing a power tether system. Several areas were difficult to address effectively in this study that could severely impact the cost estimate of the power tether

approach. One area is micrometeoroid protection for the power cable. A study of the application of nuclear power using tethers<sup>10</sup> indicates that a significant mass may be necessary to shield high voltage lines from micrometeoroids. The system examined in this article has a tether conductor weight of 330 kg/km for a design voltage of 4.5 kV including 3 conductors for redundancy and a micrometeoroid shield. This system has an estimated survival probability of .992 for a 10 year mission. This system or even a scaled down version would quickly make the electrical tether impractical. Therefore, the power tether will need a much more detailed study before it can be recommended as an alternative to standard solar arrays.

#### 1.1.2 TETHER DEPLOYER DESIGN

A system to deploy, retrieve, and control a tethered platform has been designed. Two systems will be mounted on the Space Station structure. The hardware and design requirements are identical for both a +Z and -Z tether (zenith looking and nadir looking). The major design requirements are listed below.

1. Minimize impact on Space Station interfacing (minimize special interface hardware).
2. Minimize imparting tether dynamic effects onto Space Station.
3. Power to retrieve tether will be supplied by the Space Station.
4. Power generated during tether deployment will be dissipated by the deployer.
5. Hardware elements are to be shuttle transportable and require minimal on-orbit assembly.
6. Designed to accommodate a reel containing 10 km of tether with a 10 mm diameter.

-----

<sup>10</sup>Bents, D.J.: "Tethered Nuclear Power For The Space Station", Proceedings of the 20th Intersociety Energy Conversion Engineering Conference, SAE, pp 1.210 thru 1.227, August 1985

Figures 1.1.2-1 thru 1.1.2-4 show that the deployer system consists of a carrier structure containing the reel, drive system, and tether level wind control. The second major element is the TAPPS (Tether Alignment and Platform Positioning System) mechanism for aligning the tether tension force through the Space Station CG to minimize the tether's effect on the Space Station.

#### 1.1.2.1 CARRIER

The reel carrier is based on an existing design that has been fabricated and qualified for the BASD CRRES spacecraft program. The carrier structure is essentially unchanged except for the deck where the tether hardware is mounted. The carrier is constructed from 10 cm (4 inch) aluminum honeycomb panels with internal bracing and is capable of carrying a 6590 kg (14,500 lb.) payload in addition to its own 1500 kg (3,300 lb.) weight. The carrier interfaces directly into the cargo bay using 4 longeron trunnions and one keel trunnion. Fittings on the Space Station truss would be required to accept the carrier. The carrier attaches to the Space Station truss at three points. The truss diagonal used for receiving the carrier keel fitting requires additional support to increase its stiffness as shown in the figures. All of these modifications needed to support the carrier would be EVA bolt-on operations and would not require any changes to the primary Space Station structure itself.

#### 1.1.2.2 REEL DRIVE COMPONENTS

The reel drive components consist of the tether and reel, level wind, and drive system. The reel is fabricated from a hollow steel shaft and aluminum flanges capable of supporting 10 km of 10 mm diameter tether. The drive system consists of a motor/generator, gearbox, clutch, brake, and chain drive to couple with the level wind mechanism.

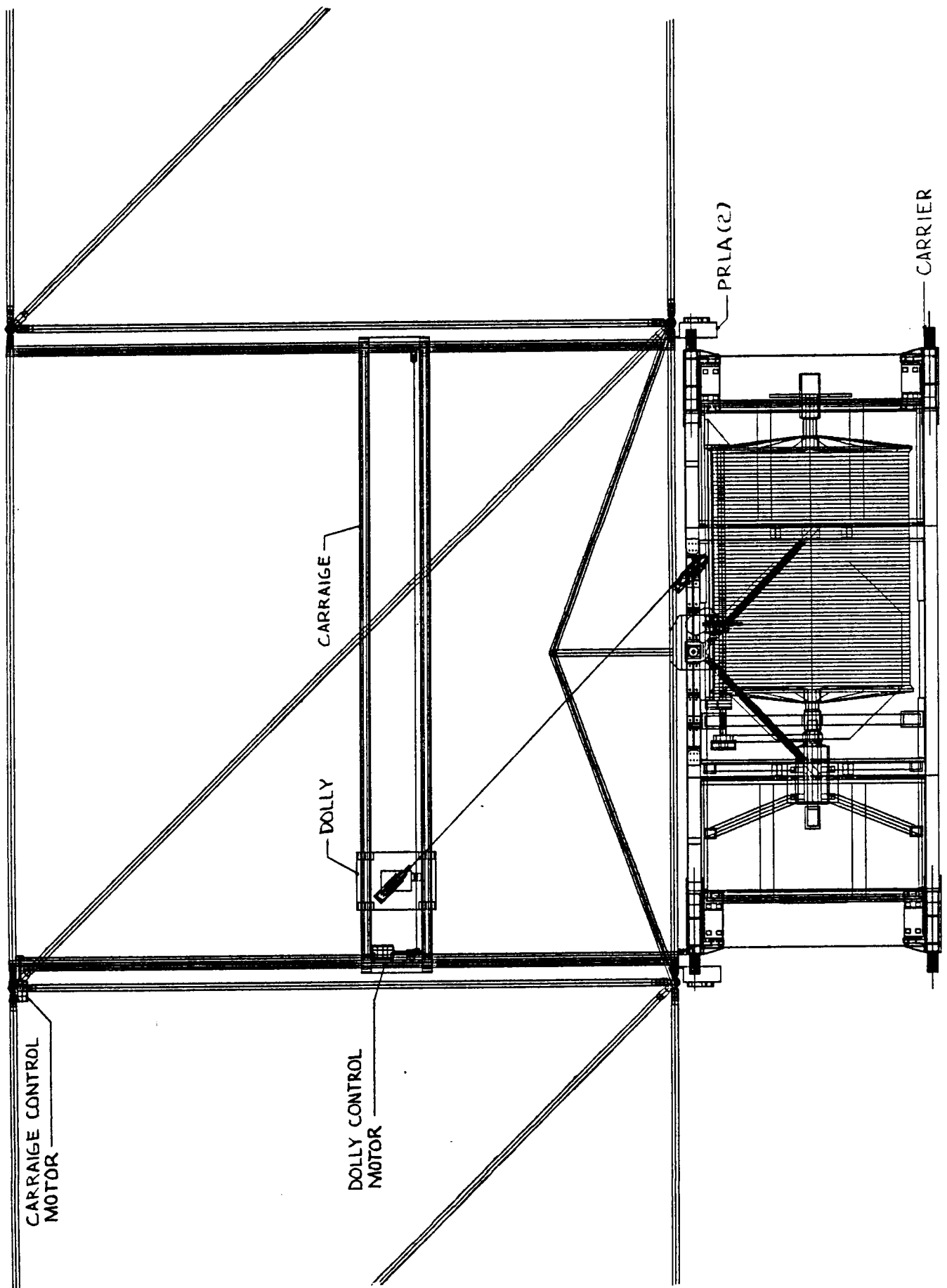


Figure 1.1.2-1 Tether Deployer - Top View

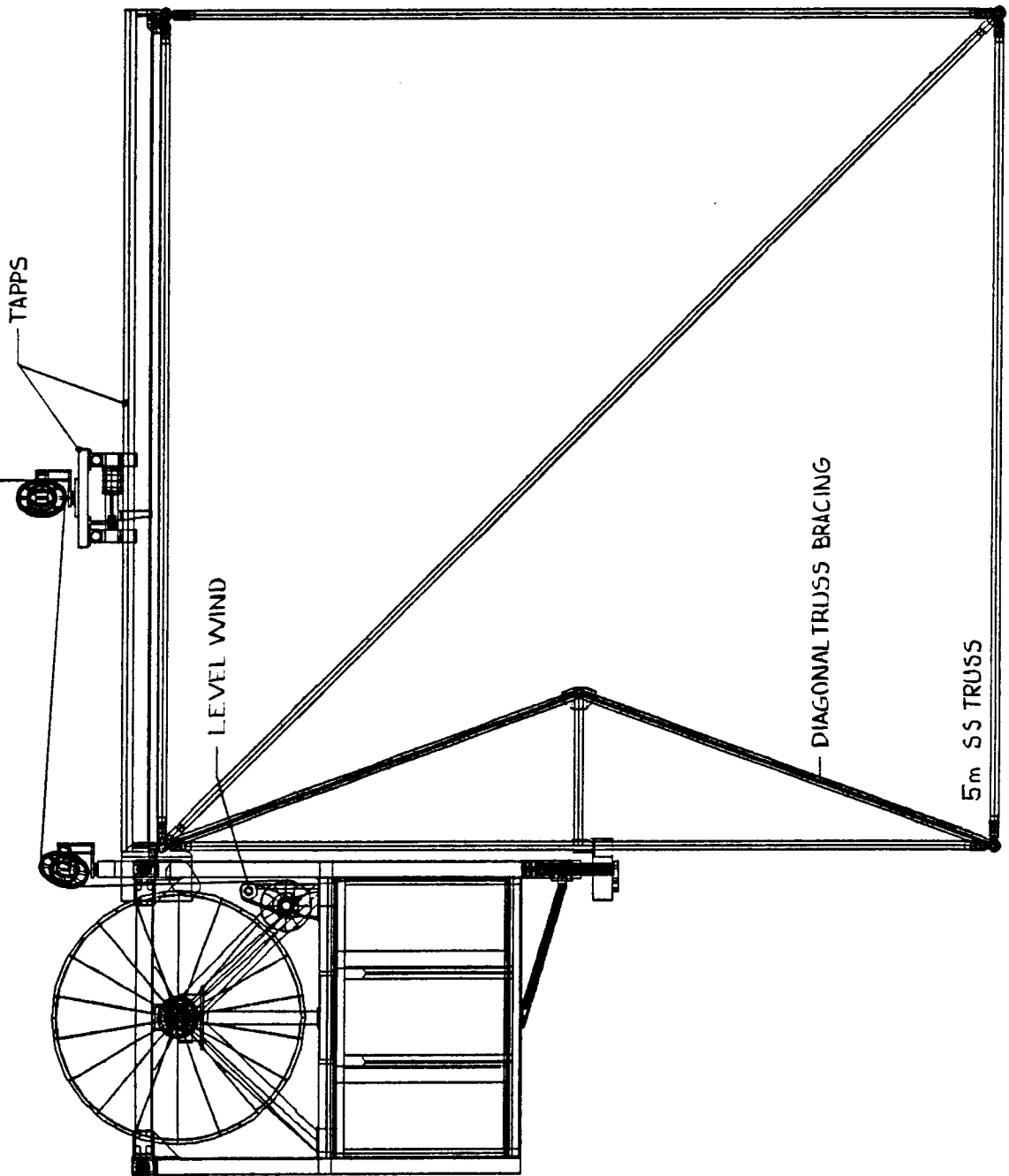
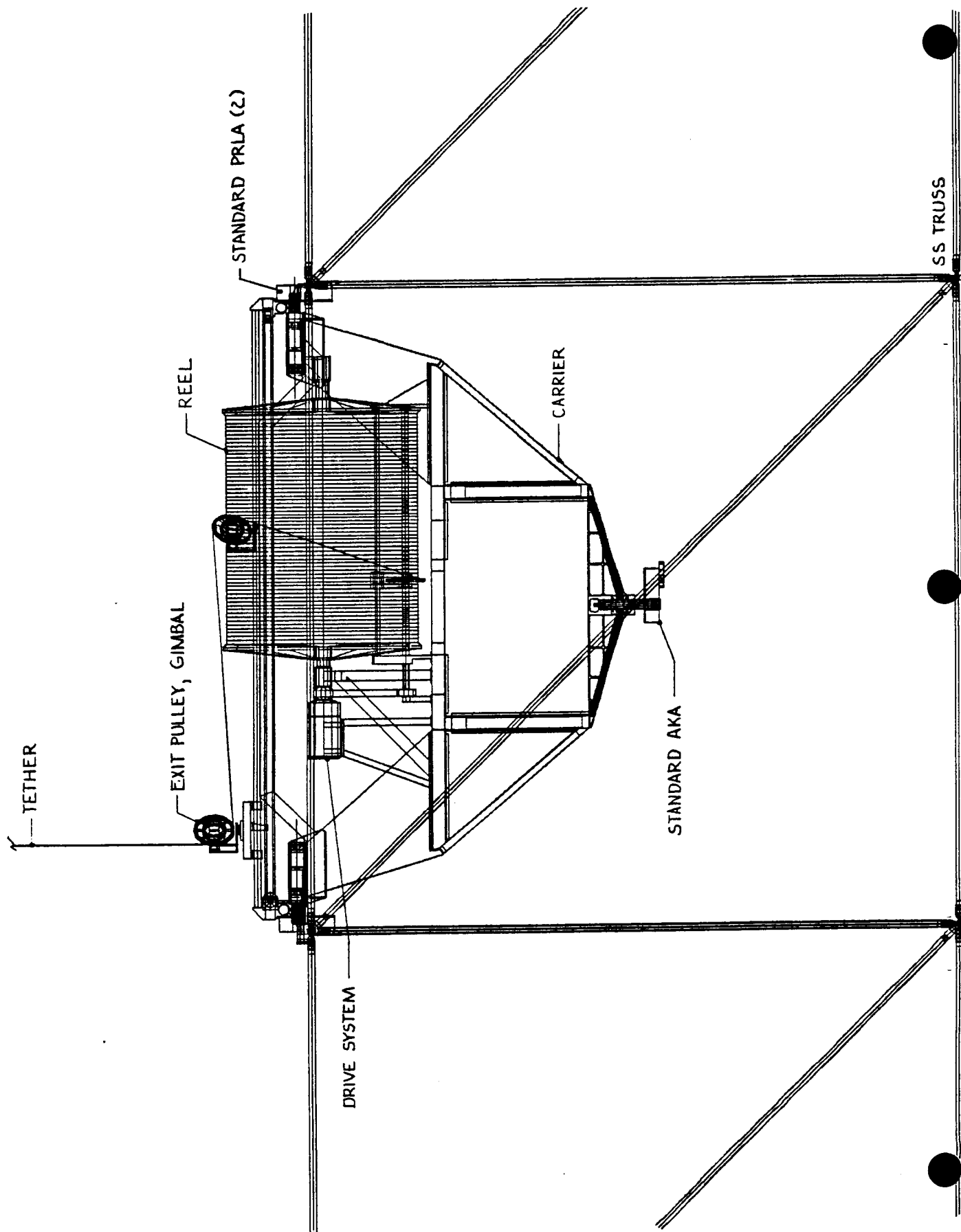


Figure 1.1.2-2 Tether Deployer - Side View

Figure 1.1.2-3 Tether Deployer - Front View





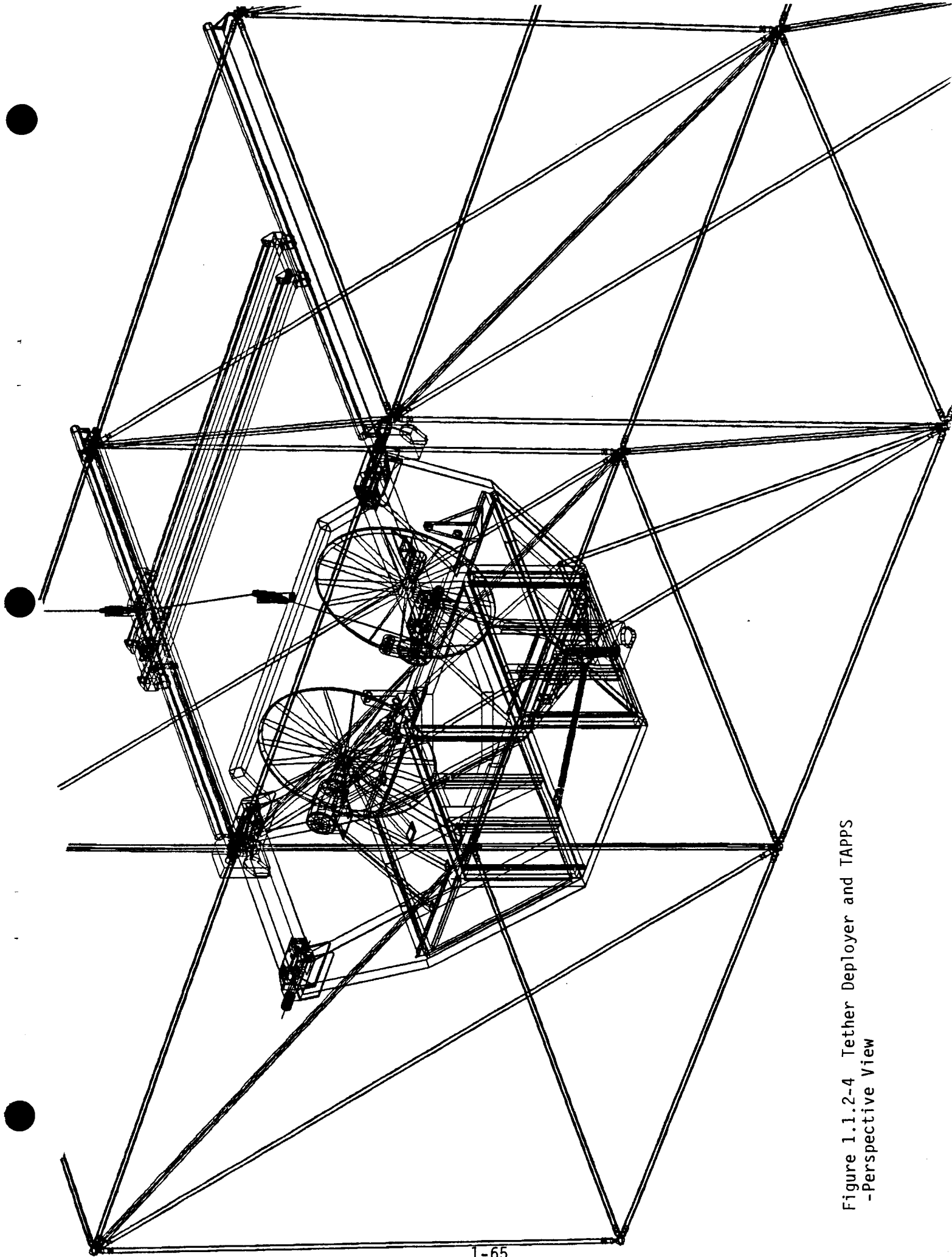


Figure 1.1.2-4 Tether Deployer and TAPPS  
-Perspective View

#### 1.1.2.3 TAPPS MECHANISM

The TAPPS is a large X-Y translator mechanism that occupies the entire truss bay face adjacent to the carrier. Its sole purpose is to locate the position that the tether pays off from the exit pulley so that the tether tension force will always be aligned through the CG of the Space Station when the latter is horizontal. Due to the dynamics of the tether and perturbations on the SS the TAPPS will include a closed-loop control system. Payload manifesting on the SS, orbiter presence, fuel usage, and tether swing dictate that the TAPPS accommodate a CG shift as large as possible and so the 5m x 5m (16.5 ft x 16.5 ft) area is baselined. The components consist of a small dolly mounted on rails onto a carriage that is also mounted on a set of perpendicular rails. The dolly contains the gimballed tether exit pulley which allows the x direction of motion along the carriage. The x position is controlled by a cable driven motor and encoder. The Y positioning is controlled by locating the carriage along the main rails that attach to the SS truss nodes. The carriage position is also controlled by a cable driven motor and encoder. The rails are fabricated from hollow steel tubes to attain the necessary stiffness. The sliding motion is attained by using linear motion ball bushing bearings in 8 locations.

#### 1.1.2.4 POWER, C&DH, AND THERMAL

Electrical power to run the tether deployer will be obtained from the standard Space Station power bus. Command and Data Handling functions will similarly be implemented by tying into the Space Station Command and Data Handling bus.

For the Thermal Control Subsystem radiator lamps will be used to dissipate the energy of Platform deployment while conventional cold plates will be used to dissipate the waste energy from electrical systems and mechanisms.

### 1.1.3 MISSION OPERATIONS

The mission operations flow from installation of the deployer on the Space Station and checkout through deployment of both the platform and dummy masses is shown in Figure 1.1.3-1. The associated timeline is shown in Figure 1.1.3-2.

Several methods for deployment and retrieval of the end masses were explored. These included using purely passive means, using crawlers, using Space Station propulsive power, using the Orbiter, using the OMV, using an active end effector, using Platform propulsive power, etc. The final choice was a combination scheme which uses the OMV as an escort vehicle during the close-in segments of the transfer process and passive means at other times. To do this the platform and dummy masses are both fitted with appropriate grapple fixtures used for temporary OMV attachment. OMV thrusters are used for initial separation and final docking maneuvers during deployment and retrieval for convenience, expediency, and safety. Tether back tension during these phases is maintained just low enough to prevent slackness. This is actually a conservative approach; the whole operation could probably be accomplished without an OMV since there will always be some low level of starting/finishing back tension by virtue of the distance of both the top and bottom keels from the Space Station center of mass.

During other portions of the deployment and retrieval sufficient tether tension exists to support both the platform and dummy masses. The deployer control system will dampen any libration build-up that occurs. Should a single tether system be implemented the operations flow relative to the dummy mass is deleted.

Figure 1.1.3 - 1  
Installation & Operational Sequence For  
Tether Deployer System

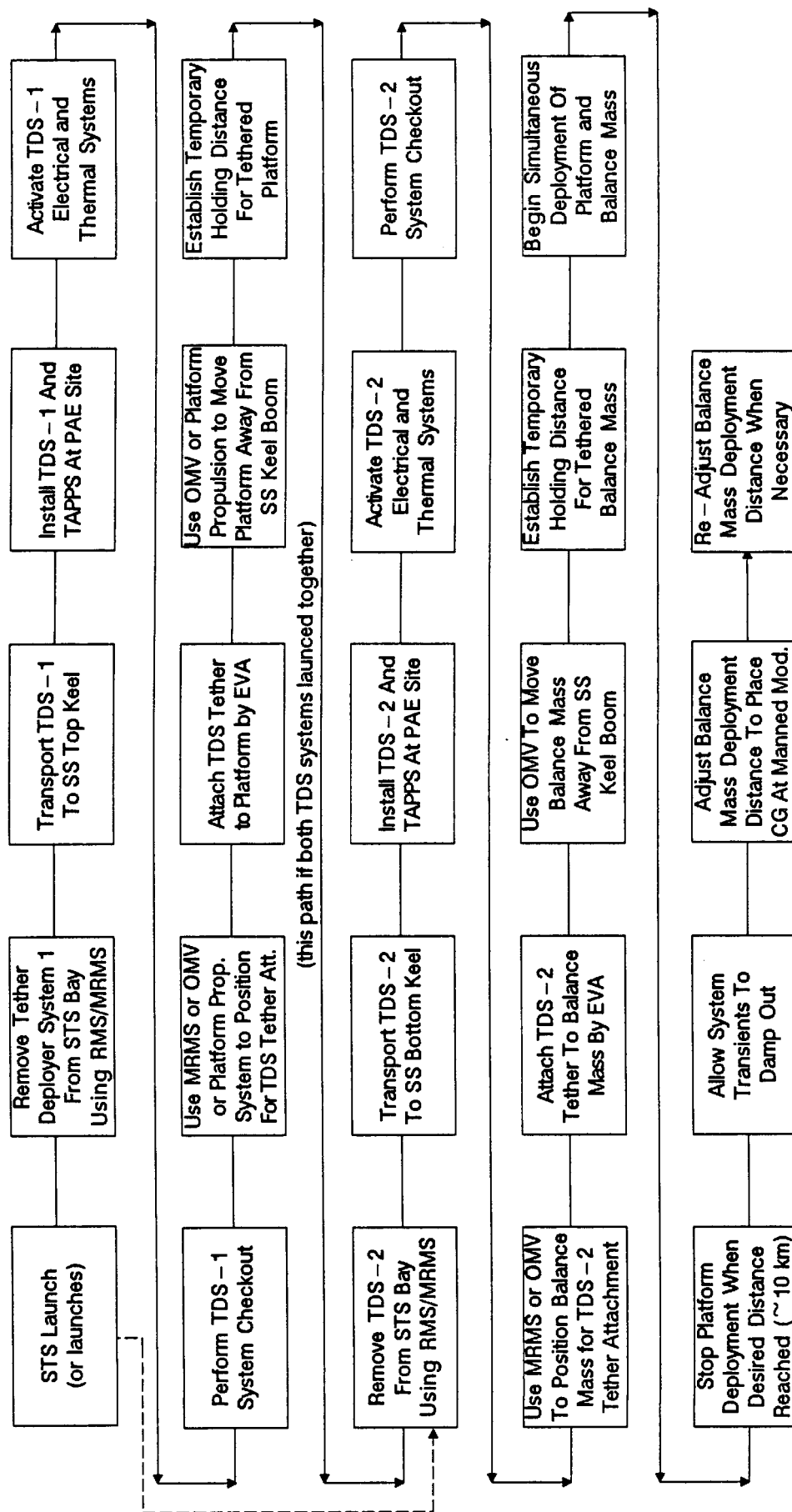
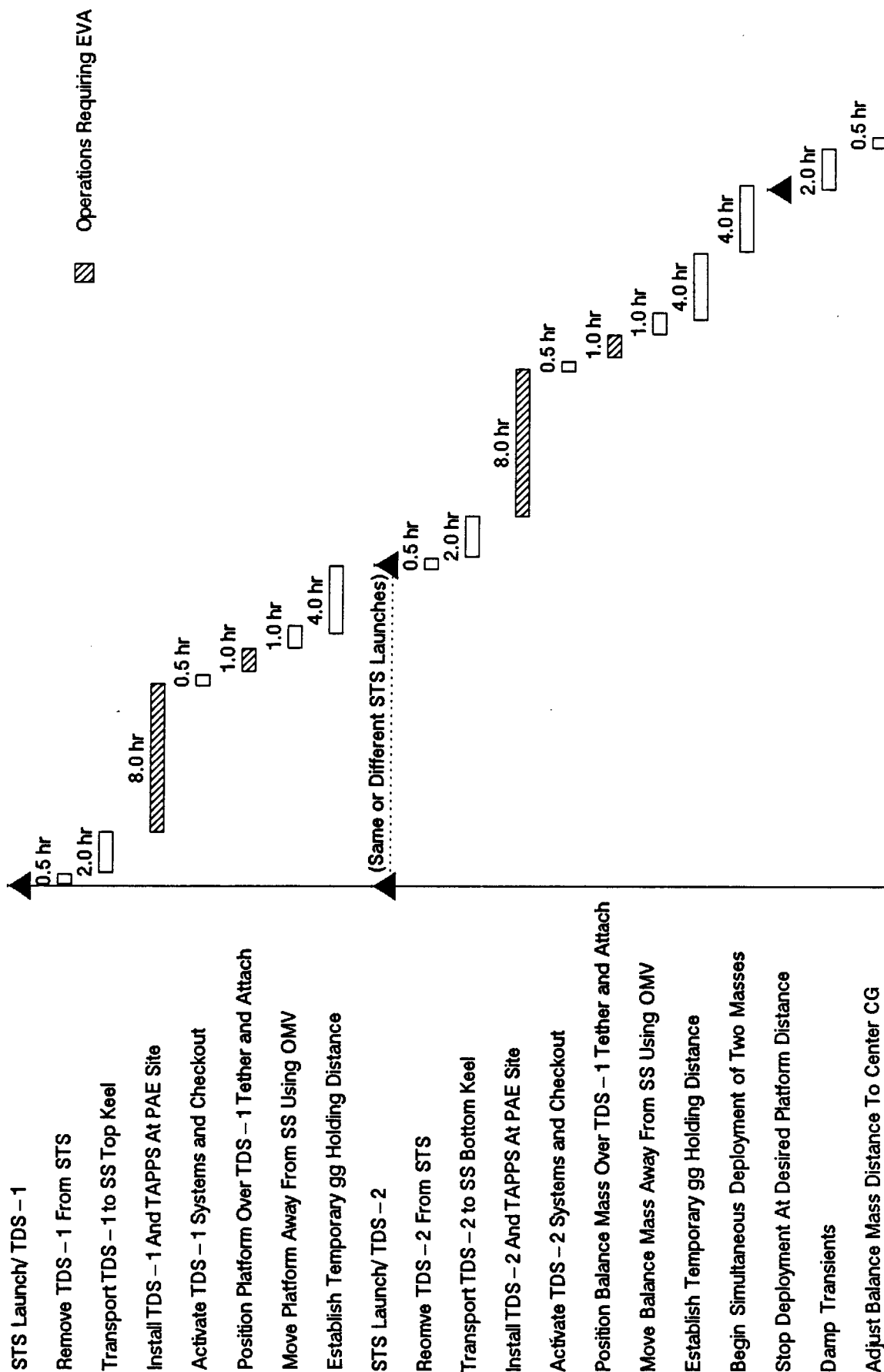


Figure 1.1.3-2  
Installation & Operational Timeline For  
Tether Deployer System



Simulations of the tether dynamics indicate that another deployment sequence could use the naturally existing gravity gradient forces to deploy and retrieve the platform without external aid from the OMV.<sup>11</sup> This approach needs further analysis to access the safety aspects of this approach.

The installation and checkout of the deployer systems occur as is shown in Figures 1.1.3-1 and 1.1.3-2. When the tether needs replacement the entire tether deployment system will be returned to Earth by the Shuttle. Although this is not cost effective from a weight to orbit standpoint it does simplify maintenance procedures which will be important during the initial phase of Space Station operation.

#### 1.1.4 TETHERED PLATFORM COST ANALYSIS SUMMARY

A cost analysis for the Tether Deployer System was performed using the RCA PRICE cost modeling system and a Lotus-123 based LCC model. A summary of the results of this analysis is presented in Table 1.1.4-1. Details of this cost effort are presented in the separate cost document accompanying the study report (DR-6 Sections 2-16 thru 2-20 and its Appendices).

Table 1.1.4-1 Tether Deployer System Costs (Constant 1987 Dollars)

Hardware Design and Development Cost	\$ 22,244,000
Hardware Production Cost	\$ 25,224,000
Operations and Support Cost	\$ 64,514,168*
Software Cost	\$ 2,102,500
	<hr/>
Total Tether Deployer Cost	\$114,084,668

\*Note: STS Launch Costs are \$30,506,215

-----

11 "Tether Applications in Space Dynamics and Control Systems Analysis",  
Control Dynamics Company, Huntsville, AL, October, 1986.

# SUMMARY TABLE PLATFORM TETHER DEPLOYER

PHYSICAL CHARACTERISTICS	QUANTITY OR DESCRIPTION
Science Platform Reference	
Mass	o 15,000 kg
Standoff Distance	o 10 km vertical
Subsystems (Elec., Comm., Prop. <sup>(1)</sup> , C&DH, AD&C., etc.)	o Integral
Power Capability	o 10,000 watts via solar arrays
Dummy Mass Reference	o 15,000 kg nominal
Tether Deployer	o 2 (to maintain Space Station CG control)
Shuttle Carrier	o CRRES cradle design
Reel Drive Components	o Reel (up to 10 km, 10 mm tether), level wind, drive control system and TAPPS (CG positioner)
Nominal Tether Diameter	o 2 1/2 mm for 15,000 kg platform
Power and C&DH Requirements	o Via standard Space Station service
OPERATIONAL CHARACTERISTICS	
	o MRMS transfer to SS from STS
	o Platform deployer installed on top keel
	o Dummy mass deployer installed on lower keel
SPECIAL TETHER BENEFITS	
	o Constant standoff distance
	o Less fuel required
	o SS CG control accommodated
COST BENEFITS	
Dual Tether System Costs	Table 1.1.4-1
TOTAL	\$114,084,668
Free-Flyer Platform Costs	
Fuel Transportation (3)	\$414,000,000
Stationkeeping Operations	TBD
TOTAL	TBD

## FOOTNOTES:

- (1) Included in case of tether break
- (2) Includes a KITE system if inertial pointers are to be accommodated
- (3) Based on average annual fuel consumption for stationkeeping of 8250 kg

1.2 TETHER CRAWLER

A review of possible missions for a crawler resulted in several observations about what a crawler might be used for. First, using a crawler as a method of moving consummables or replacement equipment or payloads between the Space Station and a tethered platform appears to be extremely complex. This is because some type of robotics would be required for the replacement of payloads, equipment or consummables at the platform if it was unmanned. The only way to avoid the robotics requirement is to locate all the interfaces very close to the tether attach point and use 'hard' docking to make the replacements. However, this would likely interfere with the tether attitude control system (KITE) and probably require dual remote interfaces, one on the crawler and one on the platform.

A second identified use of a tether crawler is as a base for a variety of experiment types that have requirements that can be met by the crawler. These 'special' requirements apply mainly to a variable g level capability, proximity operations conducted about the Space Station, and to measurements to be performed at various altitudes. No one experiment type has a sufficient experiment base identified to justify the development of a crawler, however, a generic tether crawler bus that could accommodate a variety of these experiments would be useful and desirable. Some possible experiment types are micro-gravity, contamination, and plasma measurements.

A third use of a tether crawler that has considerable merit is as a Space Station CG control device. The CG of the Space Station will undergo significant shifts due to payload arrangement, consummables movement, servicing activities, growth and STS dockings. These shifts will effect the magnitude of the micro-g environment on the Space Station and a CG management system would be beneficial.

Based on the above observations we have decided to approach the crawler design as consisting of a bus that can satisfy many experiment objectives.



## Final Report - Volume II - Study Results

Based on the requirements from the Space Station Mission Requirements Database (MRDB) and other sources, the following Crawler design parameters were used for crawler design.

### - Power

Solar arrays will provide approximately 2000 watts on an orbital average basis. This is based on a large number of micro-g experiments with power requirements in the 500 to 1800 watt area and 200 watts for crawler subsystem use. The arrays will be oriented in yaw about the tether line for increased efficiency. The ascent phase is also based upon this same 2000 watt capability.

### - Weight

Target weight of about 2000 kg including payload. MRDB experiments have typical weights of 100 to 1800 kg for the size that might be used on a crawler.

### - Drive

Based on earlier design work we will use a friction wheel and electric motor approach for the drive mechanism. The system will be designed to allow easy mounting and removal of the crawler from the tether.

### - Thermal Control

Passive cooling for crawler subsystems and payload for tether operations. Active control through the Space Station ATCS when attached to a regular payload attachment port. High temperature radiator lamps for dissipating deployment energy of crawler system and excess solar array power.

- Communications and Data Handling

A high data rate RF link for communications with the Space Station. The data rate has not been determined yet, but may be as high as 20 Mbps to accommodate some materials processing requirements for optical monitoring of experiments.

- Attitude Control

A momentum wheel will be used to control the crawler yaw motion. The yaw direction will be constantly and automatically adjusted to place the solar array normal vector in the plane defined by the sun line and local vertical. A pair of sun sensors is used in the control loop to determine direction (which is not to be of a high accuracy for this purpose). A cold gas thruster system will be used to de-saturate the wheel.

- Deployment and Retrieval Dynamics

As the Crawler will be deployed and retrieved along a previously deployed static tether line (see Mission Operations Section), the dynamics effects related to such operations are expected to be quite benign. An analysis related to Crawler transfer dynamics is presented in Appendix B of this report.

1.2.1 CRAWLER DESIGN COST DRIVERS

Our Crawler design has incorporated most of the subsystems associated with a free-flying satellite. In addition, the design has had to incorporate some forms of remateable attachment mechanisms not normally associated with free flyers. The latter include mechanisms to attach the tether to the crawler plus adjust the line of force laterally at both top and bottom positions. These are necessary to adjust for an arbitrary payload mass torques about one

Crawler geometric axis. Actually, it can be shown that only one such lateral adjust mechanism is required to maintain the system in a horizontal orientation. However, in this case tether position must be continuously adjusted to account for varying tether tension, or effectively the deployment distance. This seems unduly complicated and so we adopted the dual mechanism design. In any case, differential solar array length is used for orientation control about the second principal Crawler axis.

Other mechanisms include those needed to attach/detach the payload to the Crawler and the Crawler to the Space Station for berthing. The first device incorporates capabilities for both electrical and fluid transfer.

A dominating factor which had to be addressed concerns the need to supply the large amounts of electrical power needed for the various experiments. We have baselined this requirement at an orbital average of 2 kW which represents a practical minimum capability in light of the envisioned experiments. For an array which provides a nominal power of 108 watts/m<sup>2</sup> (10 watts/ft<sup>2</sup>) under normal illumination, after accounting for the various orbital geometric factors an array area of between 32 and 102 m<sup>2</sup> (350 and 1100 ft<sup>2</sup>) must be provided depending upon the pointing control scheme selected. Hence, 42 m<sup>2</sup> solar array was chosen as the design point from a practicality view point. However, as a cost driver the effect upon other subsystems, especially the attitude control system was not inconsequential.

#### 1.2.2 CRAWLER DESIGN AND DYNAMICS

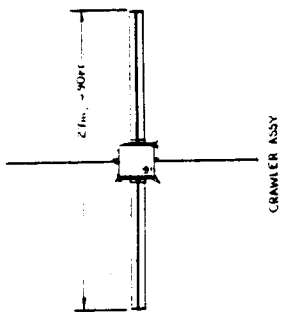
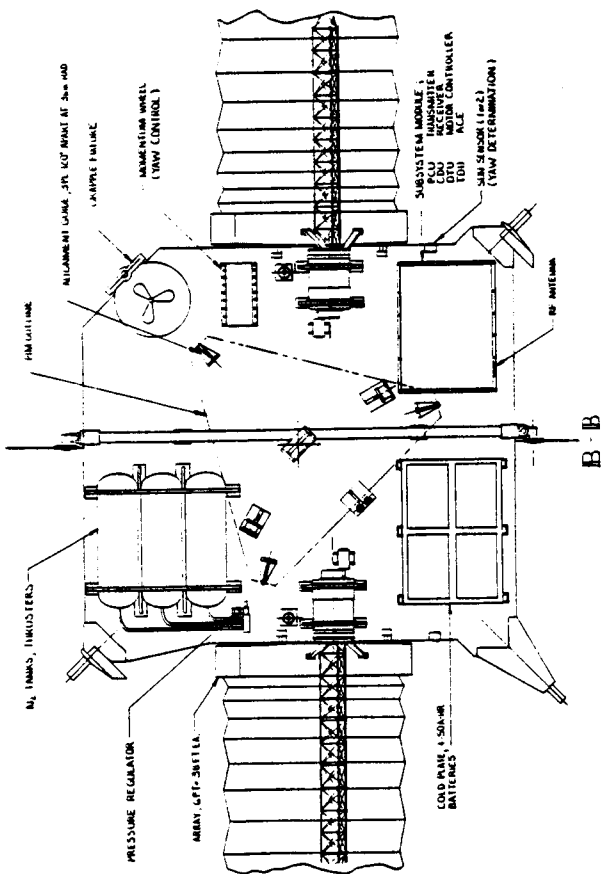
The Crawler is an independent hardware element used to locate or move a payload (instrument, experiment modules, etc.) along a tether that has been deployed from the Space Station. The Crawler has been designed to meet the following set of requirements;

## Final Report - Volume II - Study Results

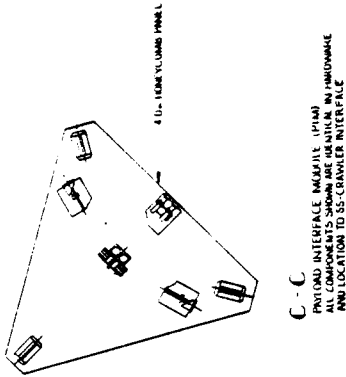
1. Contain its own power source for retrieval back to Space Station
2. Capable of accommodating a payload of 1000 kg., roughly 3m x 3m x 3m in size, and requiring 1800 watt of continuous power.
3. Capable of being placed on and removed from a previously deployed tether. (Cannot require 'threading' of tether through crawler drive system.)
4. Capable of accommodating payloads of various sizes and CG locations while still maintaining the crawler-payload CG through the line of action of the tether. (To eliminate Crawler pitch offsets during operations as well as pitch motion during acceleration and deceleration.)
5. Capable of interfacing directly into the Shuttle cargo bay (no on-orbit assembly required, no FSE required).
6. Capable of interfacing directly with the Space Station at any standard payload location (for storage).
7. Payload interface to be identical to Space Station interface (allows payload to be also mounted on Space Station and be provided with full electrical and cooling fluid services).
8. Solar Arrays to be adjustable to any arbitrary length and to be remotely stowable and deployable (for Space Station proximity operations).
9. Provide MRMS (Mobile Remote Manipulator System) interface and tether guides (to facilitate placement-on and removal-from tether, eliminating any EVA requirement).
10. Provide closed-loop yaw control (to keep system stable during movement, accommodate potential experiment pointing and low-g requirements, and point arrays as needed).
11. Capable of a one year mission lifetime (between resupply, payload exchange).

The baseline design relative to the above is shown in Figure 1.2.2-1. A standard Space Station Payload Interface Adapter (PIA) is employed, consisting mainly of a 12.7 cm (5 in.) thick honeycomb panel with trunnions for mounting in the shuttle, and actuators for mechanical, electrical, and fluid interfaces onto the Space Station. Folding type solar arrays are added to provide subsystem and experiment power and resupply power for the drive

### Figure 1.2.2-1 Crawler Design

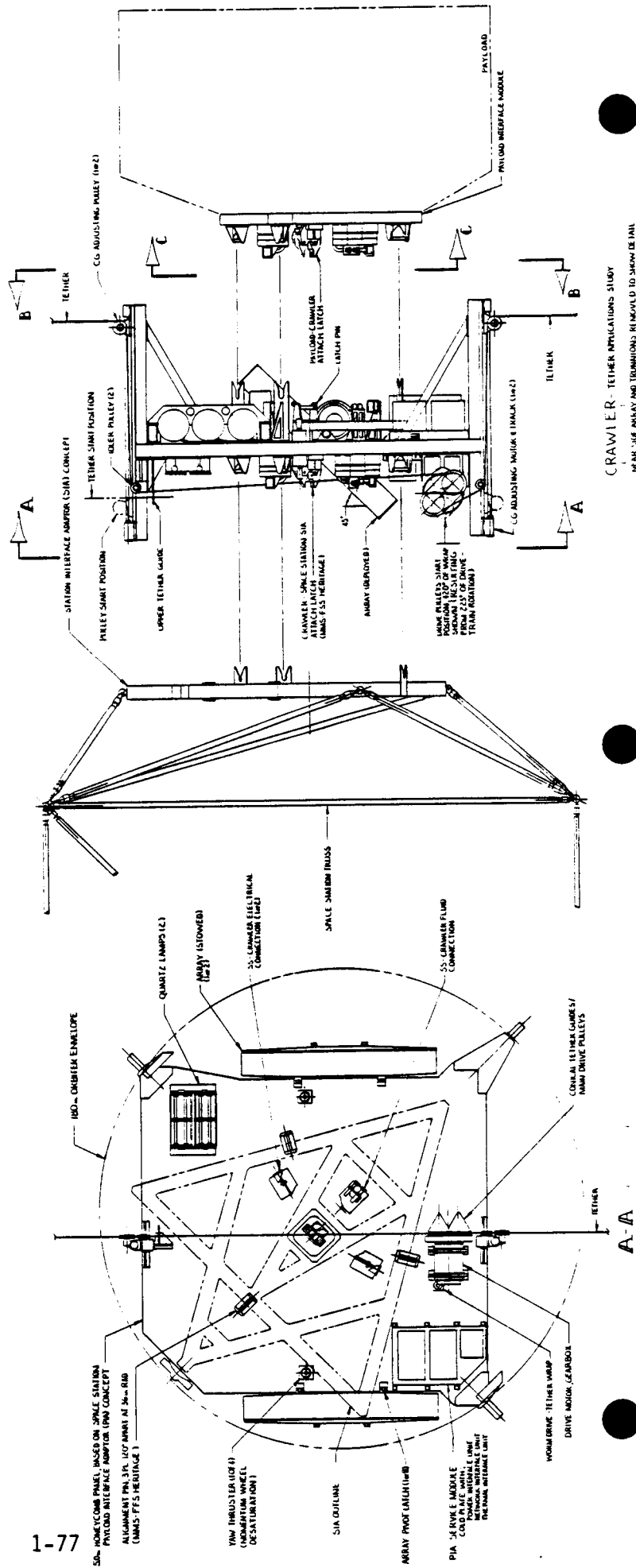


ORIGINAL PAGE IS  
OF POOR QUALITY



2-2

PROTOD INTERFACE MODULE (PIM)  
ALL COMPONENTS SHOWN ARE IDENTICAL IN HARKOVAK  
AND LOCATION TO SS-CRAWLER INTERFACE



CRAWLER - TETHER APPLICATIONS STUDY  
NEAR SIDE AWAY AND TRANSITIONS REMOVED TO SHOW DETAIL  
AKG 86.

system batteries. The arrays are mounted equidistant from the tether for balance, thus requiring the asymmetric notch in the PIA panel. Along with the motors required for actuating the array panel booms, each array also requires a motor to pivot the array  $45^{\circ}$  for more effective power generation. Subsequently each array also requires latches to secure the array during launch and servicing.

The tether drive system is mounted on the Space Station interface side of the crawler to allow the crawler to be placed on the tether with a payload already interfaced onto the crawler. The MRMS, used to transfer the integrated crawler from the Space Station to the tether, interfaces with the crawler grapple fixture. The drive system incorporates guides at either end of the structure to allow placement on the tether within the MRMS positioning accuracies. The upper guide is a simple 'Y' guide. The lower guides are incorporated onto the main drive pulleys. The guides are shaped to accommodate the pulley rotation. Once the crawler is placed on the tether, the two CG adjusting pulleys on the tracks can be activated to a predetermined (payload peculiar) position to align the tether tension through the CG of the crawler and at right angles to the adjustment track. Once the CG pulleys have set the crawler 'into' the tether, the drive pulley assembly is rotated  $225^{\circ}$  to provide about  $420^{\circ}$  of tether wrap around the drive pulleys. This wrap provides the friction needed to accelerate the crawler initially and to brake and hold the crawler at positions along the tether. Quartz lamps are used to dissipate the energy created as the main drive motor, used as a generator, brakes the crawler accelerated by gravity gradient forces.

The Crawler-Space Station interface is identical to the proposed PIA-Space Station interface. This allows the crawler to be berthed to the Space Station at any standard payload location and receive full services across the interface. The hardware is based on the MMS spacecraft FSS (Flight Support System) demonstrated on the SMM spacecraft repair mission. The mechanical interface is accomplished with a single FSS berthing latch at the center of a

3 point pin and guide arrangement symmetrically positioned at a 36 in. radius from the latch. Redundant electrical connectors, also of FSS heritage, are activated once the latch is set. The fluid umbilical to interface with the Space Station cooling loop can be activated if required. The Payload-Crawler interface is identical to the Space Station-Crawler interface. This allows the Crawler payload to be berthed to the Space Station while receiving full services as would any other Space Station experiment. The payload interface is standardized by having all users mount to a PIM (Payload Interface Module) that contains the interface hardware on one face and a flat deck for the payload on the other face.

Yaw control (rotation about the tether axis) needed for solar array pointing (and/or coarse payload pointing) is provided by a momentum wheel whose rotation axis is parallel with the tether axis. Four thrusters are used to desaturate the momentum wheel. The cold gas system uses nitrogen stored in three cylindrical tanks, supplying enough nitrogen to cover the one year servicing requirement.

### 1.2.3 CRAWLER SUBSYSTEM DESCRIPTIONS

#### 1.2.3.1 POWER SUBSYSTEM

The following first order relations and parameter values are employed in arriving at the size of components. To simplify the design we impose the same maximum continuous load requirement of 2 kW is imposed for both the transfer and on-station phases of operation.

### Transfer Phase Expressions

$$\text{Max Total Energy } \Delta E_{\max} = 3m\omega^2 L_{\max}^2/2$$

$$\text{Max rate at max distance } L_{\max} = P_{\text{peak}}/3m\omega^2 L_{\max}$$

$$\text{Max length } L_{\max} = g[a]_{\text{gmax}}/3\omega^2$$

$L_{\max}$  is determined first, based upon achieving an on-station upper acceleration limit of at least  $[a]_{\text{gmax}}$  where the latter is measured in g's. An  $[a]_{\text{gmax}}$  of 0.1 g's is desirable. However this would be impractical as the corresponding value for  $L_{\max}$  is about 270 km, using a 500 km  $\omega$  of 0.0011 rad/sec. We choose an  $L_{\max}$  of 100 km (somewhat arbitrarily) which gives  $[a]_{\text{gmax}} = 0.037$  g's. With a peak power limit at 100 km of 2 kW and a crawler-payload combination mass of 2000 kg,  $L_{\max}$  is 2.7 m/sec and  $\Delta E_{\max}$  is 37 MJ from the above. One way trip time at a constant velocity of 2.7 m/sec would therefore be 10.3 hours or one and a quarter shifts. Actually, the one way trip time could probably be less than one crew shift even for a unidirectional uncontrolled retrieval, due to the inherently benign nature of crawler dynamics.

### Solar Array Sizing

Several types of arrays and drive schemes were investigated in an effort to minimize total array area which, because of the continuous 2 kW load requirement, must be of an appreciable area in any case.

Clearly, the most efficient array from an energy standpoint is one whose area normal vector is continuously parallel to the instantaneous sun line. In this case both continuous yaw orientation control about the local vertical (tether) direction and continuous array cant angle control about a second orthogonal Crawler body axis is required. Here, average orbital power would



be limited only by the length of the eclipse periods. At the other extreme, a fixed array attached to a Crawler with an uncontrolled yaw orientation is probably least efficient since the cant angle of such an array must necessarily be restricted to zero degrees (i.e. area normal is parallel to local vertical) in order to accommodate higher solar beta angle situations.

A third class of arrays affording an intermediate performance and the one taken as baseline, uses a fixed cant array together with a Crawler, which is continuously oriented to the most favorable yaw angle about the tether using a momentum wheel. The most favorable yaw orientation angle is the one which places the array normal vector in the plane defined by the local vertical and sunline directions.

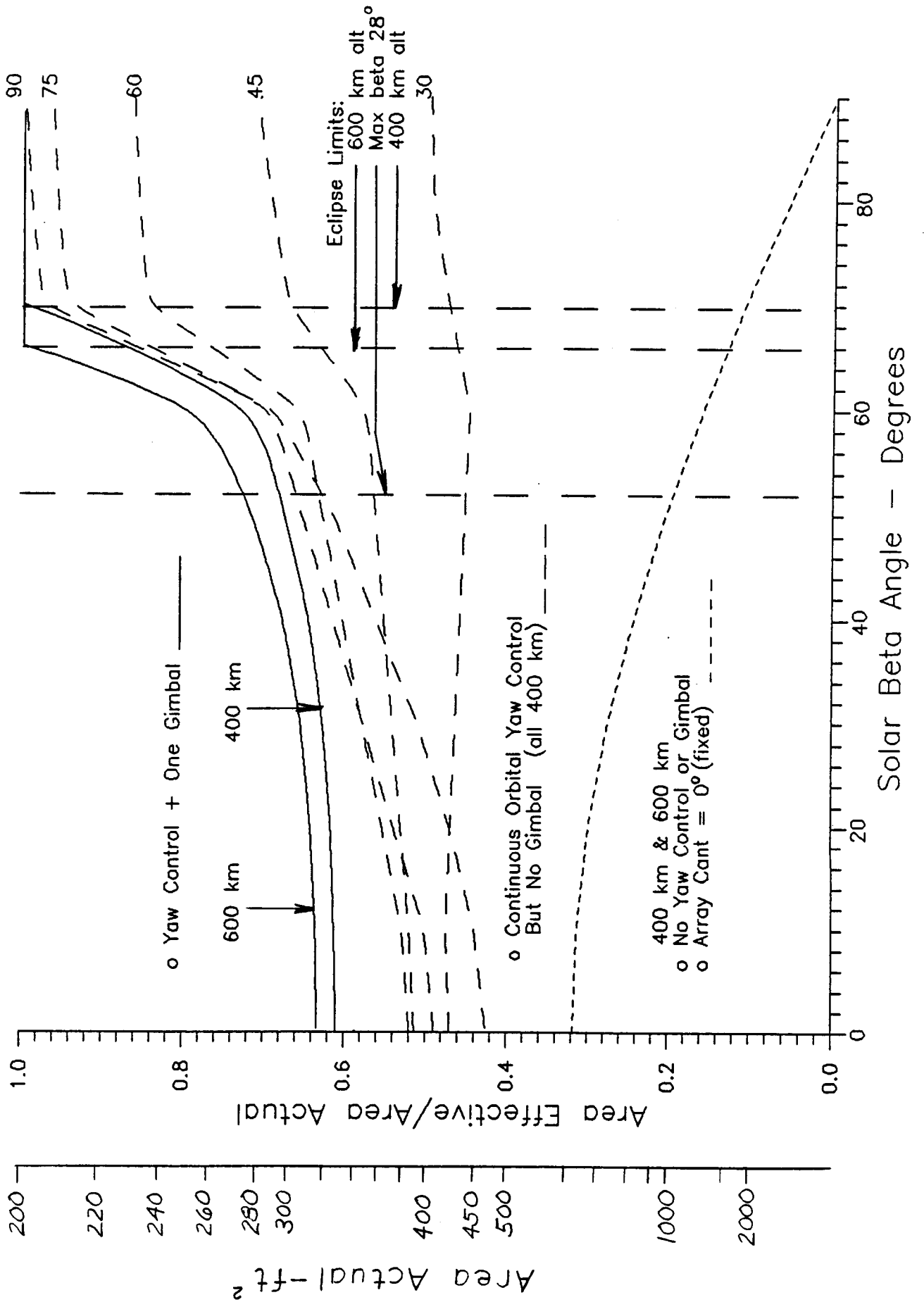
Other types of array configurations, including ones using fixed yaw position with variable cant angle capability, ones consisting of multiple panels, etc., were also considered. However, none of these appeared to offer any overall advantages to the one baselined. It is noteworthy that all forms of arrays considered required some form of yaw control, either stationary or moving, if an area of enormous proportions was to be avoided.

Relative performance with respect to the three previously described principal array designs is illustrated in Figure 1.2.3.1-1 as a function of solar beta angle. Both effective area, which is a function of eclipse duration plus non-optimal pointing, and required actual area are indicated. For a 500 km Space Station orbit Crawler eclipses can occur out to beta angles of about  $66^{\circ}$  to  $71^{\circ}$  depending upon whether the Crawler at 100 km distance is deployed up or down as shown. For a  $28.5^{\circ}$  Space Station Orbit, wherein the maximum beta angle cannot exceed  $52^{\circ}$ , the implication is that a significant portion of all Crawler orbit revolutions will be eclipsed also as shown.

From Figure 1.2.3.1-1, a baseline fixed array cant angle of  $45^{\circ}$  was chosen (See dashed curves) which yields an effective orbital average array area of just over 50% at a beta angle of zero degrees together with an essentially

Figure 1.2.3.1-1

# Crawler Array Trade-offs



flat response out to the maximum required beta angle of  $52^\circ$ . This latter characteristic simplifies the power regulation electronics as average array output is thus essentially invariant with changes in sun angle.

Assuming a conservative normally illuminated array output of  $107.6 \text{ w/m}^2$  ( $10.0 \text{ w/ft}^2$ ), a 2 kW continuous load, a 100 km downwards deployment (of the Crawler), and the additional effects of an 85% battery charge efficiency a baseline actual array area of  $41.8 \text{ m}^2$  ( $450.0 \text{ ft}^2$ ) was selected.

#### Battery Selection

During eclipse periods of the operations phase battery discharge rate at 26.4 volts would be  $2000 \text{ W}/26.4\text{V} = 75.8 \text{ A}$ . Thus, for a c/2 discharge rate, roughly 3@ 50 A-h batteries would be needed  $[(3 \times 50 \text{ A-h})/(1\text{h} \times 2) = 75\text{A}]$ .

For a 40 minute eclipse, battery depth of discharge would be  $(40 \times 75.8)/(60 \times 150) = 0.34$  which would probably be satisfactory. We, however, choose 4@50 A-h batteries as baseline which yields a c/2.6 discharge rate together with a 25% depth of discharge per cycle. At 1.1 kg/A-h this yields a battery mass of 220 kg (484 lbs).

It would probably be most convenient, though not operationally necessary, if the Crawler could return to the Space Station solely under battery power. However, this does not appear to be practical based upon a battery mass argument.

For even a 50% depth of discharge, the requirement to supply 37 MJ of energy would require a total battery capacity of  $(2 \times 37 \times 10^6)/(3600 \times 26.4) = 778.6 \text{ amp-hrs}$ , which would represent a mass of 856.5 kg. (At 25% depth of discharge battery mass climbs to 1427 kg.) Thus it is assumed that the ascent phase will be accomplished principally under solar array power with battery augmentation during eclipse periods. Since the maximum peak power requirements during ascent is also 2 kW using an L of 2.7 m/sec at  $L = 100$

km, the load at such distances, as seen by the power system closely resembles that which is required during normal operations. At closer ranges, approach speed can be increased and/or the array can be shortened and/or excess array energy can be dissipated via the quartz lamps to maintain the proper energy balance.

#### 1.2.3.2 MOMENTUM WHEEL SIZING

The yaw momentum wheel must be sized to provide angular momentum storage in an amount which corresponds to peak Crawler angular rate requirements. The wheel's torque motor must also be able to deliver yaw control torques in an amount which matches the peak angular accelerations needed to keep the solar array surface normal near the local vertical-sun line reference plane.

Pursuant to the above yaw angular rate  $d\alpha/dt$  and angular acceleration  $d^2\alpha/dt^2$  as a function of orbit anomaly  $\gamma$ , solar beta angle  $\beta$ , and orbit rate  $\omega$  were derived and are presented below without proof:

$$\frac{d\alpha}{dt} = \omega \sin\beta \cos\beta \cos\gamma / (1 - \cos^2\gamma \cos^2\beta)$$

$$\frac{d^2\alpha}{dt^2} = \omega^2 \sin\beta \cos\beta \sin\gamma (1 + \cos^2\gamma \cos^2\beta) / (r \cos^2\gamma \cos^2\beta)$$

Here when  $\gamma$  is zero the angle between the Space Station position vector and the sun line has the same values as the beta angle and is therefore at a minimum.

In the above, it can be shown that  $d\alpha/dt$  reaches a maximum when  $\gamma = 0$ , reducing the former to just

$$\left(\frac{d\alpha}{dt}\right)_{\max} = \frac{\omega}{\tan\beta}$$

The value of  $\gamma$  corresponding to maximum acceleration is

$$\cos\gamma_{\max} = [1 - 3\sec^2\beta + (1 + 8\sec^4\beta)^{\frac{1}{2}}]^{\frac{1}{2}}$$

When  $\beta$  approaches  $0^\circ$ , both  $(d\alpha/dt)_{\max}$  and  $(d^2\alpha/dt^2)_{\max}$  approach very large values. However, both angular momentum and torque requirements can be limited by simply adopting the values associated with the less stringent set of requirements of some larger value of beta at these times. This introduces only second order power production losses. If a minimum beta of say  $10^\circ$  is adopted, then the required crawler angular rate and acceleration become

$$\begin{aligned} \left(\frac{d\alpha}{dt}\right)_{\max} &= 6.28 \times 10^{-3} \text{ Rad/Sec} \quad (0.36 \text{ Deg/Sec}) \\ \left(\frac{d^2\alpha}{dt^2}\right)_{\max} &= 2.59 \times 10^{-5} \text{ Rad/Sec} \quad (1.48 \times 10^{-3} \text{ Deg/Sec}) \end{aligned}$$

Since we have computed a Crawler yaw moment of inertia equal to  $I_y = 11,240 \text{ kg-m}^2$ , this translates into wheel angular momentum and torque motor requirements of  $H = 71 \text{ N-m-sec}$  and  $T = 0.29 \text{ N-m}$ . For a momentum wheel running at a typical top speed of say 6000 RPM the peak power requirement corresponding  $\beta = 10^\circ$  and to the above torque level is 182 watts. Though this power level is not insignificant it is transitory, occurring near low  $\gamma$  values only, such that an orbital average would be just a few tens of watts. Also the peak power requirements falls-off quickly with increasing  $\beta$  angle. For example at  $\beta = 15^\circ$  instead of  $10^\circ$ , the peak requirement would drop from 182 to only 80 watts.

### 1.2.3.3 NITROGEN RCS SIZING

A nitrogen RCS system has been baselined to account for secular yaw disturbance torques which could over time saturate the yaw momentum wheel. This section estimates the amount of high pressure nitrogen gas needed to allow autonomous operation for up to one year, though it is expected that the Crawler would be serviced on a somewhat more frequent basis.

This computation is predicated upon an amount of secular drag torque equivalent to that arising from a 1/2% solar array length differential, although it is admitted that there may be other forms of disturbance torques as well. For each of two 1.8 meter (6 foot) wide array panels extending out to 12.5 meters (41 feet) this amounts to an effective differential area element of  $0.1143 \text{ m}^2$  attached to a lever arm of 12.50 m. At 400 km and an exospheric temperature of  $1200^\circ \text{ K}$  the imposed torque is thus

$$\tau = Fl = C_D \rho v^2 A l / 2 = 5.4 \times 10^{-4} \text{ N-m}$$

Since the previous argument is a characterization it will be rounded up to  $\tau = 0.001 \text{ N-m}$  as a conservative measure.

A high pressure regulated nitrogen system feeding a pair of bowtie thrusters, each acting with a center referenced lever arm of 1.4 meters is assumed. Pressure regulation is such that the exhaust to feed pressure ratio is assumed to be 0.1. The propellant  $I_{sp}$  of such a system at  $T_0 = 528^\circ \text{ R}$  is computed to be

$$I_{sp} = \left[ \frac{2\gamma}{\gamma-1} \frac{R_{N_2} T_0}{g} \left( 1 - \left( \frac{P_2}{P_1} \right)^{(\gamma-1)/\gamma} \right) \right]^{\frac{1}{2}}$$

$$= 541 \text{ N-sec/kg (55.2 lbf-sec/lbm)}$$

## Final Report - Volume II - Study Results

Each of the two thrusters forming a couple should exert a force of  $F=0.001/(2 \times 1.4)=3.6 \times 10^{-4}$  N. Thus, yearly fuel consumption is computed to be

$$\begin{aligned}\Delta m &= 2F\Delta t/I_{sp} = 2 \times 3.6 \times 10^{-4} \times 3.16 \times 10^7/541 \\ &= 42 \text{ kg/yr (92.6 lbm/yr)}\end{aligned}$$

Tank volume can be computed as follows:

Assuming that the gas is stored at 3000 psia (compressibility factor  $Z = 1.06$ ) and 293°K (68 F) its mass density would be

$$\begin{aligned}\rho &= \frac{P}{ZRT} = 3000 \times 144 \times 28/(1.06 \times 1545 \times 528) \\ &= 224.3 \text{ kg/m}^3 \quad (14.0 \text{ lbm/ft}^2)\end{aligned}$$

For a 30 cm (12 in.) diameter cylindrical tank of unspecified length its volumetric capacity per foot of length is  $\pi/4 = 0.7854$ . Thus required tank length to support a one year mission is  $92.6/(0.7854 \times 14.0) = 8.4$  ft (2.54 m). Rounded to 9.0 ft, the baseline design Nitrogen tankage calls for 3 - 1 ft. Diameter by 3 ft. long cylindrical tanks.

It should be noted that a very interesting possibility does exist which might permit flying without the nitrogen gas desaturation system altogether. This would involve using a compensating commanded solar array length differential which together with drag effects could desaturate the wheel. Since, however, such compensating torque authority might be quite small in the cases of distant upwards deployments starting from 500 km altitude, it was decided to retain the subsystem in its present form for now.

### 1.2.4 CRAWLER DEPLOYMENT AND RETRIEVAL DYNAMICS ANALYSIS

The dynamics associated with deployment and retrieval of a Crawler payload are significantly more benign than a system in which the tether itself is reeled in and out in the conventional sense. Specifically, the former system can be characterized as yielding significantly reduced in-plane equilibrium hangoff angles as well as a greatly suppressed build-up of in-plane and out-

of-plane swinging as compared to the latter system. It may in fact be possible to conduct a unidirectional Crawler retrieval profile without the use of control system design for swing suppression. This implies that significantly faster transfer scenarios might be possible, as compared to a conventional system without compromising safety.

#### 1.2.5 CRAWLER OPERATIONS TIMELINES

Crawler operations are based upon a mission model philosophy in which it is assumed that dual Space Station tethers have been previously deployed and are maintained in a deployed state more or less continuously in support of some other form of tether application such as related to a Science Platform, Mass Balancer System, etc.

The various phases of the baselined Crawler operational sequence and typical operations timeline are illustrated in Figures 1.2.5-1 and 1.2.5-2. The flow should be self-explanatory based upon the previous discussion.

#### 1.2.6 CRAWLER STUDY COST ANALYSIS SUMMARY

A cost analysis for the Tether Crawler was performed using the RCA PRICE cost modeling system and a Lotus-123 based LCC model. A summary of the results of this analysis is presented in Table 1.2.6-1. Details of this cost effort are presented in the separate cost document accompanying the study report (DR-6 Sections 2-11 thru 2-15 and its Appendices).

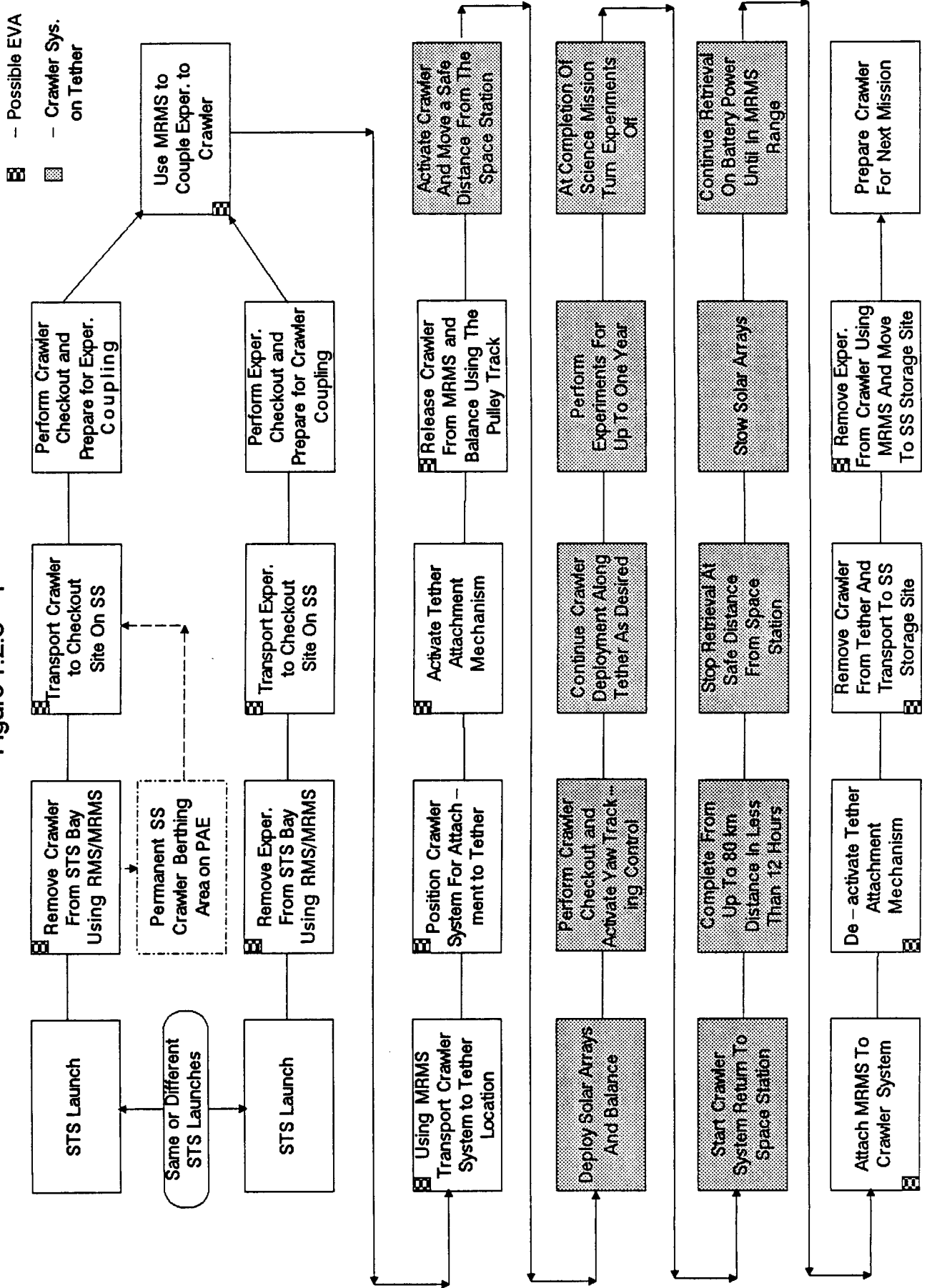
Table 1.2.6-1 Crawler Costs (Constant 1987 Dollars)

Hardware Design and Development Cost	\$ 12,896,000
Hardware Production Cost	\$ 19,617,000
Operations and Support Cost	\$ 46,661,447*
Software Cost	\$ 6,610,000
Total Crawler Cost	<u>\$ 85,784,447</u>

\*Note: STS Launch Costs are \$7,015,200



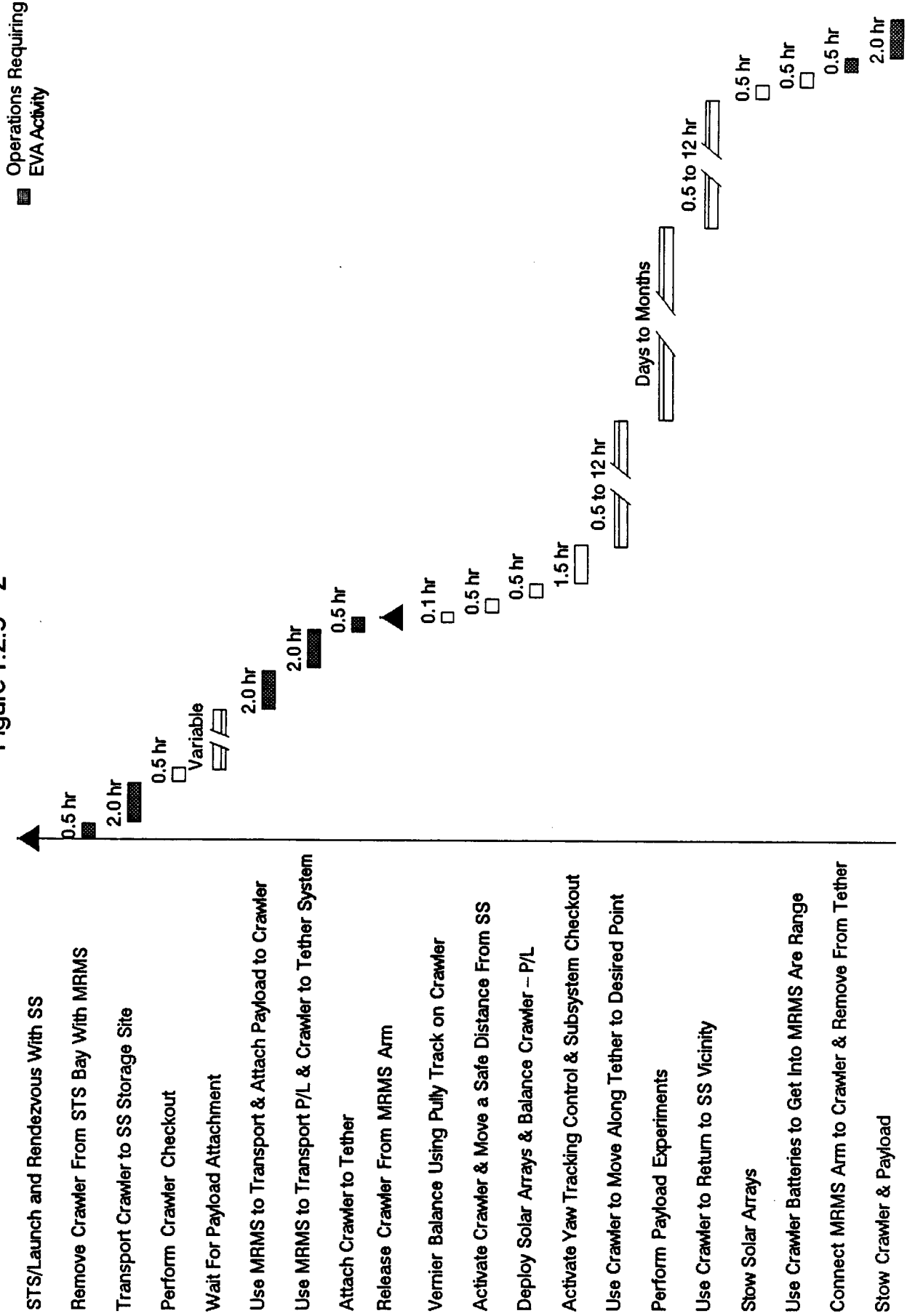
# Crawler Operational Sequence Figure 1.2.5 - 1



C-2

# Crawler Operations Timeline

Figure 1.2.5 - 2



# SUMMARY TABLE-TETHERED CRAWLER

PHYSICAL CHARACTERISTICS	QUANTITY OR DESCRIPTION
Mass	
Bus	o 1440 kg
Payloads	o 560 kg
Total	o 2000 kg
Attachment/Detachment	o Self-threading along previously deployed tether
Payload Services	o Power, fluid loop, communications
Power System Capability	
On-station	o 2000 watts
Ascent Phase	o 2000 watts
Solar Arrays	o deployable/retractable 1.8m x 11.6m = 42.4m <sup>2</sup> total, canted @ 45, oriented to most favorable yaw angle
Maximum Range	o 100 km
Maximum Stay Time	o 1 Year
Min. Descent/Ascent Time (for 100 km)	o 10.3 hours
Crawler Drive	o friction wheels
Attitude Control	plus electric motor
Yaw Wheel Angular Momentum	o 71 N-m-sec
Yaw Motor Peak Torque	o 0.29 N-m
Momentum Wheel Desaturation	o 42 kg/yr of N <sub>2</sub>
Thermal Control	o Passive plus quartz radiator lamps
OPERATIONAL CHARACTERISTICS	
Launch and Delivery Phase	o Crawler and Payloads (if any) RMS transferred to SS
	o Mating, checkout, and transferred to tether attach point by MRMS
Deployment Phase	
Tether deployment/retrieval	o TSAT or other such method assumed
Tether attachment	o Mated by attachment mechanism.
On-Station	o Dual axis balancing via pulley track and solar array length differential
	o Yaw solar tracking using yaw momentum wheel
SPECIAL TETHER BENEFITS	o Variable g capability
	o Enhanced deployment/retrieval dynamics
COSTS	o Table 1.2.6-1

## 2.0 TETHERED PAYLOAD DEPLOYMENTS FROM SHUTTLE

### 2.1 INTRODUCTION

Tethers can be used in a transportation mode to insert payloads/satellites from an orbiting host vehicle to orbits that are significantly higher than that of the host. This part of the study examines the implications of tethered payload deployments from the STS, the impact such deployment might have on shuttle operations and the cost benefits of tether deployments when compared to the conventional propulsive techniques.

The approach taken is to assume that the STS will boost a candidate payload to the standard 300 km circular orbit from which point the payload will be deployed to its higher operating orbit. The philosophy behind this approach is two-fold:

- a) The routine launching of satellites to higher orbits than the shuttle should not substantially infringe on shuttle operations other than when the deployment is being performed. If the STS is required to fly to anomalous orbits to effect a satellite deployment the shuttle launch costs, as reflected by reduced weight carrying capability and restrictions on STS orbital operations, will have to be absorbed by the payload as additional launch costs.
- b) It is more efficient from a propellant weight viewpoint to just boost the payload whatever increment of orbital altitude above the standard shuttle orbit is required than to boost the entire shuttle and payload the same increment.

The first step in evaluating the cost of tether deployments from the STS is to estimate the weight of the total tether system and compare it with the weight of a propulsion system that will accomplish the same deployment. If tether deployments are to be cost effective, the weight of the tether system

will have to be less than or equal to the competing propulsion system since the total tether deployment system will have to be launched with the STS each time a payload is to be deployed.

In the paragraphs that follow the weights of tether and standard propulsion deployment systems will be estimated and compared to each other as a first step in determining their cost effectiveness relative to each other. The results of this trade study will be used as a starting point to proceed with a design and life cycle costing for a tether deployer system and a comparison propellant system.

#### 2.1.1 TETHER SYSTEM SIZING

To estimate the weight of a tether deployment system the weight of just the tether needed to deploy a satellite of mass "M" will be determined. The deployment is assumed to be a hanging, i.e. non-swinging, tether release. The lightest tether that could be employed for satellite deployment is one that has constant stress throughout its deployed length i.e., a tether whose cross-sectional area varies as a function of length. The tension in the tether at the point of its attachment to the satellite is given by

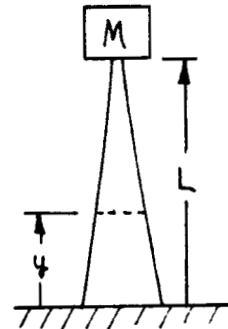
$$T_a = M(R_o + L)\omega_o^2 - \frac{GM_e M}{(R_o + L)^2} \quad (1)$$

where

M = Satellite mass

$R_o$  = Orbital radius from the center of the earth to the host (i.e. STS) vehicle

$\omega_o$  = Orbital rate corresponding to radius  $R_o$



Final Report - Volume II - Study Results

L = Tether length from host vehicle (i.e., Shuttle)

G = Gravitational constant

M<sub>e</sub> = Mass of the earth

T<sub>a</sub> = Tether tension at the point of attachment to the satellite

The underlying assumption in equation (1) is that the mass of the host vehicle is much greater than the satellite plus deployed tether which certainly applies to Shuttle deployments.

Since  $R_0 \gg L$  equation (1) can be written approximately as

$$T_a \sim 3ML\omega_0^2 \quad (2)$$

where

$$\omega_0^2 = \frac{6M_e}{R_0^3} \quad (3)$$

The tension in the tether due to its own mass at a point "y" along its length can be written as

$$T(y) = dM_y(R_0+y)\omega_0^2 - \frac{GM_e dM_y}{(R_0+y)^2} \approx 3\omega_0^2 y dM_y \quad (4)$$

where

dM<sub>y</sub> = differential tether mass at point "y"

But

$$dM_y = \rho A(y)dy \quad (5)$$

## Final Report - Volume II - Study Results

where

$\rho$  = mass density of the tether

$A(y)$  = Tether cross-sectional area at point "y"

Substituting equations (5) into (4) gives

$$T(y) = 3\omega_0^2 \rho A(y) dy \quad (6)$$

The stress in the tether at point "y" can be written as

$$s(y) = \frac{3ML\omega_0^2 + \int_y^L 3\omega_0^2 \rho y A(y) dy}{A(y)} \quad (7)$$

where

$S(y)$  = Tether stress at point y

Assuming that the stress in the tether at any point "y" is constant and equal to  $S_0$  (stress at origin) the following results

$$S_0 A(y) = 3ML \omega_0^2 + 3 \omega_0^2 \rho \int_y^L y A(y) dy \quad (8)$$

Differentiating equation (8) yields

$$S_0 \frac{dA(y)}{dy} = -3\omega_0^2 \rho y A(y) \quad (9)$$

Separating variables and integrating gives

$$A(y) = A_0 \exp \left\{ \frac{-3\omega_0^2 \rho}{2 S_0} y^2 \right\} \quad (10)$$

# Final Report - Volume II - Study Results

For the stress in the tether to be  $S_0$  at point L, the satellite attach point, the following applies

$$S_0 = \frac{3ML\omega_0^2}{A(L)} \quad (11)$$

where

$A(L)$  = Tether cross-sectional area at L, i.e., at the satellite attach point.

Substituting equation (10) into equation (11) gives

$$S_0 = \frac{3ML\omega_0^2}{A_0} \exp \left\{ \frac{3\omega_0^2 \rho}{2S_0} L^2 \right\} \quad (12)$$

Solving equation (12) for  $A_0$  and substituting into (10) results in

$$A(y) = \frac{3ML\omega_0^2}{S_0} \exp \left\{ -\frac{3\omega_0^2 \rho}{2S_0} (L^2 - y^2) \right\} \quad (13)$$

The tether mass is given by

$$M_T = \rho \int_0^L A(y) dy = \frac{3ML\omega_0^2}{S_0} \rho \exp \left\{ \frac{3\omega_0^2 \rho L^2}{2S_0} \right\} \int_0^L \exp \left\{ -\frac{3\omega_0^2 \rho}{2S_0} y^2 \right\} dy \quad (14)$$

Performing the integration indicated in equation (14) yields

$$M_T = \left\{ \frac{3\pi\rho}{2S_0} \right\}^{\frac{1}{2}} ML\omega_0^2 \exp \left\{ \frac{\omega_0^2 \rho L^2}{2S_0} \right\} \operatorname{erf} \left\{ \left\{ \frac{3\omega_0^2 \rho}{2S_0} \right\}^{\frac{1}{2}} L \right\} \quad (15)$$



For a tether of constant cross-section the tension in the tether at its attach point to the host vehicle is given by

$$SA = 3ML\omega_0^2 + \frac{3}{2} \omega_0^2 \rho AL^2 \quad (16)$$

which yields

$$A = \frac{3ML\omega_0^2}{S - \frac{3}{2} \omega_0^2 \rho L^2} \quad (17)$$

where

A = constant tether cross-sectional area

Setting the stress in the tether at the attach point to the host vehicle to  $S_0$  gives

$$S_0 A = 3ML\omega_0^2 + \frac{3}{2} \omega_0^2 \rho AL^2 \quad (18)$$

solving equation (18) for A results is

$$A = \frac{3ML\omega_0^2}{S_0 - \frac{3}{2} \omega_0^2 \rho L^2} \quad (19)$$

The constant cross-section tether mass is given by

$$M_T = \rho AL \quad (20)$$

or

$$M_T = \frac{3\rho ML\omega_0^2}{S_0 - \frac{3}{2} \omega_0^2 \rho L^2} \quad (21)$$

It is now desirable to determine the weight difference between the optimum constantly stressed tether (i.e., the tapered tether) and the constant cross-section tether for tether lengths being considered for STS payload

deployment. This can be done by noticing that the ratio between the constant cross-section and optimum tether is only a function of tether physical parameters and length and does not depend upon the mass of the satellite being deployed.

The mass properties for Kevlar are

$S_0 = 692 \times 10^6$  Newtons/m<sup>2</sup> (Includes a Safety factor of 4 over the breaking stress)

$\rho = 1,439.36$  kg/m<sup>3</sup>

$\omega_0 = 1.16 \times 10^{-3}$  rad/sec corresponding to a 300 km shuttle orbit

$R_0 = 6,668$  km

$L = 300$  km

Substituting these values into equations (15) and (21) and taking the ratio of the constant cross-section tether to the optimum tether yields

$$M_r = \frac{1.21M}{0.977M} = 1.24 \quad (22)$$

or a 300 km tether of constant cross-section will be 24% heavier than the optimum tether. This weight differential between the two would not be sufficient to dictate the use of the optimum tether when considering its manufacturing complexity, the impact it would have on the reeling mechanism design and logistics when considering storing extra tether on the reel should a defect in the tether be detected. In addition, most if not all of the tether deployments from the STS would employ tethers that are less than 100KM in which case the weight differential between the two would decrease. Hence, the constant cross-section tether will be used in the weight comparison between tether and propulsion system deployments.

Figure 2.1.1-1 shows the ratio of the tether mass to deployed satellite mass as a function of tether length. Examination of the figure indicates that for a tether 100 km long the tether mass is approximately 9 percent of the deployed satellite mass.

Weight of Fuel Needed to Boost a Payload to a Higher Orbit

The mass of fuel needed to boost a satellite from one orbit to a higher one is given by

$$M_F = M \left[ \exp \left\{ \frac{\left( \frac{GM_e}{R_o} \right)^{1/2} - \left( \frac{GM_e}{R_o + L} \right)^{1/2}}{C g I_{sp}} \right\} - 1 \right] \quad (23)$$

where

$M_s$  = Satellite mass

$C$  = 0.3048 meters/ft

$g$  = Gravitational acceleration (32.2 ft/sec<sup>2</sup>)

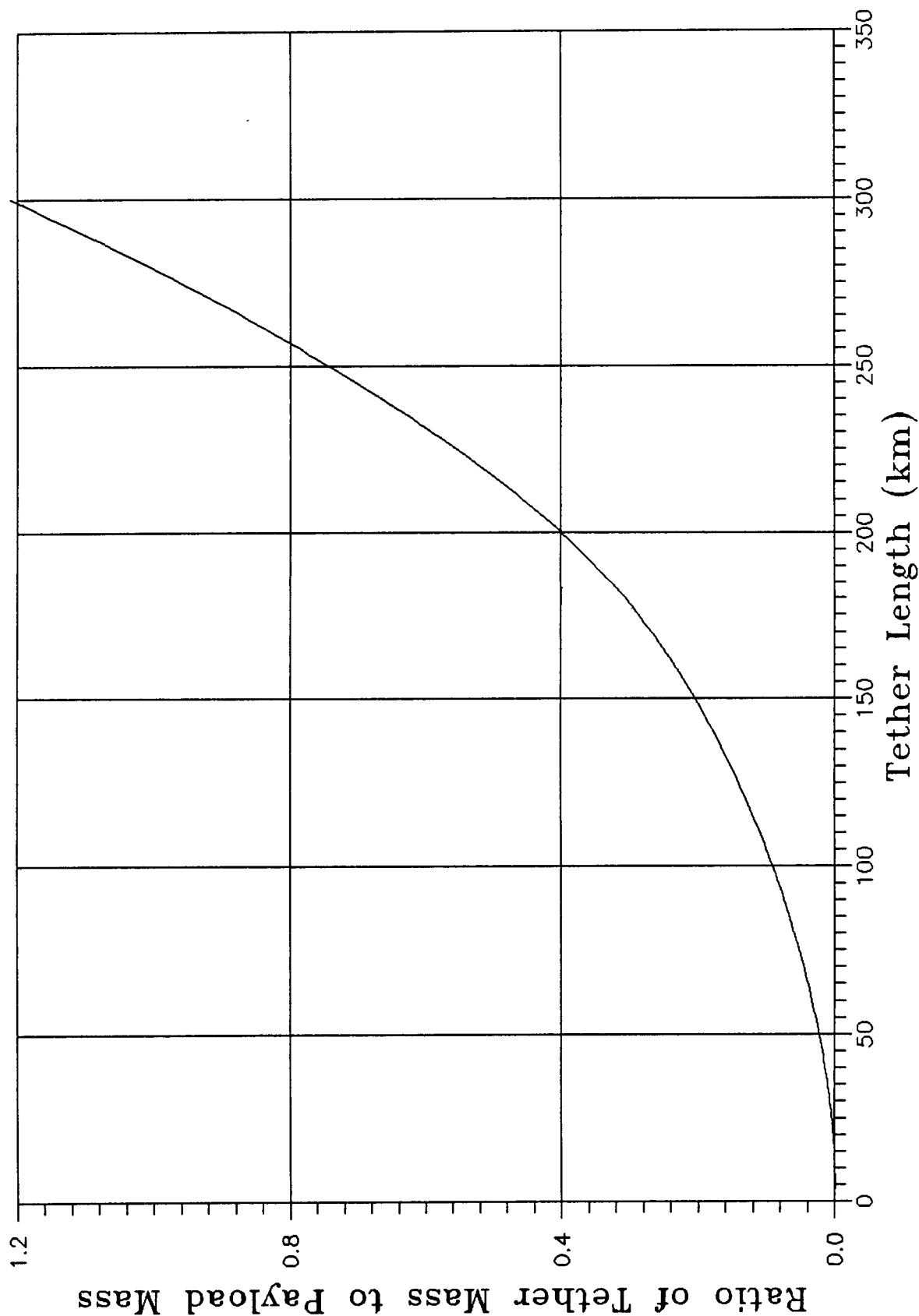
$I_{sp}$  = Specific impulse of the fuel (lb-sec)  
lbm

The weight of fuel shown in equation (23) is derived for an orbit transfer accomplished by low level thrusting along the velocity vector, which results in transferring the payload from a lower circular orbit to a higher one. However, for orbital transfers of 1000 km or less the fuel mass computed by equation (23) is within a few percent of the mass that would be used in a Hohmann transfer but the equation is considerably easier to handle.

For a non-swinging or hanging release from a tether the payload would go from the host vehicle circular orbit to an elliptical one whose apogee is the

Figure 2.1.1-1

Ratio of Tether Mass to Payload Mass  
For a Constant Cross-Section Tether



original orbital altitude plus seven times the tether length and perigee increase is approximately equal to the original orbital altitude plus the tether length. Hence, the fuel weight that would accomplish the same transfer is given by

$$M_f = M \left[ \exp \left\{ \frac{\left( \frac{GM_e}{R_o} \right)^{1/2} - \left( \frac{GM_e}{R_o+L} \right)^{1/2}}{CgI_{sp}} \right\} - 1 \right] \left[ \frac{\left( \frac{GM_e}{R_o} \right)^{1/2} - \left( \frac{GM_e}{R_o+6L} \right)^{1/2}}{CgI_{sp}} \right] - 1 \quad (24)$$

Figure 2.1.1-2 shows the ratio of fuel mass to payload mass for achieving the same orbit as a hanging tether release assuming a hydrazine system with an  $I_{sp}$  of 215 (lb-sec/lbm). Comparing these values with those of Figure 2.1.1-1 indicates that for tether lengths less than 130 km the fuel weight exceeds the tether weight however, for lengths in excess of 130 km the tether weight alone exceeds the fuel weight required to make the equivalent orbit transfer.

#### Ratio of Tether Mass to Fuel Mass for a Given Orbit Transfer

The ratio of tether to fuel mass for a given orbital transfer is given by

$$\frac{M_T}{M_f} = \frac{3\rho L^2 \omega_o^2}{(S_o - 1.5\omega_o^2 \rho L^2) \left( K_1 + \frac{1}{2} K_2 \right)}$$

where

$$K_1 = \left[ \exp \left\{ \frac{\left( \frac{GM_e}{R_o} \right)^{1/2} - \left( \frac{GM_e}{R_o+L} \right)^{1/2}}{CgI_{sp}} \right\} - 1 \right]$$

$$K_2 = \left[ \exp \left\{ \frac{\left( \frac{GM_e}{R_o} \right)^{1/2} - \left( \frac{GM_e}{R_o+6L} \right)^{1/2}}{CgI_{sp}} \right\} - 1 \right] \quad (25)$$

Figure 2.1.1-2 Ratio of Fuel Mass to Payload Mass to Achieve Same Orbit as a Hanging Tether Release

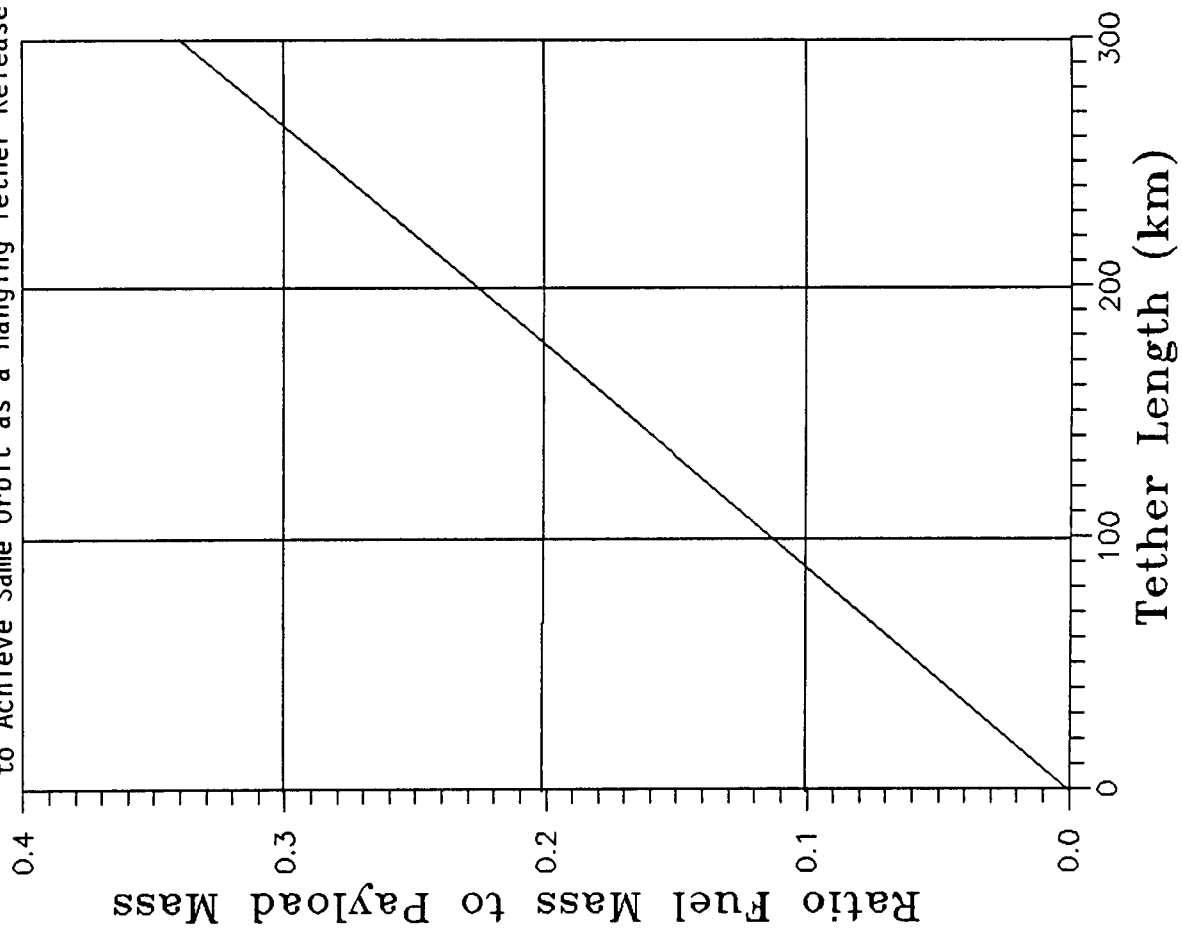
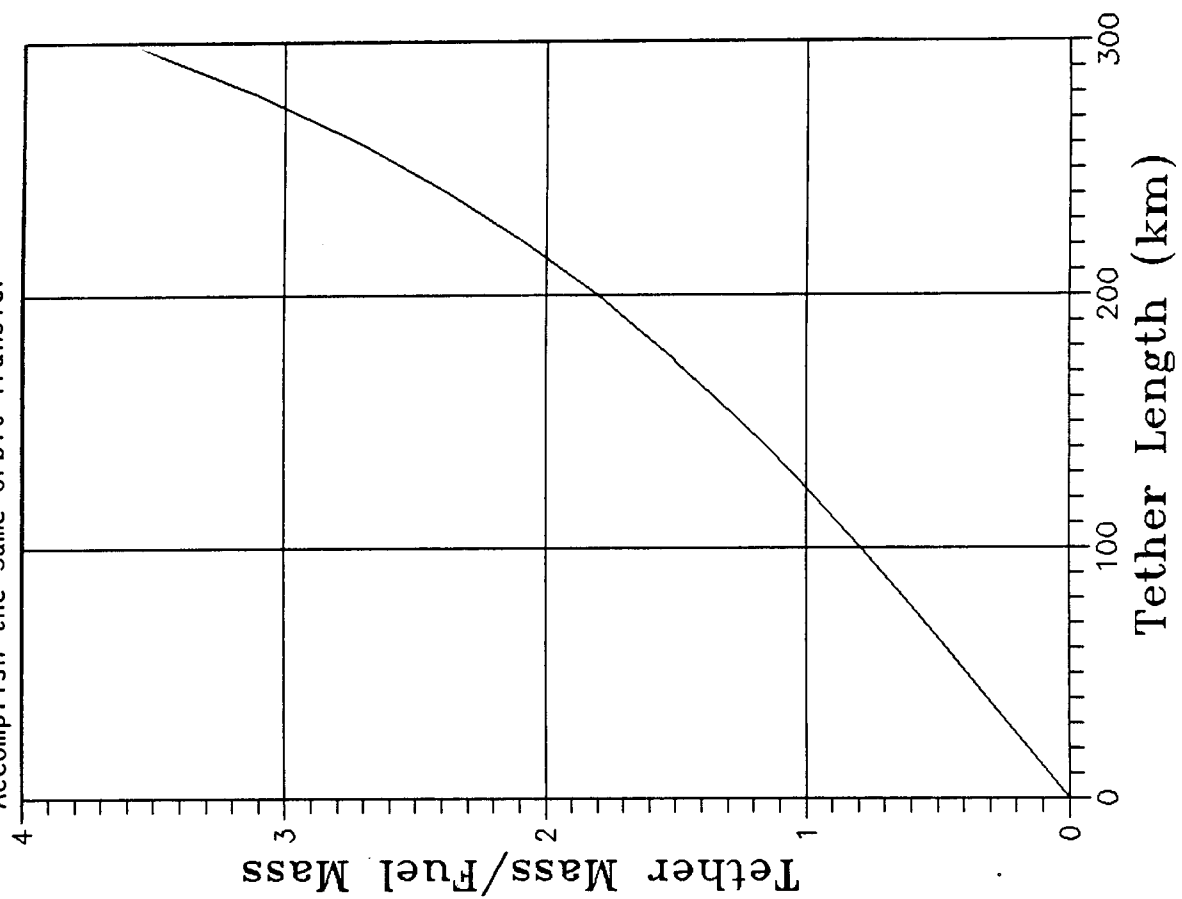


Figure 2.1.1-3 Ratio of Tether to Fuel Mass to Accomplish the Same Orbit Transfer



Examination of equation (25) indicates that the ratio of tether mass to fuel mass to accomplish the same orbit transfer is independent of the payload or satellite mass being deployed. Hence, this ratio as a function of tether length is true for any payload deployed by a tether. Figure 2.1.1-3 gives the value of this ratio as a function of tether length.

#### Estimate Tether Deployment System Weight

Examining the designs of various tether deployment systems developed by BASD and Martin Marietta Corporation (MMC) indicates that the ratio of the total tether deployment system mass to just the tether mass varies between 5 and 13 depending on length of tether and mission scenario. For a typical integral propulsion system, the propulsion system mass (i.e. the mass of tanks valves, nozzles, etc.) is approximately 15 percent of the fuel mass. Hence, if the lower value of the ratio of tether deployment system mass to tether mass is used the ratio of tether system mass to propellant system mass for equivalent orbital transfers shown in Figure 2.1.1-3 should be multiplied by the factor  $5/1.15$  or 4.35 to obtain the ratio of tether deployment system weight to propulsion system weight needed to accomplish the same orbital transfer. Using this approach gives the result that the mass of a 30 km tether deployment system equals the mass of the equivalent propulsion system with the mass of the tether system exceeding the mass of the propulsion system as the tether length is increased. Since this result is independent of payload mass the above results holds true for any payload.

Most if not all candidate orbital transfer missions will require tethers in excess of 30 km. Hence, the weight of the tether deployment system will exceed the weight of the equivalent propulsion system if current design techniques are used. If the tether deployment system is launched each time a tethered payload deployment is attempted from the STS the tether deployer design will have to reduce the ratio of tether mass to system mass. Unless

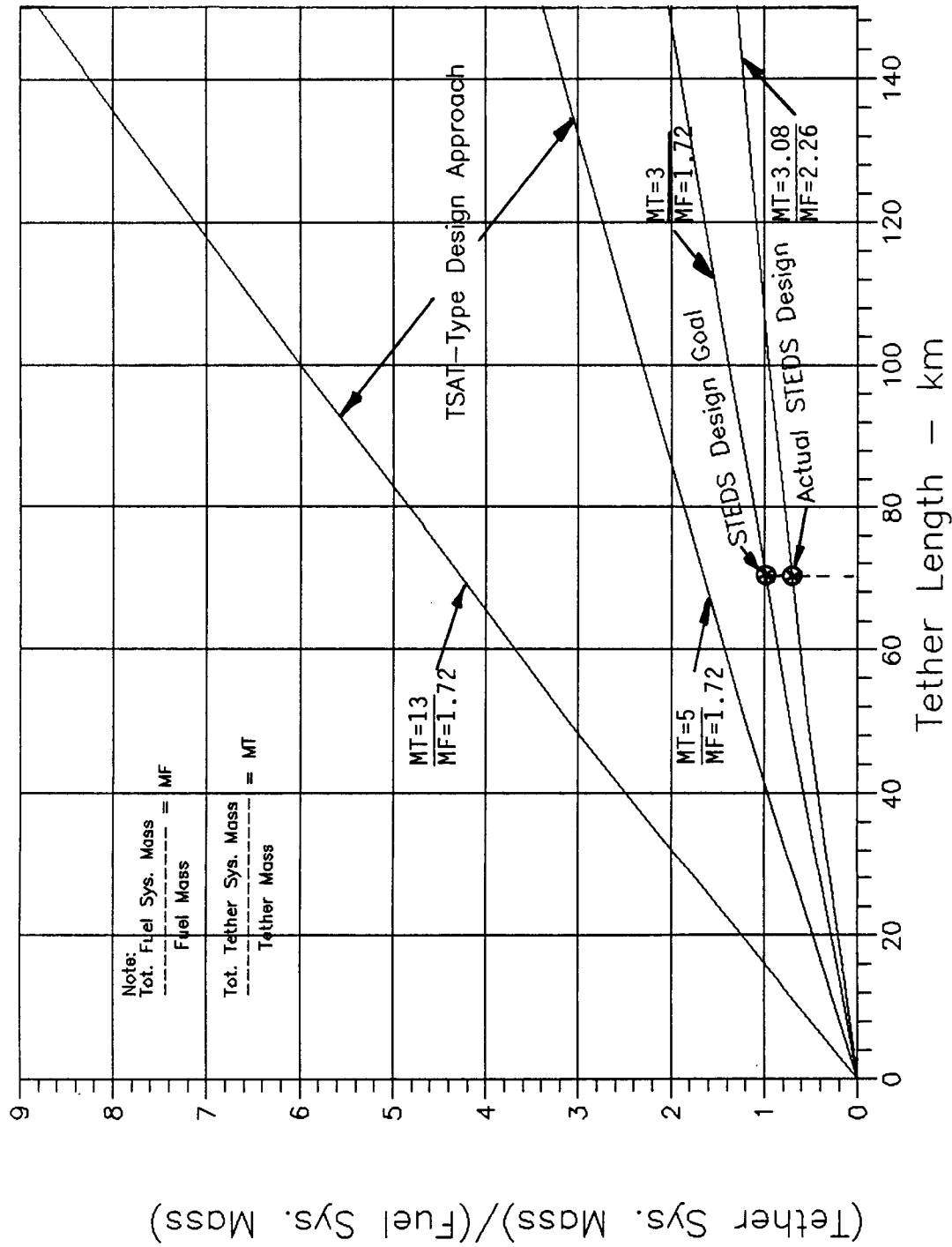
this is accomplished the technique could not be cost competitive with an integral propulsion system performing the same function since its marginal (i.e. reuse) cost exceeds those of a propulsion system.

Study of the tether system designs proposed to date indicate that potential areas for weight savings are in the reeling mechanism and accompanying support structure, and the boom mechanisms employed for terminal payload control and tether tension line-of-action positioning. An evaluation of the potential weight savings in these areas resulted in a mass ratio of 3 as being feasible.

In addition it was decided that a comparison of the cost benefit of a tether deployer vs. an integral payload propulsion system would not be feasible since the costs associated with integrating a propulsion system into a payload is payload dependent. In fact some contamination sensitive payloads cannot tolerate the by-products of propulsion systems at all. Therefore, a better defined comparison would be between the tether deployer and an external Orbital Maneuvering Vehicle (OMV) type system. Based on preliminary design parameters for the OMV it was determined that a better mass ratio for the propellant system would be 1.72 rather than the 1.15 assumed for the integral system. This resulted in a design point of 1.74 (3/1.72) (see Figure 2.1.1-4). The resulting cross over point is approximately 70 km of tether length. The orbital parameters for a payload deployed with a 70 km tether from a 300 km STS altitude would be approximately 370 x 790 km. This is the energy equivalent of a 600 km circular orbit.

The published orbit transfer capabilities of one OMV design is more than 15,000 kg from STS altitude to 900 km and 14,000 kg for a roundtrip to 600 km. This same OMV design will be capable of delivering a 10,000 kg payload to an altitude of more than 1,300 km. It is obvious that comparing the tether deployer, on a cost/benefit basis, with the proposed OMV is not valid. The two systems to be compared should have similar performance capabilities. Therefore, an alternative OMV design is proposed (referred to as the mini-





Ratio of Tether System Mass to Fuel System Mass for Design

Figure 2.1.1-4

OMV) whose performance parameters will more closely resemble the tether deployer. This mini-OMV should be capable of transporting a 10,000 kg payload from a normal STS 300 km altitude to 600 km altitude and separating itself from the payload.

#### 2.1.2 DESIGN ASSUMPTIONS/GUIDELINES

One objective of the Phase III study contract is to determine the cost benefits associated with using a tether to deploy payloads from the STS cargo bay. Therefore it is imperative that all the costs associated with the tether system be minimized. This includes design, development, production and operations.

Early trades established that the biggest cost driver is transportation to orbit. This is especially true for systems that are designed for multiple missions since the launch costs are a recurring item. The STS costing formula is based on payload length or weight, whichever results in the larger cost. Therefore an early design guideline for STS deployer systems was to minimize weight and required cargo bay length. Most payloads that fly on the STS pay by cargo bay length, not weight. This is because most payloads have a low density when it is computed on the basis of cargo bay volume occupied. So to keep launch costs at a minimum cargo bay length must be minimized.

Another part of the operations cost is the fraction of total mission time that must be devoted to the payload. Normal STS pricing includes STS operational support for 24 hours. Therefore the total accumulated time dedicated to the deployments should be less than 24 hours if additional support costs are to be avoided. Also, no EVA time or mission specialist training is included in the basic STS launch services. Therefore, EVA's should not be required and the deployment system operation should be kept simple to avoid the need for mission specialists.

The deployer system should be sized to handle a variety of payloads so that non-recurring costs can be amortized over many missions. This means the system must be capable of accommodating a range of payload masses, configurations, and final orbit altitudes. Earlier studies of the STS missions manifested for the next several years and in the planning stages indicate that payload masses will range from 1000 to 10,000 kg. The preliminary estimates of a breakeven point for tether deployments versus standard propellant systems gives an altitude design point of 600 km for 10,000 kg payloads. This is based on initial assumptions of the realizable design weights of the competing systems and the resulting tether length of 70 km. Re-calculating these numbers on the final designs presented here indicate that the true optimum design point will be between 70 and 100 km of tether length. However, this does not significantly impact the total life cycle costs (LCC) so the designs were not iterated to determine the exact optimum design point.

Another design goal for the deployer systems was to minimize the impact of the deployer system on the payload to be deployed. The deployer system should be able to easily integrate its operation into the payload deployment sequence without significantly interfering with the design and operation of the payload. This is a necessary design feature if the deployer system is going to be able to accommodate a variety of payloads.

Finally the deployer systems should not incorporate a payload retrieval capability. This is not required with rocket assisted deployments and its elimination reduces the complexity of the systems greatly.

#### 2.1.3 Mini-OMV VERSES OMV RATIONALE

In order to determine the cost effectiveness of a tether deployment it is necessary to compare it to conventional approaches to accomplish the same end. Using a propulsion system is the obvious conventional alternative to

tether deployment and two possibilities come to mind; the OMV or a newly designed propulsion stage which will be called the mini-OMV or MOMV. The following paragraphs outline the rationale for this choice.

Using the weights projected for the OMV (6636 kg) a tether system will have a weight cross-over with the OMV for an orbital transfer from the 300 km circular STS orbit to a 900 km circular orbit when using a payload of 10,000 kg.

This implies that the cost to launch a tether system capable of making the above orbital transfer would be the same as the OMV although the OMV has considerably greater capability than represented by this transfer. It does not seem likely that if one is considering transferring a 10,000 kg payload to the vicinity of 1,000 km that a tether system could possibly compete with the OMV. This follows from the fact that the recurring costs for both systems would be equivalent (STS transportation costs) and the tether system needs development while the OMV will be a developed Space Station element. In addition, considering the performance capability of the OMV vs. a tether deployer and the risk vis-a-vis the two deployment techniques makes the OMV a better choice than a tether deployment system at the weight cross-over point.

It therefore is apparent that the trade between a tether and conventional deployment systems should occur for system performance capabilities significantly below the weight cross-over point of the OMV (i.e. light payloads, 10,000 kg payloads that only require a few hundred kilometer orbit transfer) where use of the OMV can become quite expensive. However, the alternative deployment system for this class of payload would need to be designed, developed and built regardless of what the deployment system may be since no such system exists or is planned as a part of the Space Station program. Hence, if we are considering the development of an alternative small deployment system to the OMV we should be examining the economic considerations of developing a tether deployer as opposed to a conventional propulsion stage. i.e. a MOMV.

## 2.2 MINI-OMV DESIGN

### 2.2.1 REQUIREMENTS

The mini-OMV (MOMV) design is based on the following set of design requirements:

Launch/Recovery	- Shuttle
Payload Mass	- 1000 to 10,000 kg
Altitude Capability	- from STS 300 km orbit to 600 km (cir.)
Mission Duration	- 48 hours maximum
Subsystems	- Self-contained
Subsystem Redundancy	- None except for safety
Payload Attachment	- On-orbit, remote
Payload/MOMV Interface	- Mechanical only

Many of these requirements are derived from the basic set of requirements which include: Shuttle launch, minimize payload impact, and the orbit transfer requirement. The 48 hour mission time is derived from the orbital mechanics of the orbit transfer and MOMV recovery operations. The non-redundant subsystems requirement is derived from the fact that the tether deployer is a non-redundant system, so for cost comparison reasons the MOMV should be designed similarly. The requirement to limit the payload interface to mechanical only was also made for equal capabilities reasons. The payload will probably have an attitude control system that could have been interfaced to the MOMV to save this expense, but this would have resulted in extra impact on the payload and an unfair comparison with tether deployments. The on-orbit remote payload attachment requirement was also made to limit the

impact of the MOMV on the payload design. Since the attachment is made on-orbit the payload designer is given more freedom to place the mechanical attachment interface where it will impact the payload the least. This same assumption is made for the tether deployer design.

#### 2.2.2 CONFIGURATION

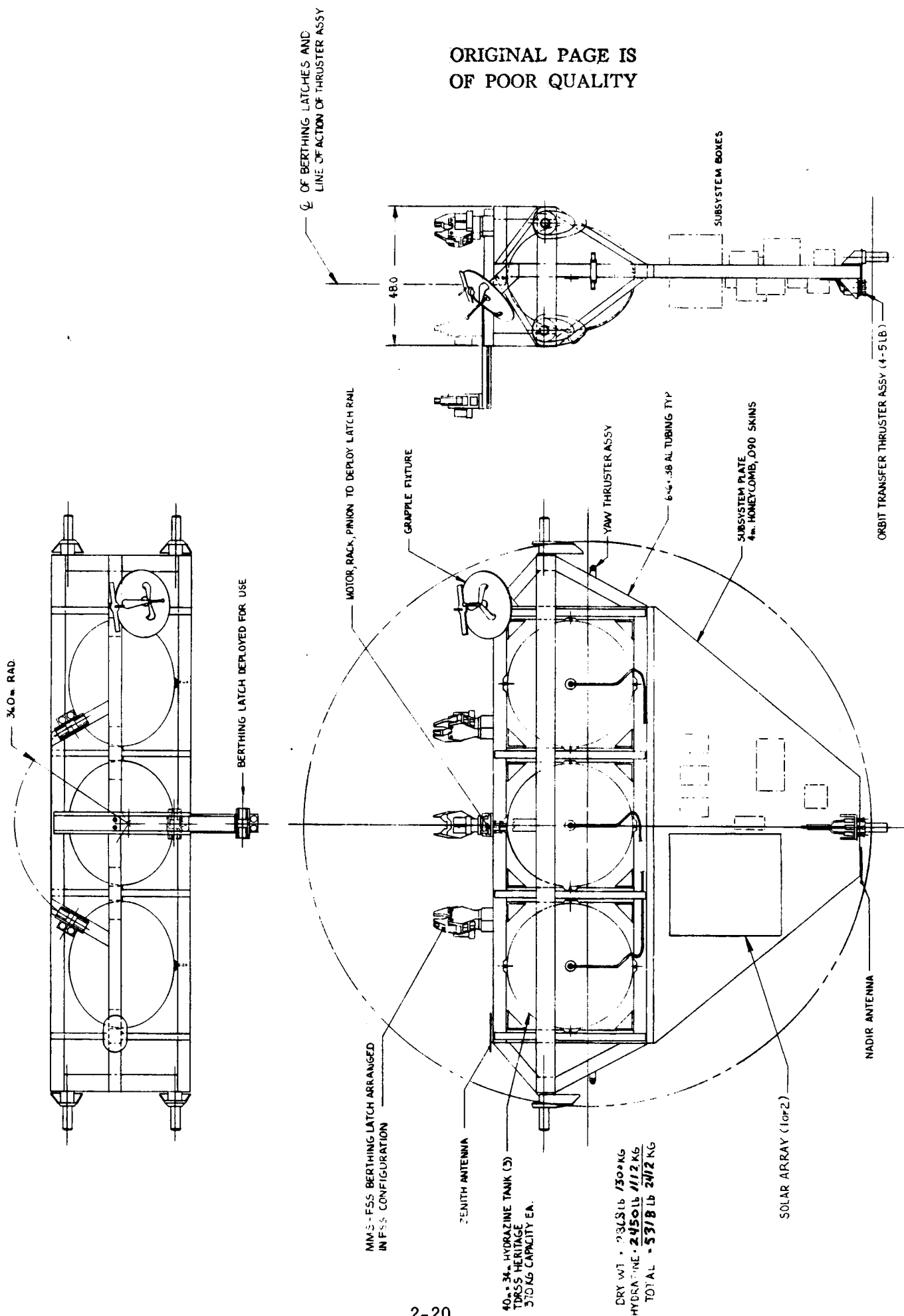
Figure 2.2.2-1 shows the configuration of the MOMV. It is basically a truss support structure with a honeycomb panel for subsystem mounting. It is optimized for minimum payload bay length and launch weight. All components are flight proven designs for low cost and risk.

The structure is fabricated from 6061-T6 aluminum and honeycomb panels. The truss structure supports the three hydrazine tanks, which are of TDRSS heritage, and the trunnions for structural interface to the STS sill attachments. This structure also provides an attachment point for the honeycomb subsystem plate, the latching mechanisms (MMS-FSS heritage) for the payload, the zenith antenna, the yaw thrusters, and the grapple fixture (ERBS heritage) for RMS operations. The truss members are 15.24 x 15.24 x .965 cm (6 x 6 x .38 in) aluminum tubing.

The honeycomb subsystem plate is 10 cm (4 in) thick and has .229 cm (.090 in) aluminum facesheets. It provides a mounting surface for the various electronic boxes, batteries, nadir antenna, solar arrays, hydrazine thrusters and the keel fitting for Shuttle interface.

The payload is attached to the MOMV using a set of MMS-FSS berthing latches located on the top of the truss assembly. One of the latches is deployed on-orbit after the payload has been removed from the cargo bay by the RMS. This is done to reduce the total cargo bay length required in the launch and recovery conditions.

Figure 2.2.2-1  
Mini-OMV Layout



ORIGINAL PAGE IS  
OF POOR QUALITY

## Final Report - Volume II - Study Results

The entire structure is designed for 24 reflights in the STS bay, including fracture considerations. A NASTRAN analysis of the structural design was completed to verify the design sizing for all the structural components.

### 2.2.3 STS INTERFACE

The MOMV interface with the Shuttle is accomplished mechanically with the Payload Retention Latch Assembly (PRLA) and Active Keel Assembly (AKA) through the trunnions supplied on the MOMV. Electrical interface with the MOMV is not required except through the S-band link provided by the STS Payload Interrogator. Figure 2.2.3-1 illustrates the MOMV/STS electrical and communications interface.

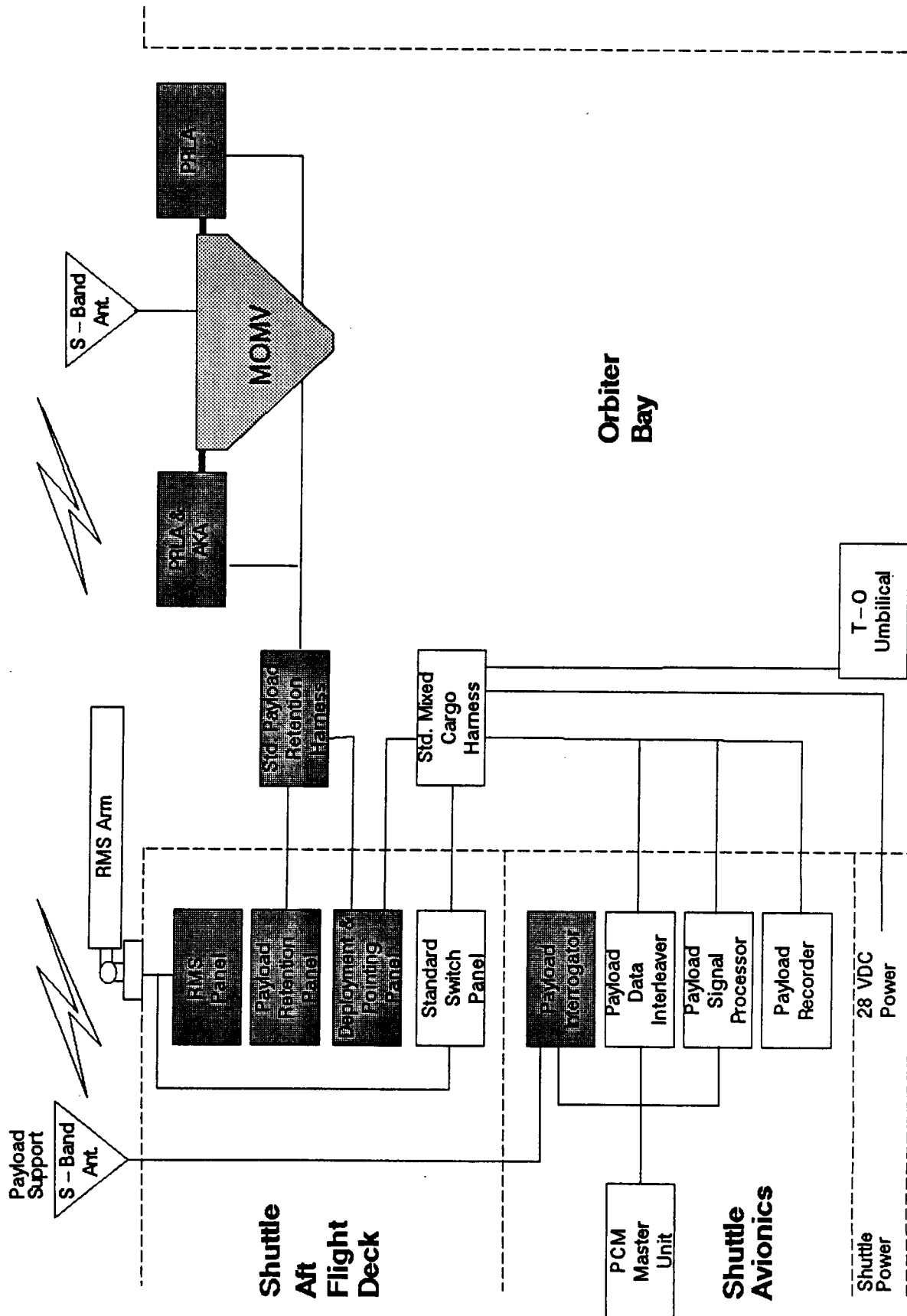
### 2.2.4 SUBSYSTEM DESCRIPTIONS

#### 2.2.4.1 ATTITUDE CONTROL

Attitude control for MOMV is provided by an attitude control electronics box, a horizon scanner, a triaxial rate gyro package, and hydrazine reaction control jets. Table 2.2.4-1 lists the AC&D subsystem components weights and power requirements. All components are based on the BASD ERBS spacecraft heritage.



Figure 2.2.3 - 1 MOMV/STS Electrical Interface



## Final Report - Volume II - Study Results

Component Name	Wt (kg)	Power (w)	%On	Ave. Pwr
AC&D Electronics	10.9	7.5	100	7.5
Triaxial Gyro Package	2.8	21.0	100	21.0
Horizon Scanner	4.0	7.4	100	7.4
<hr/>				
Totals	17.7 kg			35.9 w

Table 2.2.4-1 MOMV AC&D Subsystem Components List

The normal attitude for the MOMV during orbital transfer operations will be with its thrust axis along the orbital velocity vector and its longitudinal axis along the local vertical. This is accomplished by using errors generated by the horizon scanner and rate gyros configured as a gyrocompass to appropriately drive the MOMV thruster system. The orbital transfer is accomplished by continuously thrusting at low level along the orbital velocity vector causing the vehicle and payload to slowly spiral out to the desired orbit. The same technique is used to return the MOMV to the vicinity of the STS for retrieval. This procedure has been used successfully by the ERBS spacecraft to affect an orbit change from STS altitude to above 600 km.

### 2.2.4.2 THERMAL CONTROL

MOMV thermal control requirements include STS launch and recovery, and the normal on-orbit environment for a nadir oriented three axis stabilized spacecraft. During orbit transfer operations the sun can be in any position relative to the MOMV surfaces. The orbital altitude can range from 300 to 600 km and the MOMV thermal control system must maintain temperatures of critical

## Final Report - Volume II - Study Results

equipment with and without the payload attached. The payload will be responsible for its own thermal control during the orbit transfer. The following equipment temperature ranges were used for analysis and design purposes:

Item	Operating Temperature	
	Min (C)	Max (C)
Hydrazine	+5	+55
Electronics Boxes	-10	+55
Batteries	-5	+25
Solar Arrays	-70	+90

Based on these requirements the thermal design for MOMV was developed. The goal was to make the system completely passive, if possible, to eliminate the need for electrical power in the STS cargo bay and to minimize the solar array size for orbit transfer operations.

The external surfaces of the MOMV are completely covered with MLI blankets. The outer covers are 5 mil second surface aluminized teflon over the subsystems mounting plate area and under the solar arrays. The outer cover is .5 mil second surface aluminized Kapton over the hydrazine tank area. All blankets are assumed to be constructed of 10 layers of .25 mil doubly aluminized Mylar with dacron netting separators.

The solar arrays are thermally isolated from the rest of the spacecraft with fiberglass spacers. The MLI blankets running under the arrays are effective in providing thermal radiative isolation of the arrays from the underlying electronics boxes.

A completely passive design was not possible because of the varied environments and operating conditions encountered by the MOMV. However, heater power was minimized and the hydrazine subsystem is the only one requiring heaters. Thermal analysis of the MOMV indicates that less than 30 watts of heater power will be required.

Thermal analysis was completed for all design attitudes and variations in orbital environments. This included orbit transfer operations in high and low beta angles. Runs were made with and without a simulated AXAF type payload. The payload was assumed to be adiabatic and resulted mainly in shadowing of the MOMV. High and low beta angle runs were also completed for conditions in the STS cargo bay. There was no simulated payload for these runs and the STS bay was assumed to be in a +Z-LV attitude (bay to earth).

The results of these analyses for critical components are presented in Table 2.2.4.2-1 along with the predicted heater power requirements. The heater power will be supplied by the MOMV batteries while in the STS bay and by the solar arrays during orbit transfer operations.

#### 2.2.4.3 COMMUNICATIONS

The requirements for the Communications and Data Handling system are minimal and consist of a 1 kbps telemetry and 128 bps command link through the TDRSS satellite for orbit transfer operations. Communications will be sporadic because of the low thrust approach to orbit transfer which will require updated commands only every few hours. The downlink information consists entirely of engineering data and is for troubleshooting and health check only.

Figure 2.2.4.3-1 shows the baseline C&DH subsystem design approach for the MOMV. All components are based on the BASD CRRES and ERBS satellite programs with the exception that this system contains no tape recorder. Data storage

Table 2.2.4.2 – 1 MOMV Thermal Analysis Results

	W/O Payload		With Payload		STS Bay	
	Cold	Hot	Cold	Hot	to Earth	
	$\beta = 0$	$\beta = 90$	$\beta = 0$	$\beta = 90$	$\beta = 0$	$\beta = 90$
Elec. Mounting Panel	34.6	52.4	34.0	53.0	-1.0	-13.7
Hydrazine Tank Frame	6.9	19.9	6.9	21.0	4.6	3.8
Hydrazine	5.0 #	17.7	5.0 *	18.0	5.0**	5.0***
Battery	6.9	20.0	6.9	20.9	8.6	26.0

All Temperatures – deg C

# 7.2 W htr. power

\* 13.0 W htr. power

\*\* 8.4 W htr. power

\*\*\* 26W htr. power

TLM. ANTENNA SET

CMD. ANTENNA SET

5 WATT NASA STD. TRANSPONDER

TOP SEMI-OMNI ANT.

BOTTOM SEMI-OMNI ANTENNA

PAYLOAD MINI-OMV

HYBRID COUPLER CIRCUIT

POCC

MAX RANGE = 44,600 KM.

Corrections to Thrust Direction are Telemetered Up From the Ground

USES TDRSS S - BAND SINGLE ACCESS LINK AT 1 KBPS TLM. & 125 BPS COMMAND.

TELEMETRY INPUT CHANNELS

DTU

CDU

DISCRETE COMMANDS

TDU with Memory

## Final Report - Volume II - Study Results

requirements have not been identified, but they could be accommodated by installing solid state memory boards in the Telemetry Distribution Unit (TDU).

The NASA Standard Transponder is included in the system because of the baseline decision to use TDRSS as the communications link with the Payload Operations Control Center (POCC).

Table 2.2.4.3-1 shows the component list for the MOMV C&DH subsystem.

Component Name	Wt (kg)	Power (w)	%On	Ave. Pwr
Transponder RCV	6.5	17.5	99	17.3
XMIT/RCV		45.5	1	.5
TDU	7.1	5.0	100	5.0
DTU	4.5	13.0	100	13.0
CDU Operate	4.5	5.0	1	.1
Standby		1.5	99	1.5
Zenith Antenna	1.0			
Nadir Antenna	1.0			
Cabling & Misc.	4.0			
Totals	28.6 kg			37.4 w

Table 2.2.4.3-1 C&DH Component List

### 2.2.4.4 POWER

The power system for the MOMV is designed to meet subsystem orbit transfer requirements of Table 2.2.4.4-1 and the survival power requirements of the STS cargo bay environment during non-operating conditions.

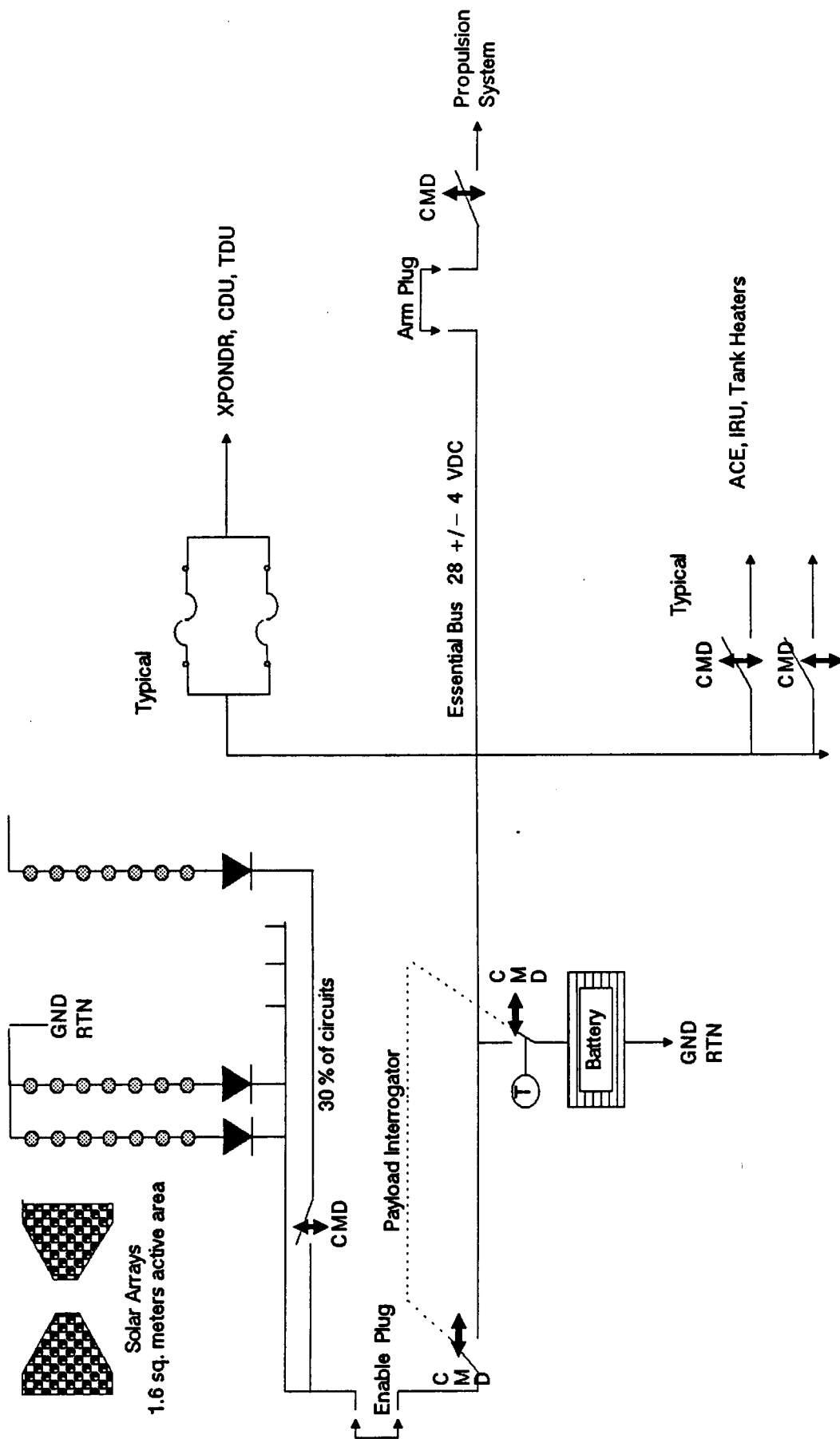


**Figure 2.2.4.4 – 1 MOMV Electrical Power System Concept**



# Final Report - Volume II - Study Results

Component/Subsystem	Quant.	Power (w)	%On	Ave. Pwr	
C&DH Subsystem					
Transponder RCV	1	17.5	100		
XMIT		45.5	1	17.8	
TDU	1	5.0	100	5.0	
DTU	1	13.0	100	13.0	
CDU Operate	1	5.0	1		
Standby		1.5	99	1.6	37.4 w
AC&D Subsystem					
AC&D Electronics	1	7.4	100	7.4	
Gyro Package	1	21.0	100	21.0	
Horizon Scanner	1	7.5	100	7.5	35.9 w
Thermal Control					
Hydrazine Line Htrs.	1	20.0	60	12.0	
Hydrazine Tank Htrs.	3	40.0	15	18.0	30.0 w
Propulsion Subsystem					
Valve Heaters	8	0.75	100	6.0	
Catalysts Bed Heaters	8	0.25	100	2.0	8.0 w
Power Subsystem					
Distribution Losses	1	5.0	100	5.0	
Batteries	2	9.0	100	18.0	
Power Control Box	1	5.0	100	5.0	28.0 w
Total for all subsystems					139.3 w

Table 2.2.4.4-1 MOMV Power Subsystem Requirements

The component list for the electrical power system is given in Table 2.2.4.4-2. All components are based on the ERBS spacecraft design except they have been resized for the significantly lower MOMV power system requirements. The solar arrays have a total active area of 1.6 square meters (18 sq.ft.) with half of the array on each side of the MOMV subsystem plate. The main function of the power control box is to disconnect or reconnect strings of solar array cells from the bus to keep the battery from overcharging. This function could

actually be performed by ground command for this system since the powers are so low and the batteries are oversized to handle the STS heater requirements. However for this design a power control box was included to handle this automatically.

Component Name	Wt (kg)	Pwr. (w)	%On	Ave. Pwr
Solar Arrays	28.0	N/A		N/A
Power Control Box	54.4	5.0	100	5.0
Batteries (2 50 amp-hr)	50.0	9.0	100	18.0
Electrical Harness	45.4	5.0	100	5.0
Totals	177.8 kg			28.0 w

Table 2.2.4.4-2 MOMV Power Subsystem Component List

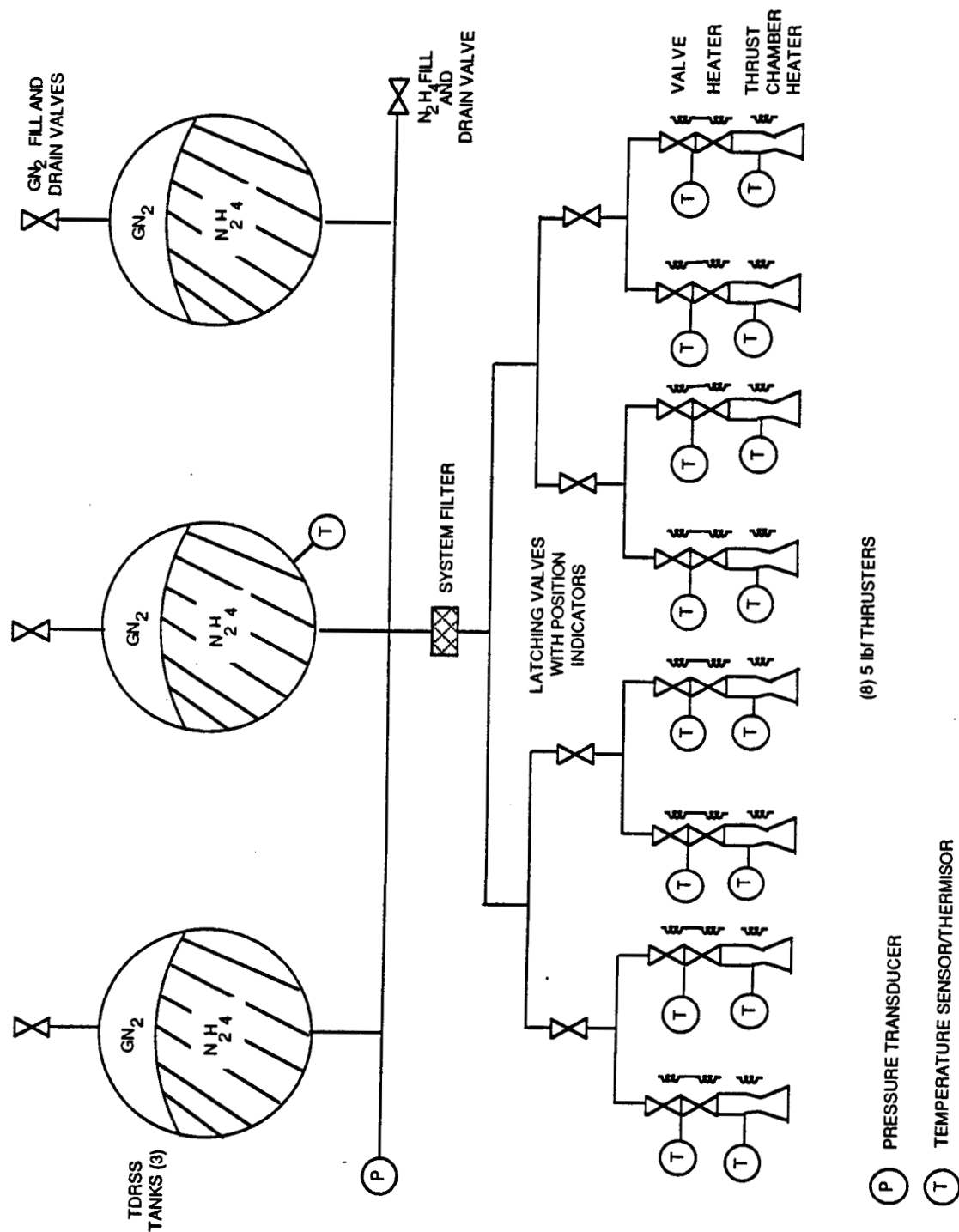
Figure 2.2.4.4-1 illustrates the layout and function of the MOMV power subsystem. The propulsion system is activated through a separate command relay so that the system can be deactivated for recovery by the STS and return to earth. The hydrazine tank heater circuits will be wired directly to the batteries and controlled by a set of redundant thermostats. This will allow operation of the heater circuits from the batteries at all time to prevent freezing of the hydrazine tanks and lines. The battery system has been sized to accommodate the hydrazine heater requirements for up to two days in a worst case cold STS attitude. If the MOMV stays in the bay for longer periods than this the solar arrays will have to be put on line to recharge the batteries.

#### 2.2.4.5 PROPULSION

The propulsion system is designed according to standard spacecraft practice for this type of system and is based on flight proven components and techniques. A schematic of the system is shown in Figure 2.2.4.5-1.

Figure 2.2.4.5-1

# MOMV PROPULSION SUBSYSTEM



# Final Report - Volume II - Study Results

Propellant storage is provided by three TDRSS type tanks that can hold 370 kg (815 lbs) of hydrazine each. Orbit transfer thrust is provided by a cluster of four 5 lbf thrusters aligned along the centerline of the MOMV. Roll control is provided by two pairs of thrusters aligned perpendicular to the transfer thrusters on the tank support structure. Table 2.2.4.5-1 is a component list for the propulsion subsystem.

Component Name	Quant.	Wt (kg)	Pwr (w)	%On	Ave.(w)
Hydrazine		1112.0			
TDRSS Tanks	3	103.4	N/A		N/A
Latching Valves	4	4.0	N/A		N/A
Fill & Drain Valves	4	4.0	N/A		N/A
Pressurant Tank	1	9.0	N/A		N/A
Lines	1	1.0	N/A		N/A
Thrusters 5 lbf	4	14.0	1.00	100	4.0
Thrusters 1.5 lbf	4	14.0	1.00	100	4.0
Totals		1261.0 kg			8.0 w

Table 2.2.4.5-1 MOMV Propulsion Subsystem Component List

The hydrazine tanks are sized to provide orbit transfer capability up to 600 km from an STS orbit altitude of 300 km for payloads with a mass of 10,000 kg maximum. Payloads with smaller masses could be transported to a higher orbit

and those with a larger mass to lower orbits. Figure 2.2.4.5-2 shows the relation of required propellant load to a circular orbit payload drop-off altitude for a 10,000 kg payload.

Mission analysis for the MOMV indicate that the minimum time required to transport a 10,000 kg payload from a 300 km STS orbit to 600 km and return to the STS orbit is a little under two days. This is based on the differences in the orbit periods of the 300 and 600 km orbits. The synodic period for minimum transfer time can be estimated from:

$$P_s \sim \frac{P_{450} P_{300}}{P_{450} - P_{300}}$$

where:  $P_{450}$  = Orbital period at mean altitude (1.560 hr)

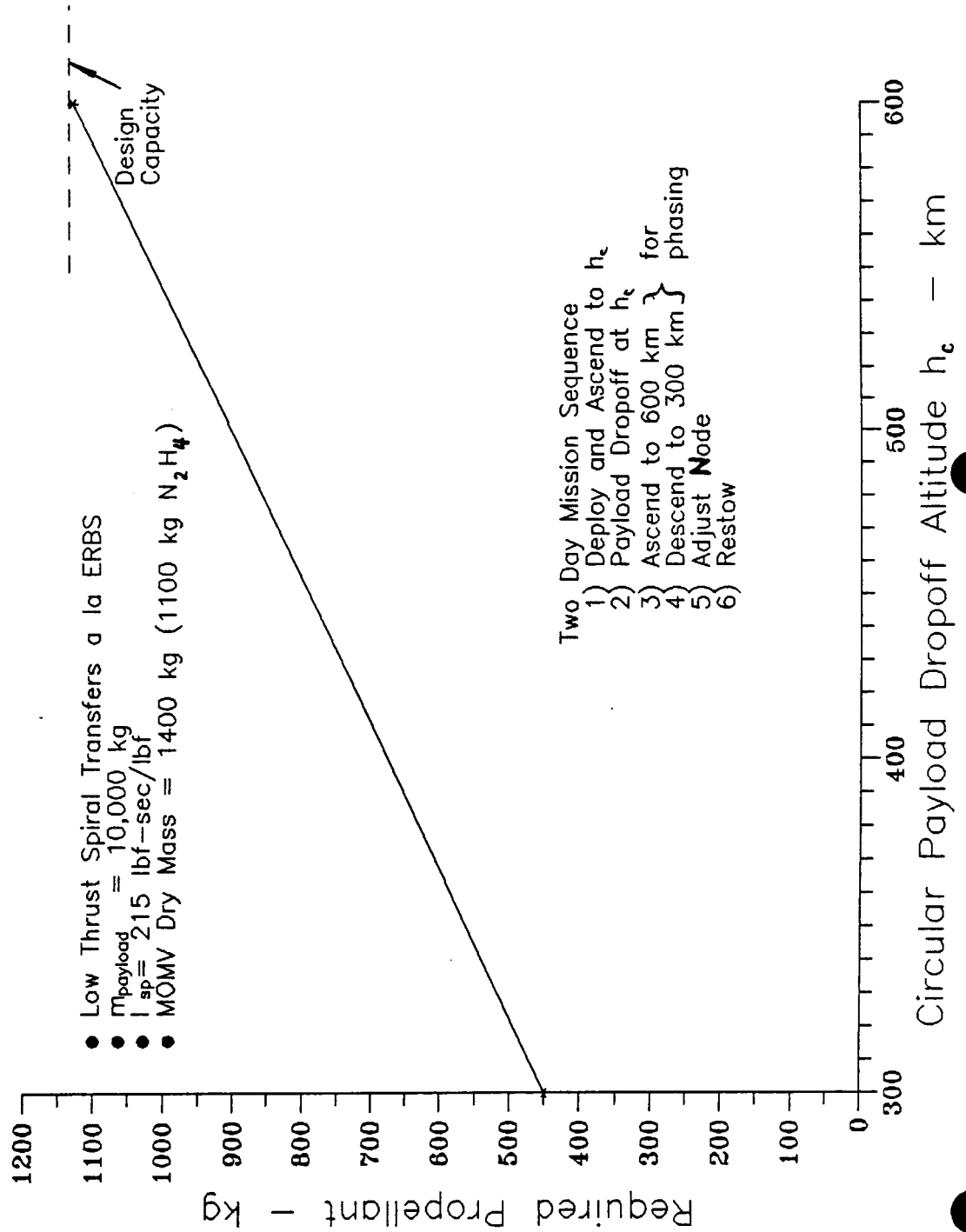
$P_{300}$  = Orbital period at STS orbit altitude (1.509 hr)

This results in an approximate period of 46.2 hours before the MOMV and Orbiter celestial longitudes are again equal. This equation assumes uniform ascent and descent rates and a short payload drop-off time. For mission planning purposes it is assumed that if the desired payload drop-off altitude is less than 600 km that the MOMV will continue up to 600 km before starting its descent back to the STS altitude for rendezvous.

The propellant sizing for the MOMV also includes provision for maximum required nodal readjustment due to the difference in the orbit altitudes during the payload transfer operations. The amount of change required is dependent on the orbit inclinations and the difference in orbit altitudes. The maximum value will occur for an inclination of 45 degrees, and for the MOMV baseline mission this results in a differential nodal regression of 0.86 degrees which requires a plane change of 0.61 degrees and a velocity change of 82 m/s (270.6 ft/s).

Figure 2.2.4.5-2

# MOMV Propellant Manifest Sizing



#### 2.2.5 OPERATIONAL TIMELINE

MOMV operations can be divided into three main areas; STS cargo bay prior to payload transfer, free-flyer operations, and STS cargo bay for de-orbit and landing. Figure 2.2.5-1 shows the operational sequence from STS launch through completion of the payload orbit transfer and return to the STS cargo bay for landing. Figure 2.2.5-2 is a mission operations timeline for a typical MOMV flight.

Following the STS launch and opening of the cargo bay doors a payload in-bay checkout will probably be performed to verify the readiness of the payload for deployment by the MOMV. Once this checkout is completed the MOMV will be activated by astronaut command from the aft flight deck. A short checkout sequence will follow to verify the operation of all MOMV systems except the propulsion system. This system will not be activated until the MOMV is clear of the STS.

Once the MOMV checkout is completed the RMS will be used to remove the payload from the cargo bay. A command is sent to the MOMV to extend the MMS-FSS berthing latch while the payload is attached to the RMS and clear of the bay. After the berthing latch has reached its fully extended position the RMS will position the payload attachment fitting over the MOMV berthing latches. When the attachment fittings are properly aligned a signal will be sent to the MOMV to close the latches.

The RMS will then be used to lift the combined stack (MOMV and payload) out of the cargo bay and prepare for release. While the MOMV is still attached to the RMS the communications link through the TDRSS satellite will be verified. When the stack is clear of the STS the RMS will release it and the STS will use its RCS thrusters to back away. Crew interaction is now complete for this phase of the MOMV mission. This part of the MOMV mission will occupy about 1.5 hours of crew/STS time.

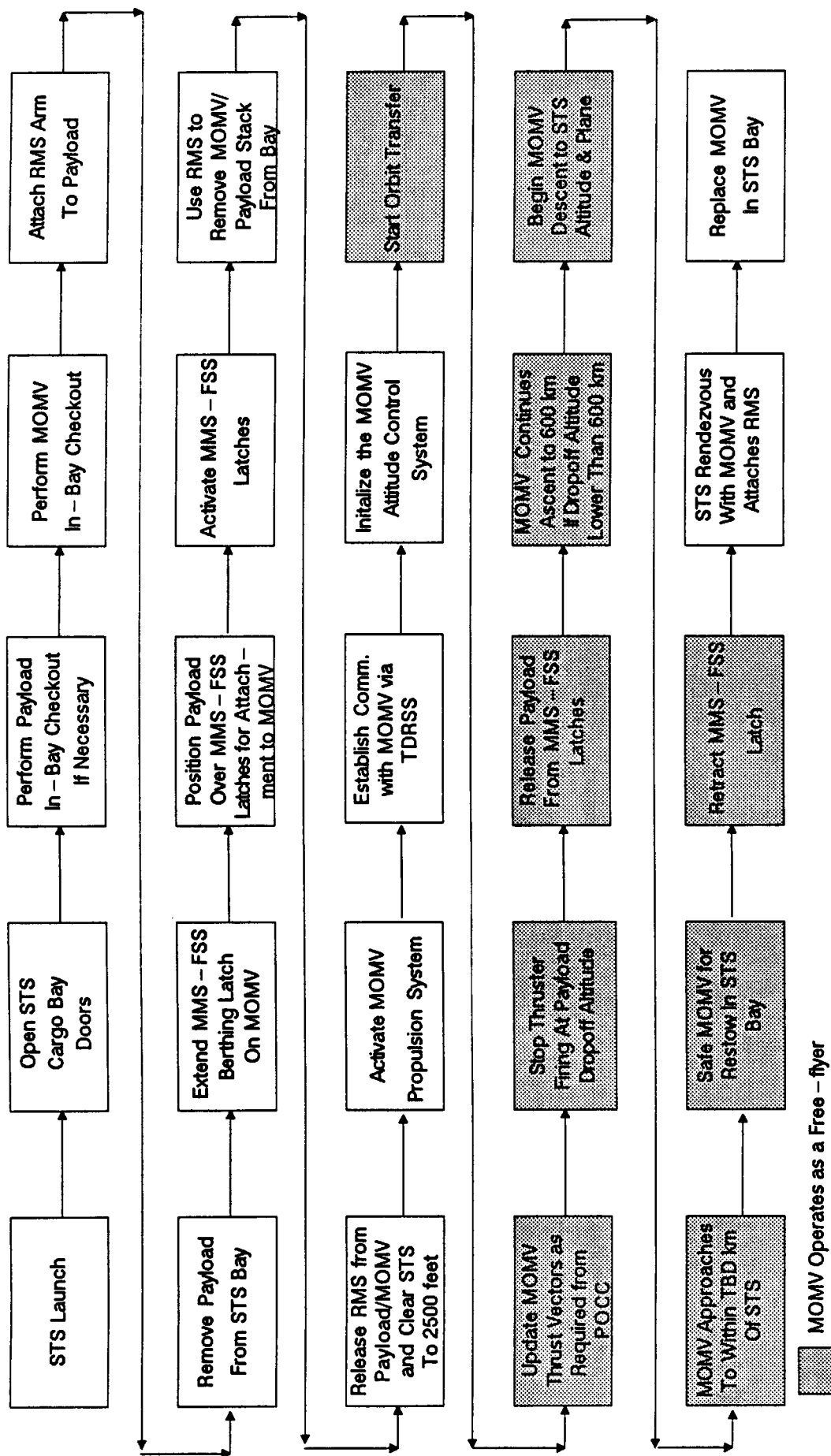
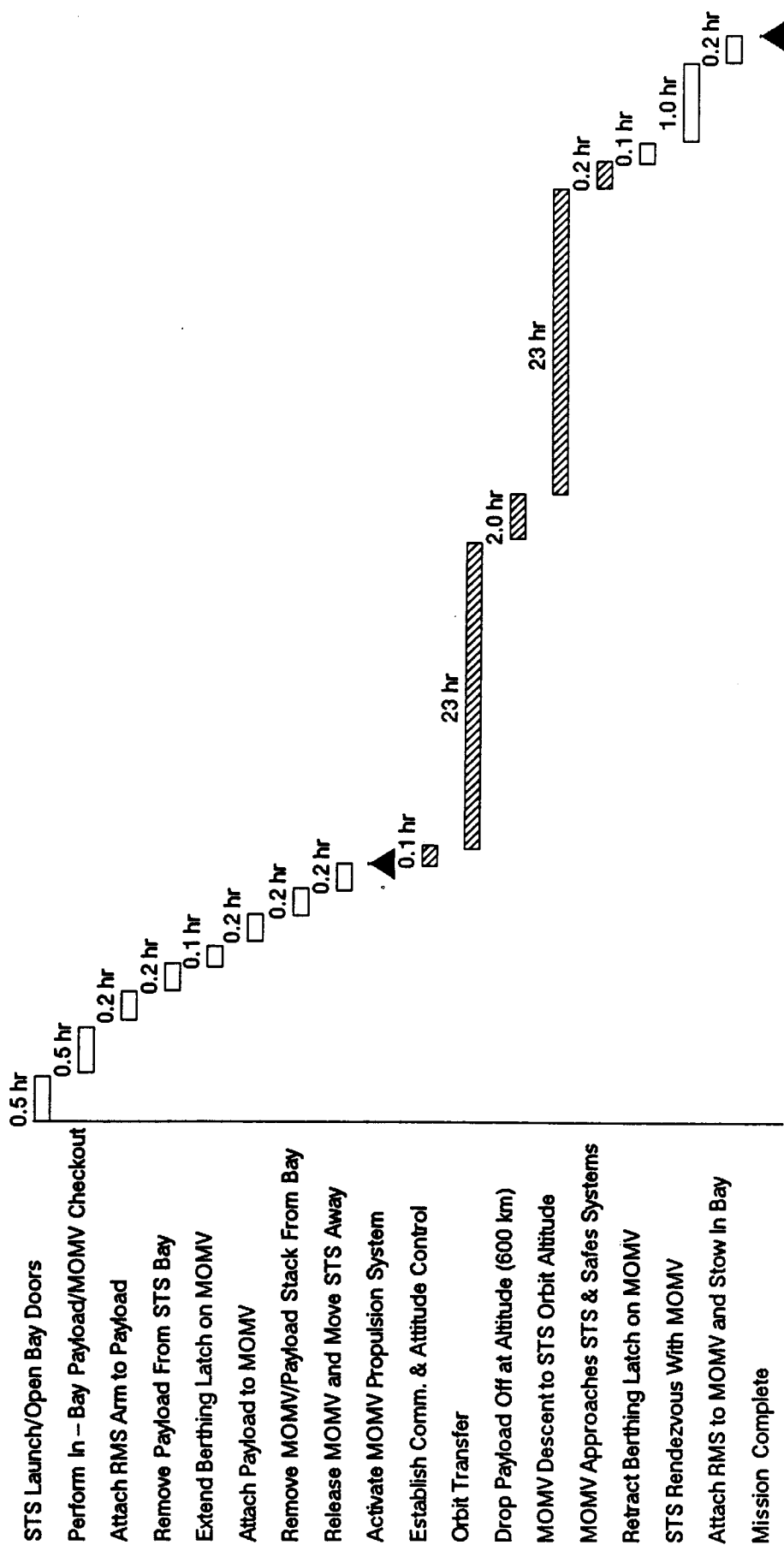


Figure 2.2.5 - 1 MOMV Operational Sequence



Figure 2.2.5 – 2 MOMV Deployment Timeline



When the STS is clear of the MOMV its propulsion system will be activated and initial transfer attitude established. Once it is determined that all MOMV systems are operating properly, a command will be sent by ground controllers to start the orbit transfer phase of the mission. The normal attitude for the orbit transfer is with the keel thrusters aligned with the velocity vector and the solar array surface normal vector 45 degrees out of the orbit plane.

The orbit changing maneuver occurs very slowly and allows plenty of time to make mid-course corrections, if necessary. Normally the progress of the transfer will be monitored by ground tracking stations and this information will be used to update the MOMV attitude control commands. The MOMV thrusters are sized to make the trip from 300 km to 600 km with a 10,000 kg payload in less than 24 hours.

When payload drop-off altitude is reached the MOMV thrusters are commanded off. At this time the berthing latches are commanded open. The opening of the berthing latches provides a small separation velocity between the payload and the MOMV. This velocity is augmented by a short firing of the yaw thrusters, which are canted 20 degrees to give a thrust component toward the payload attach plane. The MOMV and payload are allowed to drift apart for up to 2 hours before the MOMV is reoriented for the return to STS orbit altitude.

If the payload drop-off altitude was less than 600 km the MOMV will be commanded to continue its ascent to 600 km before starting the descent. This is to assure the proper phasing between the orbits and to decrease the total time required to rendezvous with the STS. To start the descent the MOMV is yawed 180 degrees to orient the orbit transfer thrusters to fire opposite the orbital velocity vector. The orbit descent is essentially the same procedure used for the ascent. Orbit tracking and corrections are provided by ground stations as necessary.

The MOMV will continue its descent and adjust thruster firing to arrive at the STS altitude in the vicinity of the STS. The exact meaning of "vicinity"

will have to be coordinated with regard to STS safety, but will probably mean that the MOMV approaches to within 1 km. At this time the MOMV attitude will be stabilized and the berthing latch retracted in preparation for STS rendezvous and pickup by the RMS. Once the attitude is stabilized the MOMV propulsion system will be deactivated.

The STS will now use its RCS system and rendezvous radar to approach the MOMV and attach the RMS to the MOMV grapple fixture. Once this is accomplished the MOMV will be placed back in the cargo bay for return to earth, refurbishment, and reflight.

In the cargo bay the hydrazine line and tank heaters will remain connected to the MOMV batteries so that and remaining hydrazine can be kept from freezing. The batteries are sized to allow operation of the heaters for 48 hours following replacement in the cargo bay.

#### 2.2.6 MOMV COST ANALYSIS SUMMARY

A cost analysis for the MOMV was performed using the RCA PRICE cost modeling system and a Lotus-123 based LCC model. A summary of the results of this analysis is presented in Table 2.2.6-1. Details of this cost effort are presented in the separate cost document accompanying the study report (DR-6 Sections 2-1 thru 2-5 and its Appendices).

Hardware Design and Development Cost	\$ 13,019,000
Hardware Production Cost	\$ 15,345,000
Operations and Support Cost	\$315,175,000*
Software Cost	\$ 4,025,000
Total Mini-OMV Cost	<hr/> \$347,564,000

\*Note: STS Launch Costs are \$296,227,692

Table 2.2.6-1 Mini-OMV Costs (Constant 1987 Dollars)

# SUMMARY TABLE-MINI-OMV

PHYSICAL CHARACTERISTICS	QUANTITY ON DESCRIPTION
Mass	
Structure	o 1300 kg (2868 lb)
Propellant	o 1112 kg (2450 lb)
STS Attachment	o Normal keel and sill trunnions
Power System	o Batteries
	o Solar arrays
Attitude Control	o ERBS-type 3-axis
Propulsion System	o hydrazine
OPERATIONAL CHARACTERISTICS	
Launch/Recovery	o STS cargo bay
Payload Attachment	o on-orbit using RMS and FSS latches
Transfer Capability	o 10,000 kg (22046 lb) payload from nominal STS altitude (300 km) to 600 km.
	o 48 hour mission time
SPECIAL TETHER BENEFITS	o none-tether alternative
COSTS	o Table 2.2.6-1

### 2.3 SHUTTLE TETHER DEPLOYMENT SYSTEM (STEDS)

Deploying payloads on a tether from the STS Orbiter is a technically challenging task. The dynamics of two orbiting bodies connected by a tether have been studied for several years by many investigators. These studies have identified a variety of control techniques to facilitate the deployment process, especially the initial separation phase. One of the early efforts in this study was to evaluate these various techniques in terms of the cost to develop a system to implement them for payload weights and deployment distances of interest in this study.

It has been assumed for this study that payload retrieval is not a requirement for the tether deployer system considered here. This leaves two main areas of tether deployment design where significant cost savings are possible. One area is in the control of the initial deployment and the other is in the management of the energy created by the payload deployment.

One promising approach that addresses both of these design drivers is referred to as SEDS (Small Expendable Deployer System). This concept is under study for NASA by another contractor and has been presented at several technical meetings.

The SEDS concept is to use the Shuttle RMS to place the payload above the cargo bay and then release it. The deployment is initiated by firing the RCS thrusters to cause the Shuttle to drop down and away from the payload until a small separation distance is achieved. At this point a second RCS stops the separation and allows the deployment to continue using the Coriolis forces.

The advantage of this approach is that the initial separation control is simplified and the required energy dissipation is significantly reduced because of the lower back tensions involved.

SEDS relies principally upon back tension for control of its smaller sized tether and payload. The tether sizes and payload weights of concern to our study are two to three orders of magnitude greater than in the SEDS study. A scale-up of this magnitude would certainly require significant modifications, if not radically different system element design concepts than those proposed for the present SEDS concept. Thus the development of a realistic cost model based upon this type of system is not believed to be feasible at this time.

A modified SEDS type of horizontal deployment was considered in which the orbiter provides control using its thrusters, as opposed to using back-tension. It was felt that this approach might well turn out to be both a technically simpler and less expensive alternative for our larger payloads.

Appendix A presents considerable analysis relative to some basic aspects of this latter approach. Unfortunately the results of this analysis indicated that there are just too many uncertainties in this approach to base a credible design or cost model on. Therefore, our design and cost model is based on a more conventional system that uses a vertical gravity gradient type deployment without reel-in capability.

#### 2.3.1 REQUIREMENTS

The design requirements for a Shuttle Tether Deployment System (STEDS) are derived from the general guidelines stated earlier. These include STS safety, minimum weight and cargo bay length, payload design impacts, and mission requirements. The mission requirements consist of transporting a payload of up to 10,000 kg from a nominal 300 km STS orbit to a 600 km orbit. The mission orbital parameters are a derived requirement based on earlier analysis (see Section 2.1.1).

The orbit resulting from the tether release may be either circular or elliptical depending on the shape of the original STS orbit. However, the general case for the STEDS will result in an elliptical orbit for the payload and the Orbiter.

To minimize the impacts on the payload design the attachment to the tether will be accomplished on-orbit with the RMS. This will allow the payload designer a certain amount of freedom in the placement of the tether attach point on the payload.

In addition the payload side of the tether release mechanism must be autonomous. This will allow the tether deployer to operate without interaction with the payload subsystems. The tether release should be accomplished in a manner that will assure non-impact of the tether on the payload surfaces after release.

Safety requirements for the STEDS mainly concern those items associated with flying on the Orbiter. In particular the design must assure that the tether does not come into contact with any of the Orbiter structure, it must have a method of detecting a broken tether detection system, and a method of quickly cutting the tether when a break is detected. The STEDS must also manage the heat generated during the deployment sequence.

To minimize costs the STEDS should be lightweight and occupy the minimum amount of cargo bay space.

#### 2.3.2 CONFIGURATION

The STEDS is optimized for weight and bay length. These are important considerations in life cycle cost (LCC), since the transportation costs are the biggest cost drivers.

Weight has been minimized by designing the system for a one time use of the tether and limiting the size of the tether positioning boom. The use of a disposable tether allowed a weight reduction by eliminating the need for a reel and level wind mechanism, which also reduced the total structural weight and system complexity.

Figure 2.3.2-1 is a view of the STEDS system in the Orbiter cargo bay. The structure is made of aluminum tubing. The tubing is 10 x 10 x .5 cm (4 x 4 x .2 in) and joined together with machined end-fittings. The replaceable tether spool is contained within the structure and is sized to accept 70 km (42 miles) of .457 cm (.18 in) diameter Kevlar tether. The "A" frame structure to support the radiator assemblies and tether positioning boom is also constructed of the same light weight aluminum tubing.

The generator, brake, clutch and control electronics are mounted on a freon cooled cold plate in the middle of the structure. The open design of the truss structure allows easy access to these items for installation and checkout.

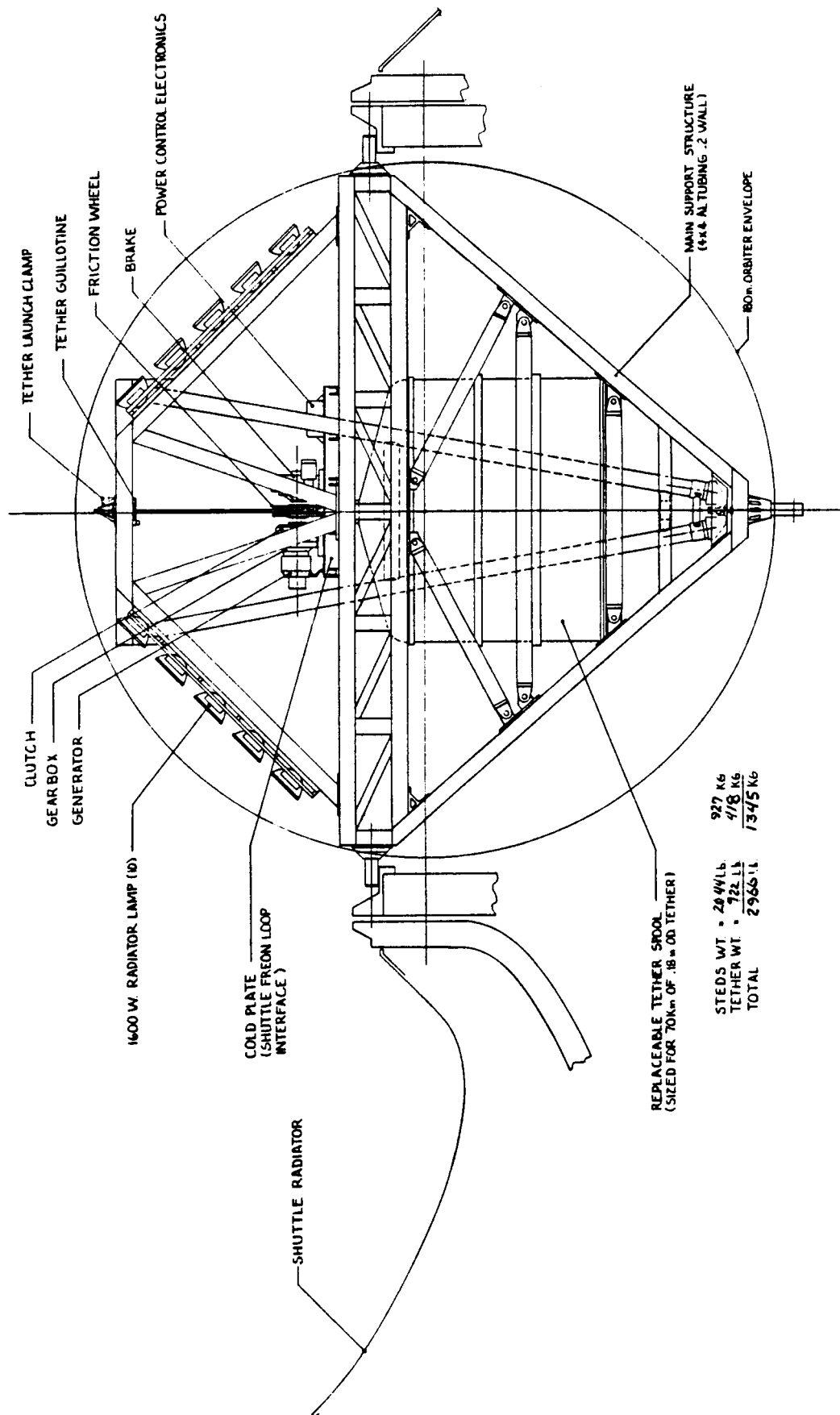
Figure 2.3.2-2 is a side view of the STEDS. In this view the tether positioning boom is shown in both its stowed and deployed positions. The boom deployment cable is used to transmit tether tension forces to the keel area of the STEDS and to position the tether line of action relative to the Orbiter CG. A motor at the base of the structure controls the position of the boom with inputs from the tether control electronics.

This view of the STEDS also shows the unique tether canister design employed. The canister is not cylindrical, but rather bath tub shaped to minimize the amount of cargo bay length occupied in the stowed configuration. Further study of this tether packing concept will be required before actual detailed design of a STEDS system could begin.



# SHUTTLE TETHER DEPLOYMENT SYSTEM (STEDS)

Figure 2.3.2-1



SHUTTLE TETHER DEPLOYMENT SYSTEM (STEDS)

# STEDS - SIDE VIEW

Figure 2.3.2-2

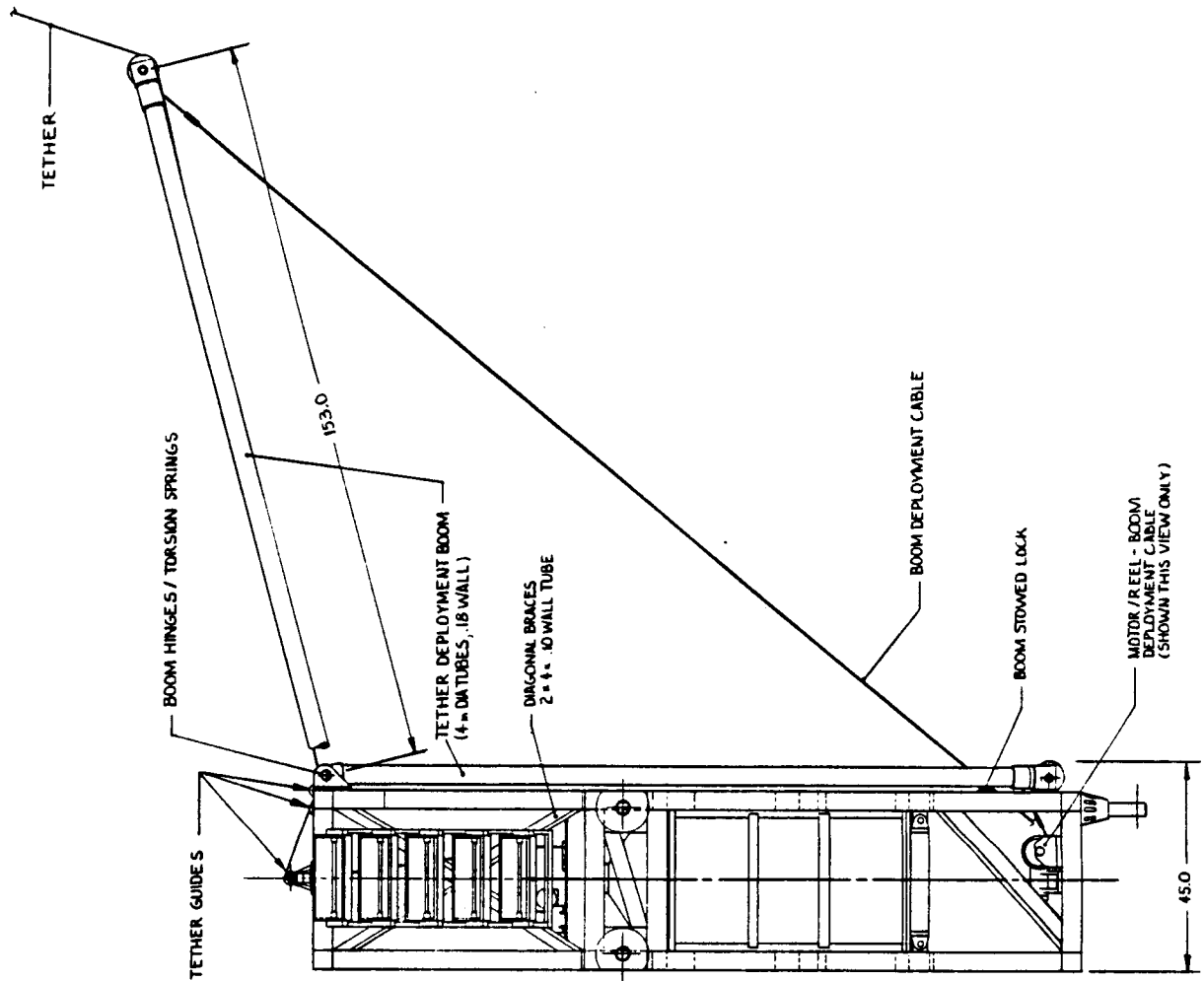


Figure 2.3.2-3 shows the details of the tension control system. The friction pulleys are connected to the generator drive shaft through three separate drive belts. The rotary motion is transferred from the shaft to the clutch assembly and simultaneously to the friction brake. The clutch transmits the motion to the generator which converts it into electricity and back tension to control the payload deployment rate.

Figure 2.3.2-4 is a detail drawing of the payload/STEDS end effector. This device is used to attach the payload to the tether and to automatically separate it when the deployment is completed or if a broken tether is detected by the integral load cell.

Everything above the "Tether Terminal Fitting" is attached to the payload on the ground, and is referred to as the "tether end-effector." This device is designed to detect a decrease in the tether tension due either to a break or deliberate cutting at the completion of the deployment. When the "break" is detected the system releases itself at the clamp assembly and is pushed free of the payload by the positive separation spring.

The tether is attached to the device by positioning the tether clamp collet over the tether terminal fitting and applying a slight downward pressure with the RMS. This activates the over-center locking mechanism in the collet.

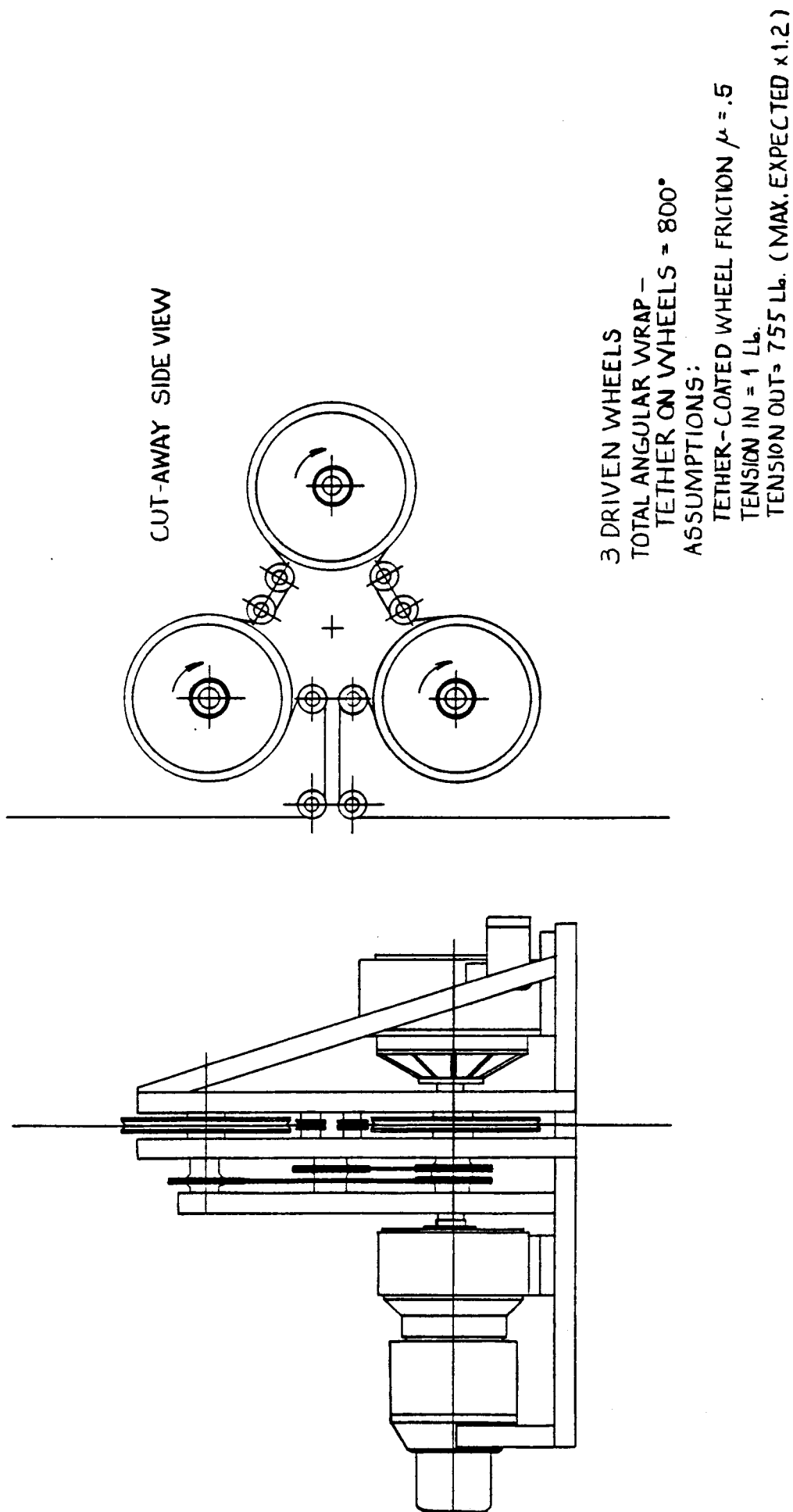
### 2.3.3 STS INTERFACE

The STEDS electrical interface with the Orbiter is shown in Figure 2.3.3-1. The standard switch panel (SSP) is used to allow the astronauts to control the activation of the various STEDS subsystems. There will be a total of five switches used on the SSP.

One switch will allow activation of the STEDS control electronics. A second switch is used to activate the freon fluid pumps to cool the STEDS equipment mounted on the cold plate. A third switch is used to activate the boom. This

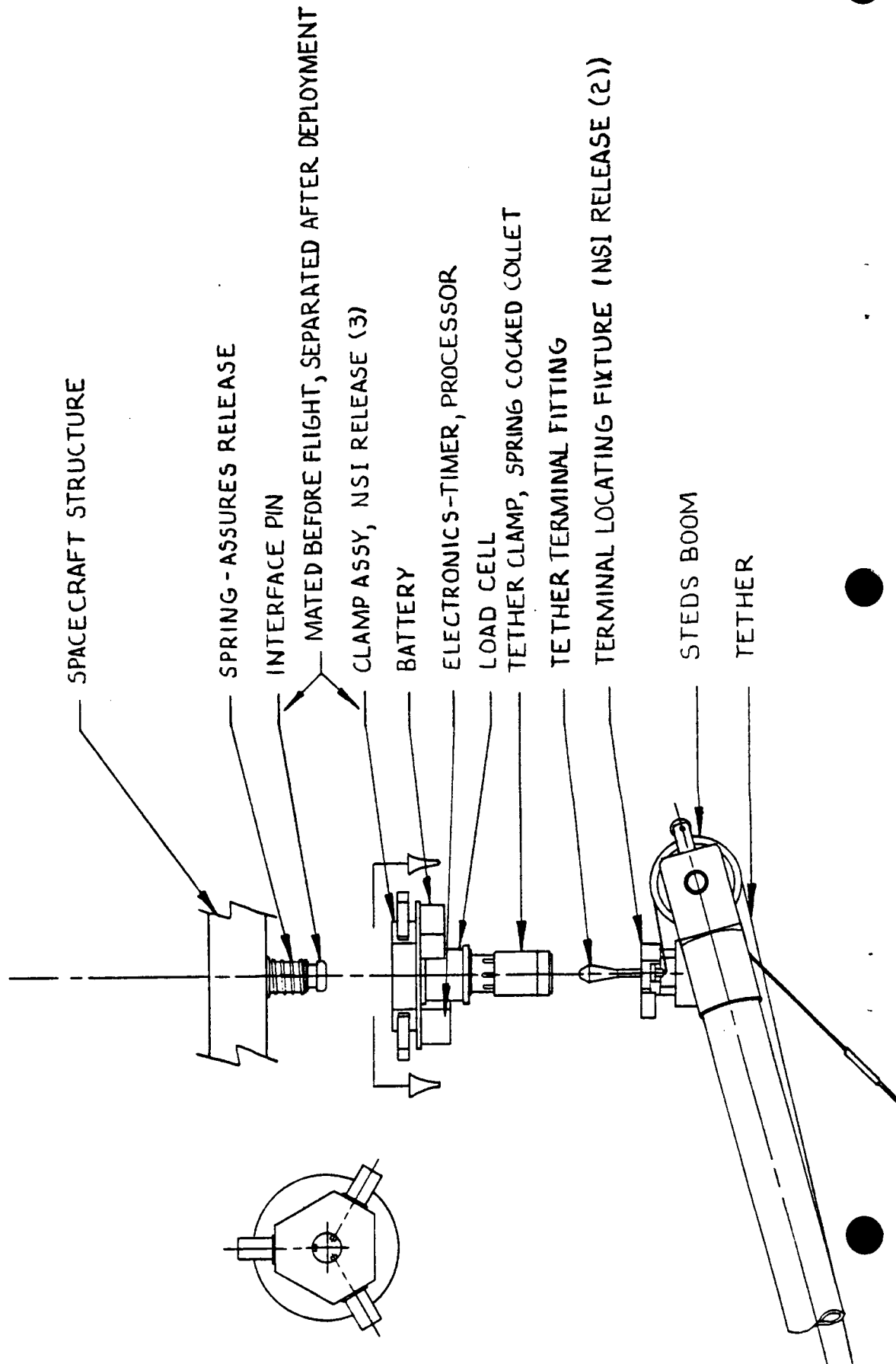
# ALTERNATIVE STEDS TETHER DEPLOYMENT CONTROL CONCEPT

Figure 2.3.2-3



# STEDS REMOTELY MATEABLE TETHER END EFFECTOR CONCEPT

Figure 2.3.2-4



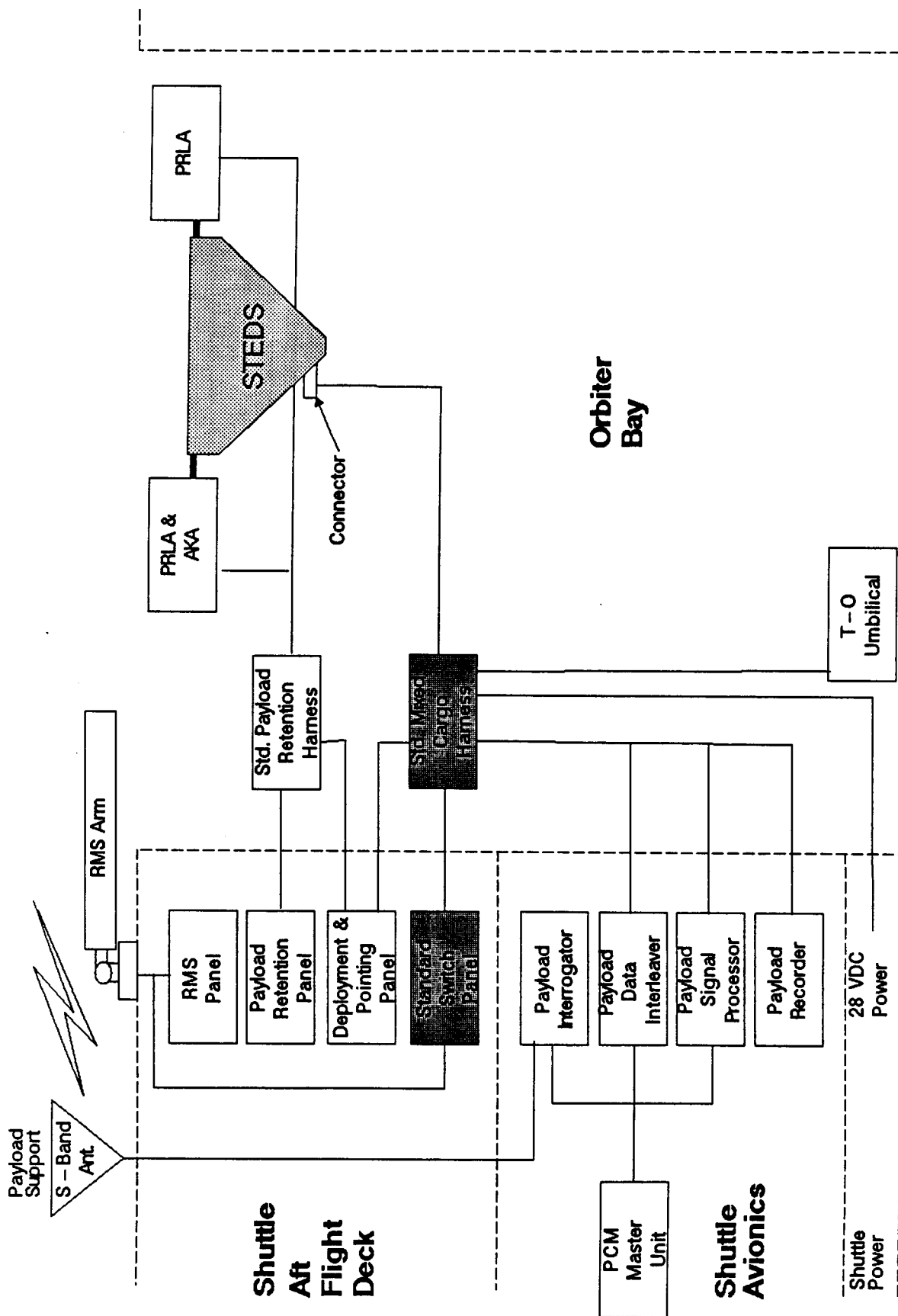


Figure 2.3.3 – 1 STEDS/STS Electrical Interface

switch will deploy the boom when it is placed in the "On" position, and the boom will retract and stow itself when the switch is placed in the "off" position. A fourth switch is used to start and stop the payload deployment. This switch will open the tether launch locks when put in the "deploy" position. In the "Stop Deployment" position a command will be sent to the controller to apply required tether tension by activating the generator and the friction brake. The final switch is used to manually activate the tether guillotine in case of emergency or failure of the STEDS control electronics to activate the switch separating the tether from the STS at the end of the payload deployment.

#### 2.3.4 SUBSYSTEM DESCRIPTIONS

##### 2.3.4.1 STEDS STRUCTURE

The STEDS structural design and configuration was driven by several key requirements placed on the system. The two that had the largest impact on the design were cargo bay length and Orbiter safety.

To reduce operational costs the total cargo bay space occupied by the STEDS must be minimized. This is due to the STS pricing formula that relates the total launch cost to payload weight and length. A payload must have a weight per unit length of more than 1500 kg/m (1000 lb/ft) before the launch cost will be based on weight instead of length.

The STEDS structure keeps cargo bay length to a minimum by using a deployable boom and an innovative tether container design. The boom design depends on the placement of STEDS next to the payload to be deployed, or next to another payload that will be deployed from the Orbiter bay before the STEDS boom needs to be deployed. If this is not possible then the STEDS would be charged with the extra bay length needed to deploy the boom and operations costs would increase significantly.

The tether canister is mounted in the center of the truss structure below the Orbiter sill line. This allows easy connection to the main structural supports and ideal placement of the tether guide mechanisms. The tether canister has a stretched cylindrical cross section to minimize required bay length. The current design assumes a 70 km tether for sizing of the canister. However, longer and larger diameter tethers could be supported without changing the length of STEDS by re-designing the structure below the sill line to more efficiently use the available cargo volume. A study of the effects canister shape has on tether deployment dynamics is needed before the actual scaling limits of this design approach can be determined. This type of study is beyond the scope of the present contract.

The structure above the Orbiter sill line is used to support the high temperature thermal radiator lamps and to serve as a pivot point and support for the boom.



## Final Report - Volume II - Study Results

Table 2.3.4.1-1 is a list of the STEDS structural components.

Table 2.3.4.1-1 STEDS Structural Components List

Component Name	Quant.	Unit Wt (kg)	Total Wt (kg)
Main Structure	1	332.4	332.4
Rad. Support Frame	1	108.8	108.8
Trunnions	5	12.9	64.5
Tether Canister	1	188.7	188.7
Tether Boom	1	41.3	41.3
Total			735.7

### 2.3.4.2 STEDS TENSION CONTROL

The STEDS tether deployment system utilizes a tension only control technique. This method of deployment was adopted to simplify the design and to reduce the operational cost of the system. The tension in the tether can be controlled with a simple generator arrangement by varying the voltage to the excitor field windings in response to the desired back tension in the tether and the sensed tether velocity. The generator will act as a brake by converting the rotational energy to electrical energy. The electrical output of the generator will be dissipated in high temperature lamps and internal joule heating and friction in a fluid cooled cold plate assembly. A tether tension and velocity sensor will be incorporated in the tether guide at the end of the boom to provide control feedback for the electronics. A clutch is provided in the design to allow the generator to be disconnected from the

drive during the early part of the deployment. This is needed because of the low tensions during this phase of the deployment and the residual back tension in the generator.

The tension force in the tether during deployment will induce a moment on the Orbiter if the line of action is not through the Orbiter center-of-mass. This moment will cause the Orbiter attitude to change until the tether tension force vector passes through the CM. If the STEDS did not have a boom and was not mounted at the Orbiter CM the Orbiter movement in response to the tension forces might cause the tether to come into contact with the Orbiter. Since it would be very restrictive to require that the STEDS always be mounted at the Orbiter CM a boom has been designed into the system to allow some control over the alignment of the tension vector during payload deployment.

Figure 2.3.4.2-1 shows the optimal placement for the STEDS in the Orbiter cargo bay. Also shown is the STEDS mounted at the Orbiter CM. This aft position allows the boom to maintain good clearance from all Orbiter surfaces even during tether librations of up to 15 degrees. It also allows the Orbiter to maintain a level attitude during the deployment. In this mounting location the payload to be deployed would be placed in the cargo bay immediately in front of the STEDS system.

Figure 2.3.4.2-2 shows the STEDS system positioned in the cargo bay for maximum payload length capability. However, in this position the orbiter attitude will be nose up for the deployment because of the distance from STEDS to the Orbiter CM. This arrangement will result in Orbiter oscillations in response to tether librations because the limited control authority of the boom in this position. The dynamic response of the tethered payload and Orbiter system in this configuration will have to be simulated to verify that this system is stable.

Figure 2.3.4.2-1  
STEDS Optimally Positioned in STS Bay

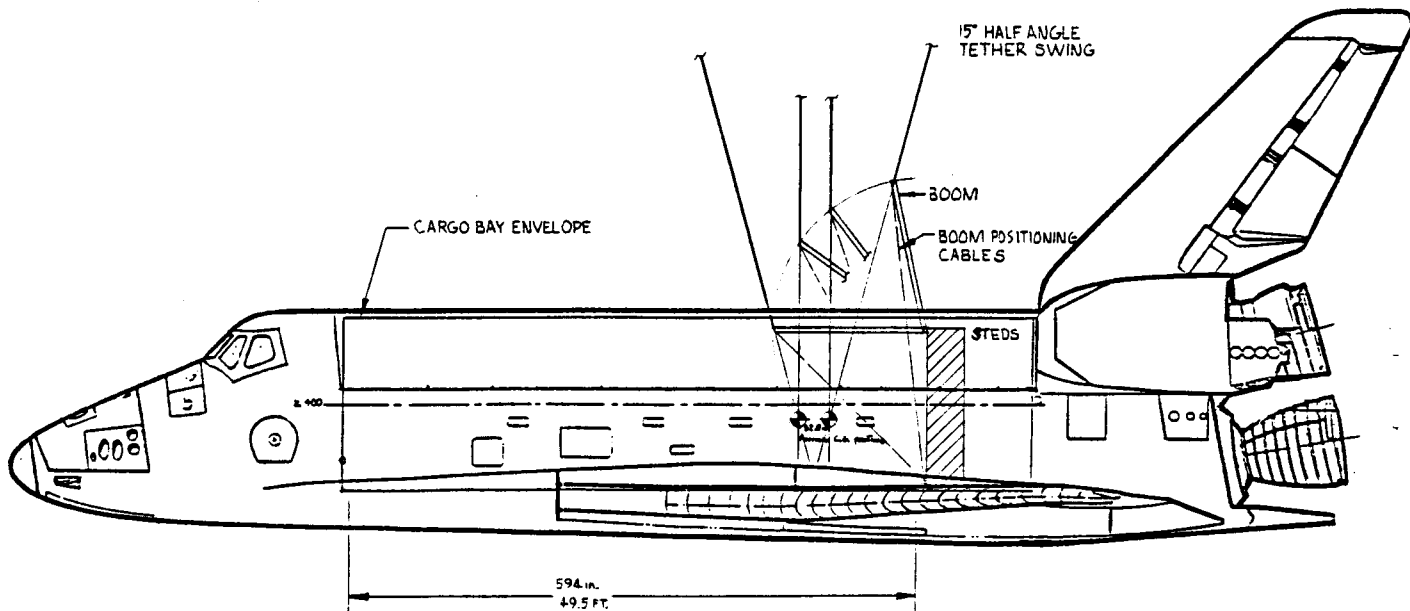
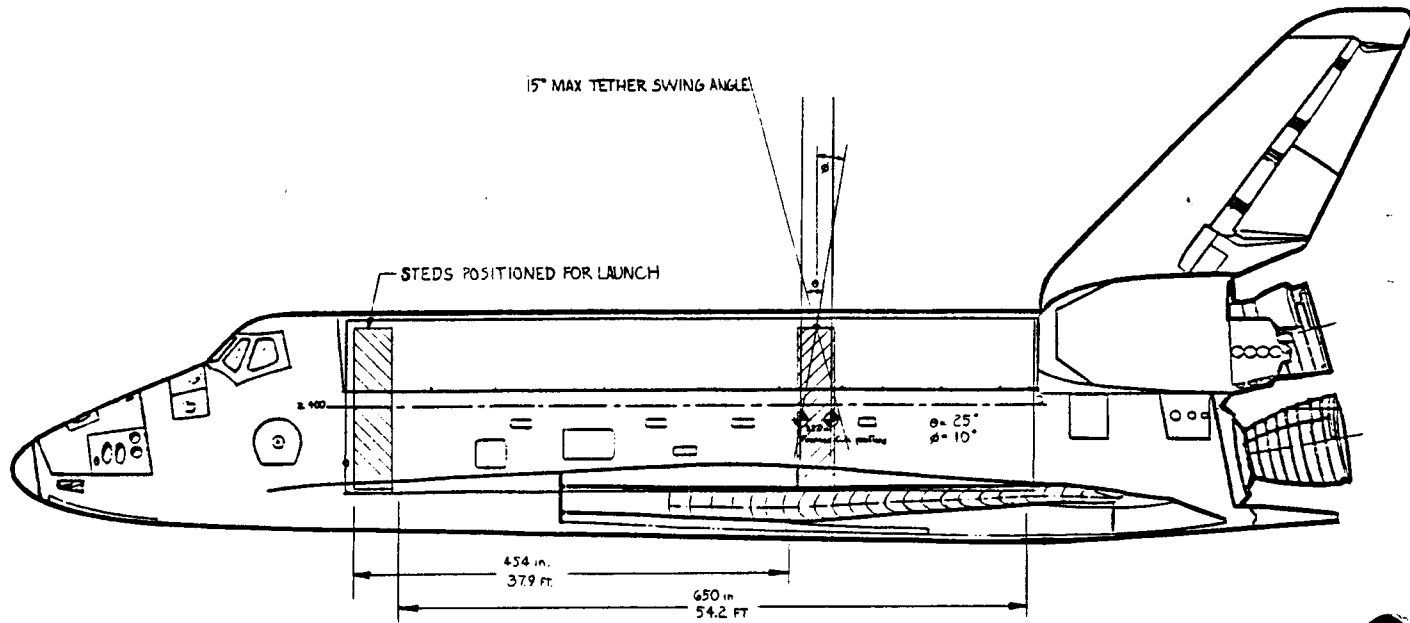
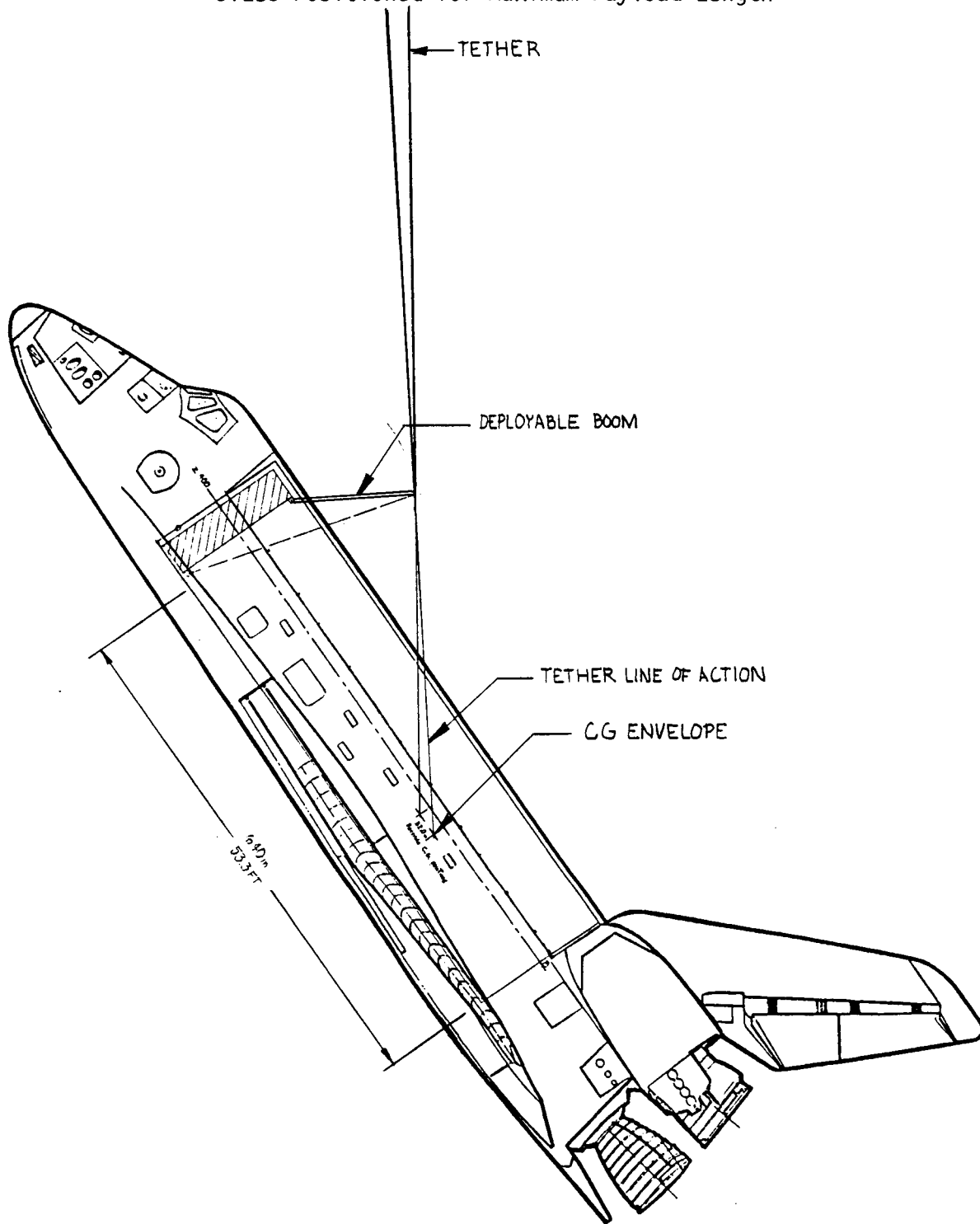


Figure 2.3.4.2-2  
STEDS Positioned for Maximum Payload Length



Tether control starts at the canister where the tether has been carefully wrapped about a mandrel to assure that as it departs no binding of the tether occurs. As the tether departs the canister it passes through a set of friction wheels that control the tension force. The resistance to tether movement is provided by linking the three friction wheels to a drive shaft that connects through a clutch and gear box to an aircraft type generator. The generator output is connected to a load composed of high temperature quartz lamps similar to those used for Orbiter bay lighting. The output of the generator is controlled by the control electronics box. Figure 2.3.2-3 shows the primary component arrangement for the tension control devices.

The control electronics box monitors the output from the tether sensors and adjusts the generator excitor winding voltage to control the electrical output. This box also controls the number of lamps that are connected as load to the generator, operation of the friction brake, and sends status information to the boom controller electronics.

The tether is routed through the friction pulleys and up through the guillotine and launch lock mechanisms. From there it is routed over a guide pulley out to the end of the boom where it is attached to the tether terminal fitting (see Figure 2.3.2-4). Attachment to the payload is accomplished on-orbit by the RMS using the tether end effector mounted to the payload.

The boom control mechanisms and electronics are mounted in the keel area of the STEDS system (see Figure 2.3.2-2). The boom control electronics sense the current position of the boom and activate the motor in response to inputs from the tension control electronics and/or the SSP. This device also controls the launch lock mechanism for the boom.

## Final Report - Volume II - Study Results

The following is a list of tension control components.

Component Name	Wt (kg)	Power (w)
Tension Control Electronics	4.5	35.0
Tether (70 km)	417.2	--
Tether End Effector	6.8	5.0
Clutch	11.3	--
Generator	22.7	--
Gear Box (64:1 ratio)	9.1	--
Friction Brake	13.6	--
Friction Wheel Assy.	5.0	--
Launch Clamps	1.4	--
Guillotine	0.5	--
Electrical Harness	11.3	--
Tether Guides/Sensors	2.3	5.0
Boom Controller/Motor	6.8	35.0
Totals	512.5 kg	80.0 watts

Table 2.3.4.2-1 STEDS Tension Control Components

### 2.3.4.3 THERMAL CONTROL

The thermal requirements include dissipation of the energy generated by payload deployment and controlling the temperature of the electronics and other equipment in all Orbiter environments. Figure 2.3.4.3-1 illustrates the main components and approach taken for the STEDS thermal control system (TCS).



The main features of this design are; high temperature quartz lamps, active fluid loop control of major components and passive control for the tether canister and boom control mechanisms.

Deployment energy dissipation presented the biggest design driver for the STEDS TCS. Figure 2.3.4.3-2 presents the dissipation requirements for various deployment scenarios for a 10,000 kg payload. The faster the deployment time the higher the peak dissipation that must be dissipated. The curves indicate that for an 8 hour deployment the peak dissipation is about 9.2 kW and for a 24 hour deployment about 2.0 kW. These dissipation levels present a serious challenge to the TCS design task.

Several options were considered before the current design was baselined. The standard options of passive radiator, fluid pumped radiator, peak energy storage devices and heat pipe radiator were considered and quickly eliminated do to inability to handle the load across a small enough temperature gradient or excessive weight and/or size requirements.

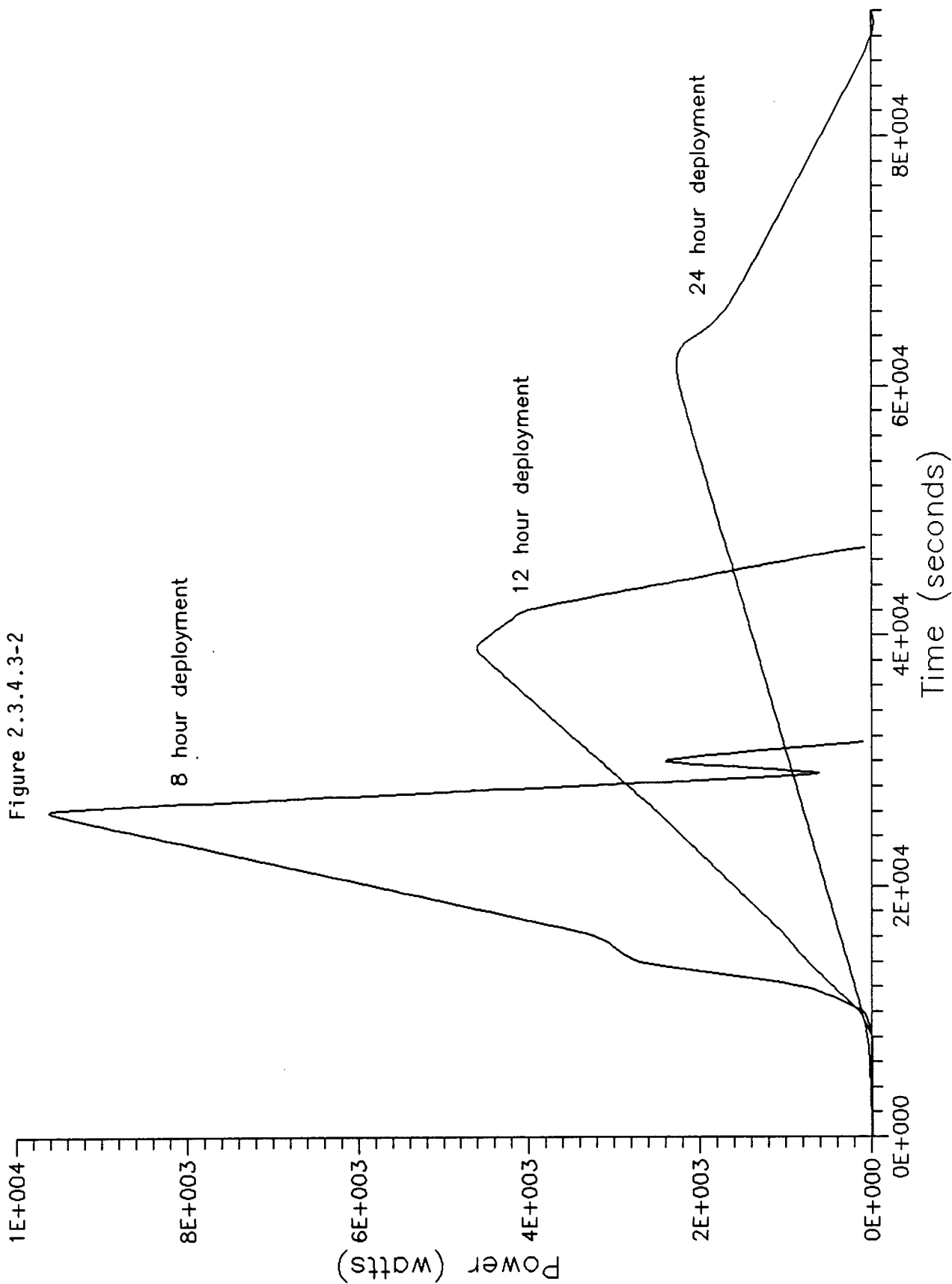
The options that survived the initial screening included; high temperature resistive radiators, high temperature quartz lamps, direct dump to the STS fluid loop, and an innovative approach consisting of transferring the energy to the departing tether.

Direct dump to the Orbiter fluid loop is a straight forward approach to the problem, however it has several drawbacks that make it unsuitable in comparison with the other approaches considered. The biggest problem with this approach would be that it would restrict deployment times for larger payloads to more than 24 hours due to the heat dump capability of the Orbiter radiators. If the orbiter is powered down and the extra radiator kits are flown the Orbiter coolant system can provide a maximum of 8.5 kW of payload coolant. This would be available to a dedicated payload, but a mixed cargo payload would have to share this load capability. In addition the Orbiter would not want to stay in a powered down condition for several hours while



# Power Generation vs Deployment Time (10,000 kg Payload to 70 km)

Figure 2.3.4.3-2



the deployment was taking place. The capability of the system during normal Orbiter operations is only 1.5 kW continuous. This level would not even handle the peak requirements of the 24 hour deployment scenario. This approach was rejected for the STEDS deployer design, but should be reconsidered in latter studies if payload size can be reduced and/or deployment times increased.

High temperature resistive radiators are a viable concept for the STEDS system. The resistive element could be constructed from nichrome wire or some other high temperature metal. The device would essentially be a radiant heater, and would use ceramic spacers for isolation from the main structure. A polished reflector would be installed behind the high temperature element to direct the energy away from Orbiter and STEDS surfaces. This concept is essentially equivalent to the selected baseline concept and can be considered as an alternative to it.

An innovative concept for the energy dissipation problem is to allow the energy to heat the tether as it is deployed, thus carrying the energy away with it. The tether can be thought of as a stream of fluid that is heated as it passes through a heat exchanger. The tether as it enters the "heat exchanger" area will be at some bulk temperature near 20° C. The tether would then be allowed to pass around the friction drum several times before it continued on out of the cargo bay with the payload. The friction drum would be heated by the frictional energy dissipated in controlling the tether deployment rate. This heat would be transferred to the tether as it passed over the drum.

The drum and tether temperatures would peak at several hundred degrees centigrade as the tether velocity was slowed near the end of the deployment. However, kevlar has very good mechanical properties at elevated temperatures and the tether would quickly cool as it radiated to space.

The major uncertainties with this approach are determining the heat transfer coefficient between the tether and the friction drum, and how closely the force applied to the friction drum by the brake could be controlled with elevated temperatures. It is also doubtful that the tether could be warped around a drum several tens of turns and not cause knotting of the tether as it exits the tether canister.

Another concern with this approach was the restrictions placed on the deployment in terms of stops at intermediate deployment distances. Since the drum gets very hot an intermediate, unplanned, stop would probably result in tether burn through. This idea was rejected in favor of the baseline approach because of these uncertainties and restrictions.

The baseline concept involves connecting the electrical output of the generator to a series of high temperature quartz lamp assemblies. Each of the quartz lamps is capable of dissipating 1.6 kW. There are a total of ten lamps giving a total system capability of 16 kW. The maximum dissipation expected from the deployment scenarios examined is 9.6 kW or the equivalent of six lamps. The other four lamps provide backup in case of on-orbit failure and the ability to run the lamps at less than their rated capacity to increase their expected life.

This approach was selected over the high temperature resistive radiators because of the availability of design information for these units, and their previous application in space. The quartz lamps selected are similar to those used on the Orbiter for bay lighting, except they are higher power versions.

Temperature control for the control electronics, friction brake, clutch and gear box are provided by a freon cooled cold plate. As shown in Figure 2.3.4.3-1 this cold plate is connected to the Orbiter payload heat exchanger and dumps its heat into the Orbiter fluid cooling system. Maximum dump is

## Final Report - Volume II - Study Results

expected to be around 850 watts from all sources including environmental heating. This same loop will provide heating to these components during cold orbit conditions.

The entire lower portion of the STEDS structure, including the tether canister, will be wrapped in Multi-Layer Insulation (MLI). The MLI will be constructed of 10 layers of mylar with dacron netting separators. The outer cover will be beta cloth. The boom arms will also be covered with MLI. The radiator lamp support structure will be painted white to assure radiation of any heat that soaks through from the high temperature lamps.

Thermostatically controlled heaters will be supplied for the boom controller, reel, and motor

The following is a listing of the STEDS thermal control components.

Component Name	Wt (kg)	Power (w)
Quartz Radiator Lamps	32.0	N/A
Cold Plate/Fluid Lines	36.3	N/A
Freon Pump/Accumulator	20.4	40.0
MLI/Paint/Misc.	10.0	N/A
Heaters/thermostats	1.0	25.0
	<hr/>	<hr/>
Totals	99.7 kg	65.0 watts

Table 2.3.4.3-1 STEDS Thermal Control Components

### 2.3.5 TETHER DESIGN TRADE

A technique for reducing the weight of a tether deployment system is to employ a tether where the cross-sectional area varies along its length such that constant stress is maintained throughout the length of the tether. This report examines the weight savings that could be realized by using a tapered as opposed to a constant cross-section tether for hanging and swinging deployments.

#### Mass of Tapered Tether

For a swinging tether payload deployment the maximum tension in the tether occurs when its aligned along the nadir. It can be shown that the tension in the tether at the payload attach point is given by:

$$T = ML \omega_0^2 \left[ 2 + (1 + \sqrt{3} \sin \theta_0)^2 \right] \quad (1)$$

where

M = Payload Mass

L = Tether Length

$\omega_0$  = Orbital frequency of host vehicle

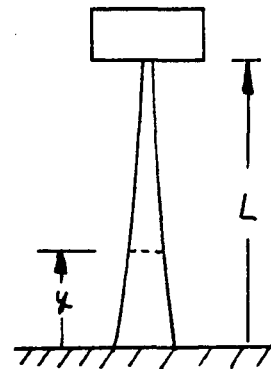
$\theta$  = Tether swing angle, i.e., initial angle between tether and nadir

The tension in the tether due to its own mass can be written as:

$$dT(y) = dm y \omega_0^2 \left[ 2 + (1 + \sqrt{3} \sin \theta_0)^2 \right] \quad (2)$$

and

$$dm = \rho A(y) dy$$



where

$\rho$  = mass density of the tether

$A(y)$  = Tether cross-sectional area at point "y"

The tension in the tether at point "y" is given by

$$T = \omega_o^2 \left[ 2 + (1 + \sqrt{3} \sin \theta_o)^2 \right] \left[ ML + \rho \int_y^L A(y) dy \right] - S_o A(y) \quad (3)$$

where

$S_o$  = The constant stress level in the tether

Differentiating equation (3) gives

$$S_o \frac{dA(y)}{dy} = -\rho \omega_o^2 \left[ 2 + (1 + \sqrt{3} \sin \theta_o)^2 \right] y A(y) \quad (4)$$

Separating variables and solving for  $A(y)$  gives

$$A(y) = A_o \exp \left\{ \frac{- \left[ 2 + (1 + \sqrt{3} \sin \theta_o)^2 \right] \rho \omega_o^2 y^2}{2 S_o} \right\} \quad (5)$$

However

$$S_o A(L) = M L \omega_o^2 \left[ 2 + (1 + \sqrt{3} \sin \theta_o)^2 \right] \quad (6)$$

Substituting equation (5) into equation (6) and solving for  $A_o$  gives

$$A_o = \frac{M L \omega_o^2 \left[ 2 + (1 + \sqrt{3} \sin \theta_o)^2 \right]}{S_o} \exp \left\{ \frac{\left[ 2 + (1 + \sqrt{3} \sin \theta_o)^2 \right] \rho \omega_o^2 L^2}{2 S_o} \right\} \quad (7)$$

Substituting equation (7) into (5) yields

$$A(y) = \frac{ML\omega_o^2 \left[ 2 + (1 + \sqrt{3} \sin \theta_o)^2 \right]}{S_o} \exp \left\{ \frac{\left[ 2 + (1 + \sqrt{3} \sin \theta_o)^2 \right] \rho \omega_o^2 (L^2 - y^2)}{2 S_o} \right\} \quad (8)$$

The mass of the tether is given by

$$M_{To} = \int_0^L \rho A(y) dy \quad (9)$$

Substituting equation (8) into (9) and performing the indicated integration gives

$$M_{To} = \left\{ \frac{\pi \left[ 2 + (1 + \sqrt{3} \sin \theta_o)^2 \right]}{2 S_o} \rho \right\}^{1/2} ML\omega_o \exp \left\{ \frac{\left[ 2 + (1 + \sqrt{3} \sin \theta_o)^2 \right] \omega_o^2 \rho L^2}{2 S_o} \right\} \operatorname{erf} \left\{ \left[ \frac{\left[ 2 + (1 + \sqrt{3} \sin \theta_o)^2 \right] \omega_o^2}{2 S_o} \right]^{1/2} L \right\} \quad (10)$$

#### Mass of Constant Diameter Tether

The tension in a constant diameter tether at the host vehicle attach point is given by

$$T_a = S_o A = L \omega_o^2 \left[ 2 + (1 + \sqrt{3} \sin \theta_o)^2 \right] \left[ M + \frac{\rho A L}{2} \right] \quad (11)$$

where

$T_a$  = tension at host vehicle

$A$  = Tether cross-section area

Solving equation (11) for the "A" gives

$$A = \frac{2M\omega_o^2 \left[ 2 + (1 + \sqrt{3} \sin \theta_o)^2 \right]}{2S_o - \omega_o^2 \rho L^2 \left[ 2 + (1 + \sqrt{3} \sin \theta_o)^2 \right]} \quad (12)$$

The constant cross-sectional area tether mass is given by:

$$M_{TC} = \frac{2M\rho L^2 \omega_o^2 \left[ 2 + (1 + \sqrt{3} \sin \theta_o)^2 \right]}{2S_o - \rho \omega_o^2 L^2 \left[ 2 + (1 + \sqrt{3} \sin \theta_o)^2 \right]} \quad (13)$$

Ratio of Constant Cross-Section to Optimum Cross-Section Tether Mass

The ratio of the mass of a constant cross-section tether to that of an optimum cross-section tether can be written as:

$$\frac{M_{TC}}{M_{TO}} = \frac{2L\omega_o \left\{ 2 + (1 + \sqrt{3} \sin \theta_o)^2 \right\}}{\sqrt{T_L} \left\{ 2S_o - \rho \omega_o^2 L^2 \left[ 2 + (1 + \sqrt{3} \sin \theta_o)^2 \right] \right\}} \left\{ \frac{1}{\theta} \right\} \quad (14)$$

where

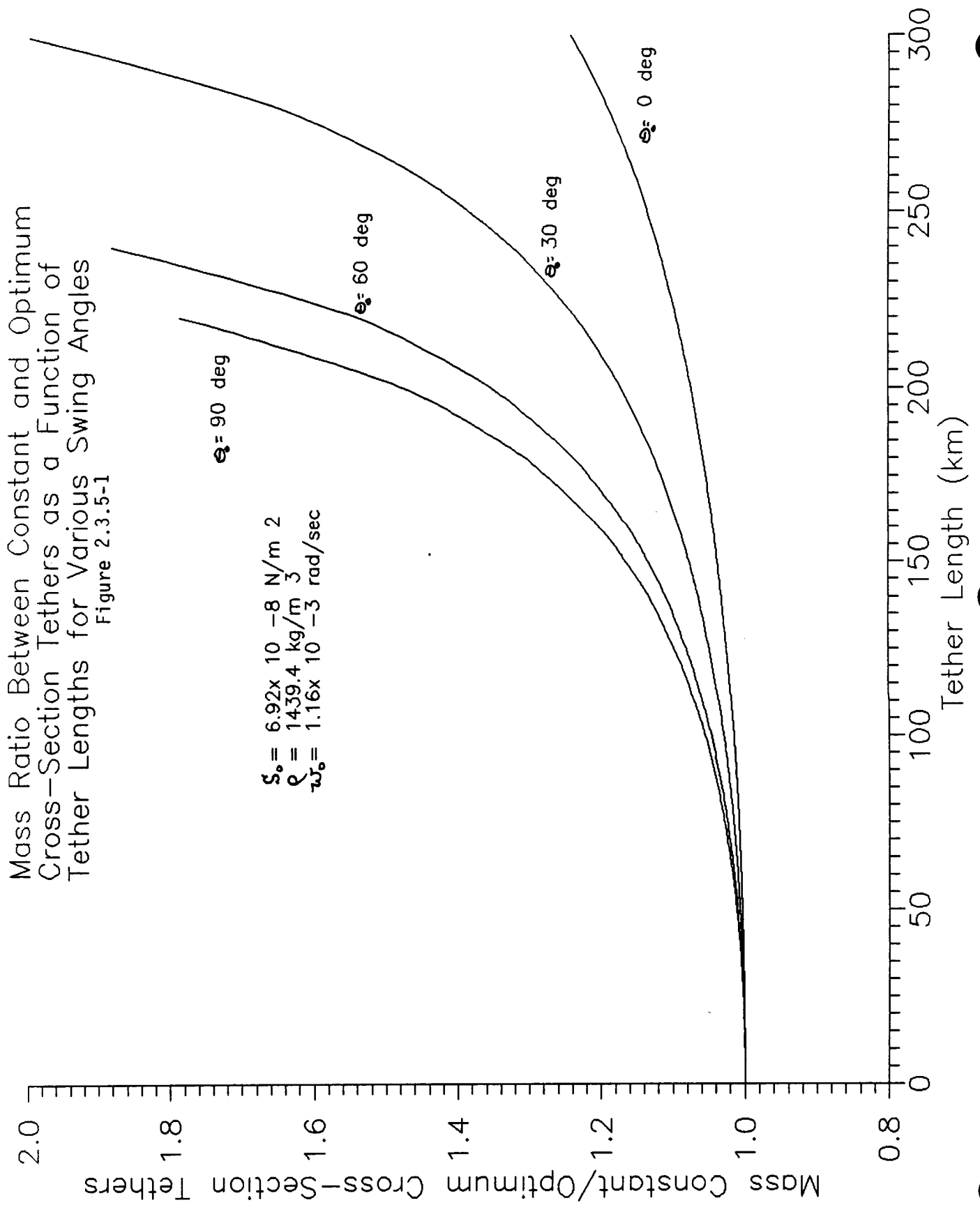
$$\phi = \exp \left\{ \frac{\left[ 2 + (1 + \sqrt{3} \sin \theta_o)^2 \right] \rho \omega_o^2 L^2}{2 S_o} \right\}$$

$$\operatorname{erf} \left\{ \left[ \frac{\left[ 2 + (1 + \sqrt{3} \sin \theta_o)^2 \right] \rho \omega_o^2}{2 S_o} \right]^{1/2} L \right\}$$

Examination of equation (14) indicates that the ratio of constant to optimum cross-section tether mass is independent of the payload being deployed and hence, is a fundamental property of tethers.

Figure 2.3.5-1 is a plot of equation (15) showing tether mass ratio as a function of tether lengths for various swing angles. Examination of the figure indicates that for tether lengths below 130 km the weight savings that could be realized is less than 10 percent for any tether swing angle. For a





hanging release (i.e. swing angle equal to  $0^\circ$ ) only a 24 percent weight savings would be realized for a tether length of 300 km. However, as the figure indicates, for tether lengths approaching 200 km and swing angles in excess of  $30^\circ$  appreciable weight savings could be achieved by the use of an optimum cross-section tether.

The tether mass ratio experiences a rapid increase as the tether length approaches 250 km for swing angles of  $60^\circ$  or greater. This is due to the phenomenon that a constant diameter tether will reach a point where it cannot support its own weight. The tether length at which a constant diameter tether cannot support its own weight decreases as the swing angle increases, however, even at a zero swing angle that point will be reached. The optimum cross-section tether has no such point and in theory a tether of arbitrary length could be realized.

For the tether deployment system being considered for STS as an alternative to a conventional propulsion system, a tether length of 100 km or less will be employed. This is due to the detrimental weight situation of a tether deployment system relative to a conventional propulsion system when the tether length exceeds 100 km. Hence, for the range of interest for an STS tether deployment system the weight savings that could be realized by an optimum tether is small while the complication introduced in its manufacture would be significant. It is therefore, judged that the use of an optimum tether is not cost effective and will be eliminated from further consideration as a candidate for the STS tether deployment system.

#### 2.3.6 TENSION CONTROL LAW AND SIMULATIONS FOR STEDS

A subcontract was awarded to Control Dynamics Company to assist BASD in the development of control laws and simulation models for the Shuttle tether deployments. The information presented in this section are the results of that effort and were supplied by Control Dynamics Company.

In proposing a control law for upward, tension controlled deployment, we have tried to keep it simple so that no elaborate sensors would be required. The current concept requires knowledge of tether deployed length, rate and tension. Of these, determining tether tension appears to be the most difficult. A study of tether tension error tolerance needs was also completed to establish the required sophistication of the tensiometer.

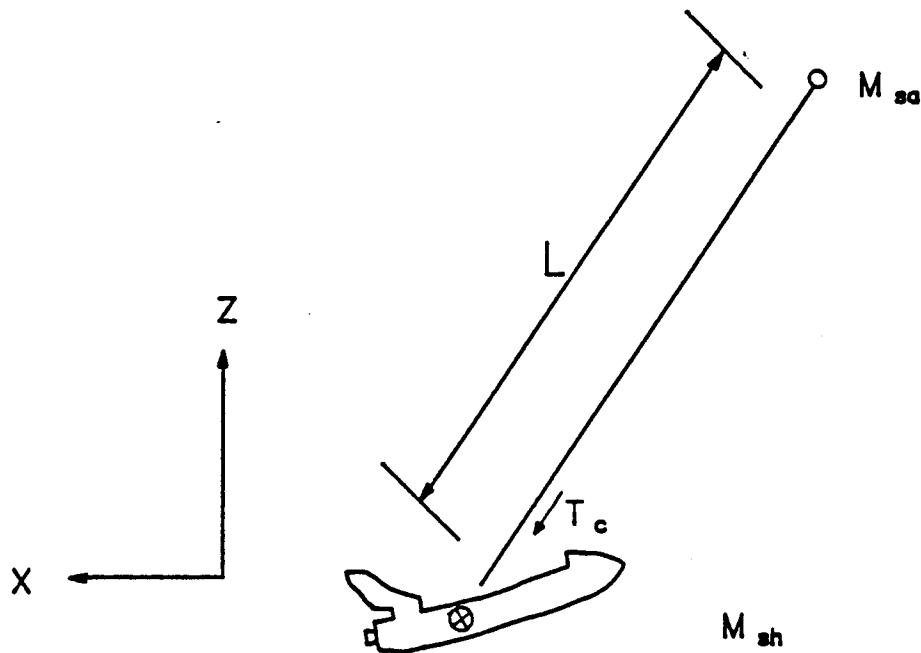
The control law for tether tension we have selected consists of two parts. The first part is an estimate of the tension required to counteract gravity gradient forces and to allow the satellite to accelerate away from the shuttle at the rate required to maintain it on the desired deployment profile. The second part is the feedback part which adjusts the tension to compensate for unmodeled forces and off nominal tip off rates, etc. This control law is shown in Figure 2.3.6-1 along with values for the control gains.

There are four distinct phases of deployment as shown in Figure 2.3.6-2. The first is the initial separation phase. In this phase, the satellite is raised out of the shuttle cargo bay by the remote manipulator system (RMS). The shuttle must be oriented such that this deployment is along the outward local vertical direction.

Once the satellite has been released by the RMS with whatever initial separation rate it can provide, the shuttle thrusters must fire to provide the minimum safe separation rate required by shuttle safety rules. These values have not been established yet. In the simulations, an initial separation rate of 1 m/sec was assumed. This rate is too high to be allowed to persist for long. The gravity gradient forces which are being used to deploy along the local vertical are too small in close proximity to the shuttle to overcome the coriolis forces produced by this large rate. Thus, tether tension is adjusted to decelerate the deployment to allowable levels within a short time. The allowable separation rate is proportional to the separation distance and thus, the deployment profile to be used for the

Figure 2.3.6-1

# TENSION CONTROL LAW



$$T_c = \underbrace{K_L(L - L_c)}_{\text{Feedback Terms}} + \underbrace{K_D(\dot{L} - \dot{L}_c)}_{\text{Gravity Gradient}} + \underbrace{K_G L_c}_{\text{Deployment}} - M_R \ddot{L}_c$$

$$K_L = 6M_R \omega_o^2$$

$$K_D = 2\sqrt{3}\zeta M_R \omega_o$$

$$K_G = 3M_R \omega_o^2$$

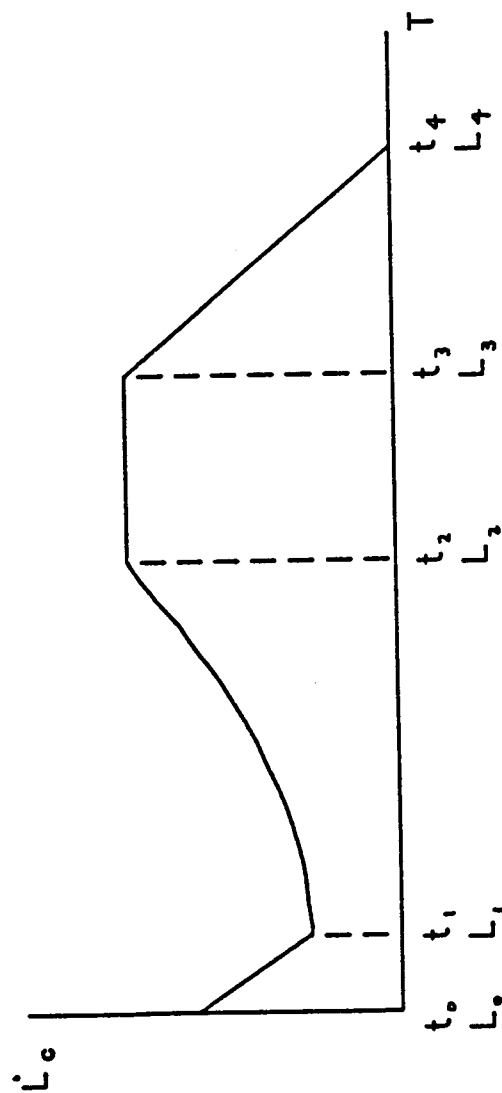
$$M_R = \frac{M_{sh} M_{sa}}{M_{sh} + M_{sa}}$$

$$\omega_o = \sqrt{\frac{GM_o}{R_o^3}}$$



Figure 2.3.6-2

## DEPLOYMENT SCENARIO



$$L_e = L_1 e^{\alpha(t-t_1)}$$

$t_0 \leq t < t_1$  : Rapid initial separation (for safety)

$t_1 \leq t < t_2$  : Exponential deployment

$t_2 \leq t < t_3$  : Constant rate deployment

$t_3 \leq t < t_4$  : Deceleration to full deployment



second phase of the deployment is exponential. That is the commanded deployment rate is proportional to the commanded distance and the commanded acceleration is proportional to the commanded rate. The first phase deceleration must slow the deployment to the exponential rate within approximately 3-4 minutes to prevent the buildup of large in-plane swing angles. The second phase is allowed to persist until the desired deployment rate is attained.

At this point the second phase is terminated and the third phase is begun. This phase consists of deployment at a constant rate. During this phase the distance away from the local vertical stays approximately constant. During the exponential deployment, the in-plane angle stays approximately constant. The fourth phase of the deployment is a constant deceleration of tether deployment to zero rate to bring the satellite to the desired distance at the desired time.

The physics of the situation limits the maximum exponential deployment factor shown in Figure 2.3.6-2 as alpha to be approximately  $.00087 \text{ sec}^{-1}$ . The absolute minimum deployment time theoretically possible if one were to deploy exponentially with a sudden stop at the end would be just over two hours and would end with an in-plane angle of 45 degrees. A more practical minimum time would be 6-8 hours depending upon how much power can be dissipated and how much residual in-plane angle can be tolerated. We have selected an alpha of .0005 to have some margin of safety. Three deployment profiles have been simulated giving deployment times of approximately 8, 12 and 24 hours.

To demonstrate the energy dissipation requirements of a typical tethered subsatellite deployment scenario, three simulation runs of various deployment profiles were performed on a simple model. The simulation follows three different command schemes which pay out 70 kilometers of tether in approximately 8, 12, and 24 hours. When each run was concluded, tether length, velocity, in-plane angle, commanded tension, power, and energy were all plotted as functions of time. In the plots that are included, the

commanded tether length and velocity are plotted at the same time as the achieved length and velocity which are shown as dashed lines. The dashed lines are difficult to distinguish on the tether length plot because it lays almost directly on the command line, some thickening can be detected, along with small overshoots.

Figures 2.3.6-3 thru 2.3.6-7 present tether length, velocity, in-plane angle, tension, and power dissipation for an 8 hour deployment scenario. The payload was assumed to be 10,000 kg and it was deployed to 70 km before release.

#### 2.3.7 OPERATIONAL TIMELINES

The STEDS mission begins with STS launch followed by opening of the cargo bay doors once orbit is established. STEDS is designed to survive all STS launch/orbit/re-entry/landing environmental conditions. This is important because the STEDS operational mission may not begin immediately after cargo bay door opening. In fact, depending on what other payloads and experiments are manifested with the STEDS, its mission may not start for several days after orbit is achieved.

Figure 2.3.7-1 is a proposed operational sequence for a typical STEDS mission and Figure 2.3.7-2 is a typical mission timeline. Once the payload and STEDS systems have passed any in-bay checkout procedures the RMS is used to lift the payload out of the cargo bay. Once the payload is clear a switch on the SSP is thrown by the astronaut and the boom deploys.

The astronaut now uses the RMS to position the payload tether end-effector over the tether terminal fitting attached to the boom (see Figure 2.3.2-4). The payload is lowered slightly to trip the over-center locking device that completes tether attachment to the payload. Once attachment is visually

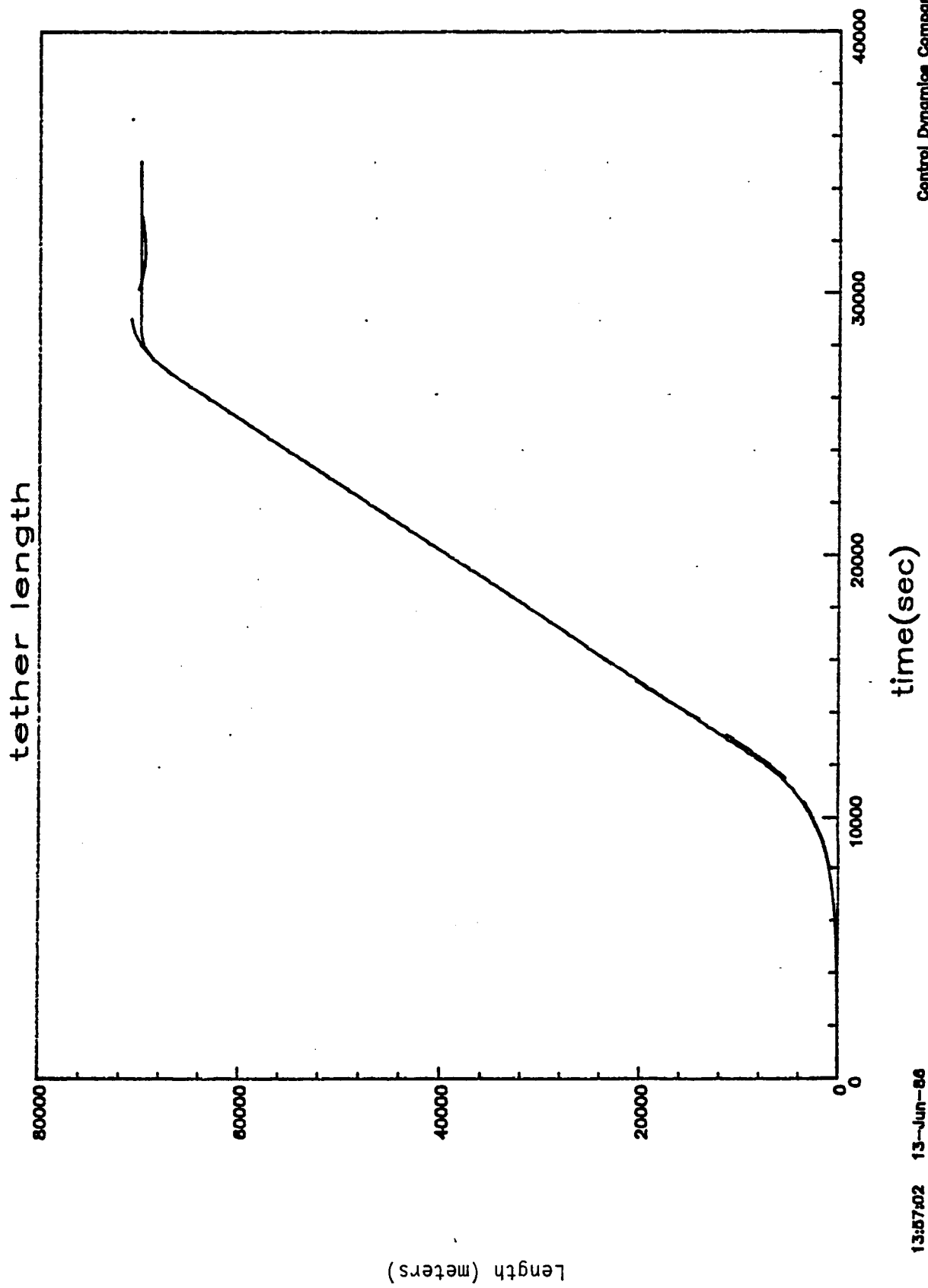
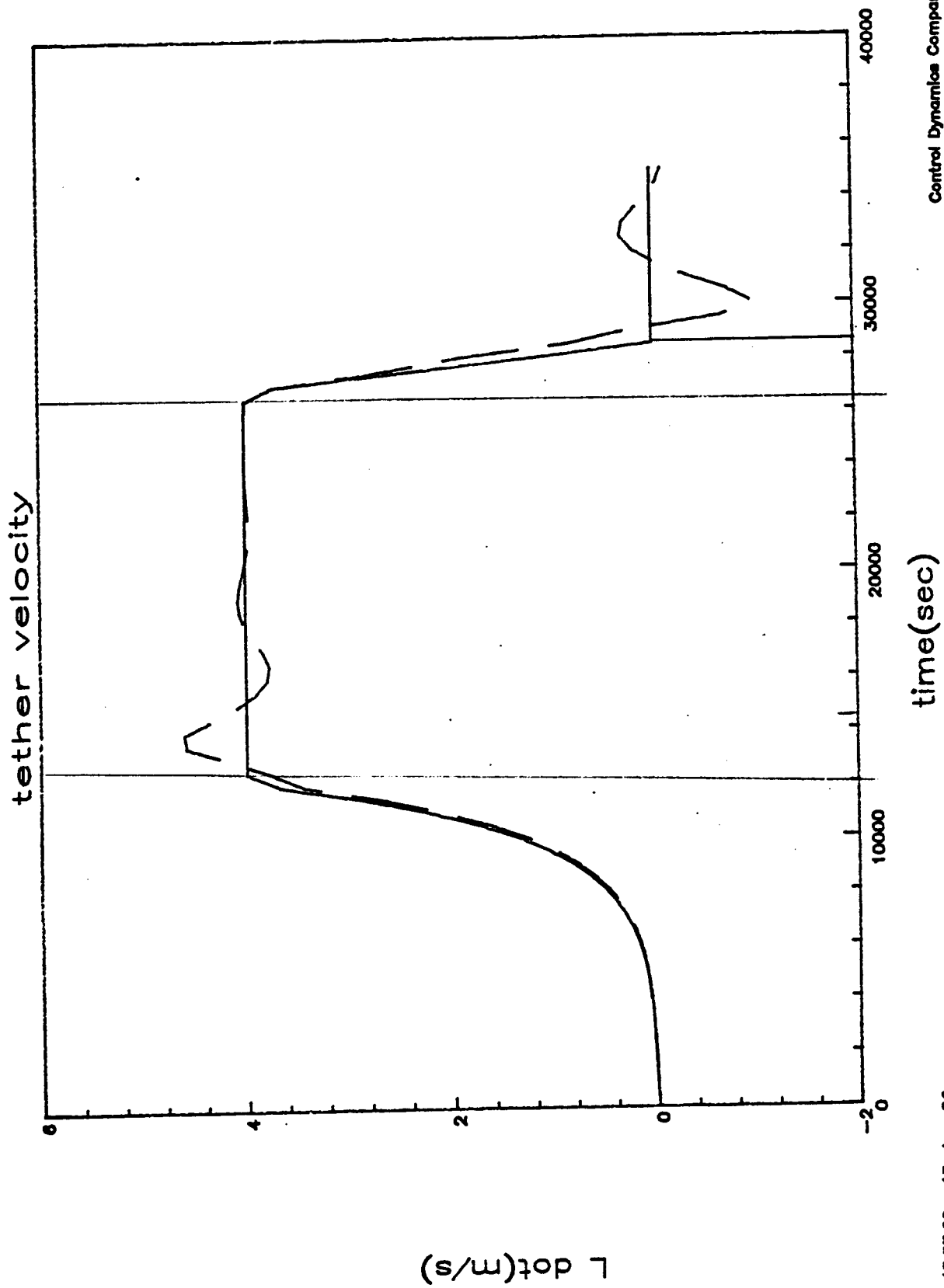


Figure 2.3.6-3 Tether Length vs Time (8 hr deployment)

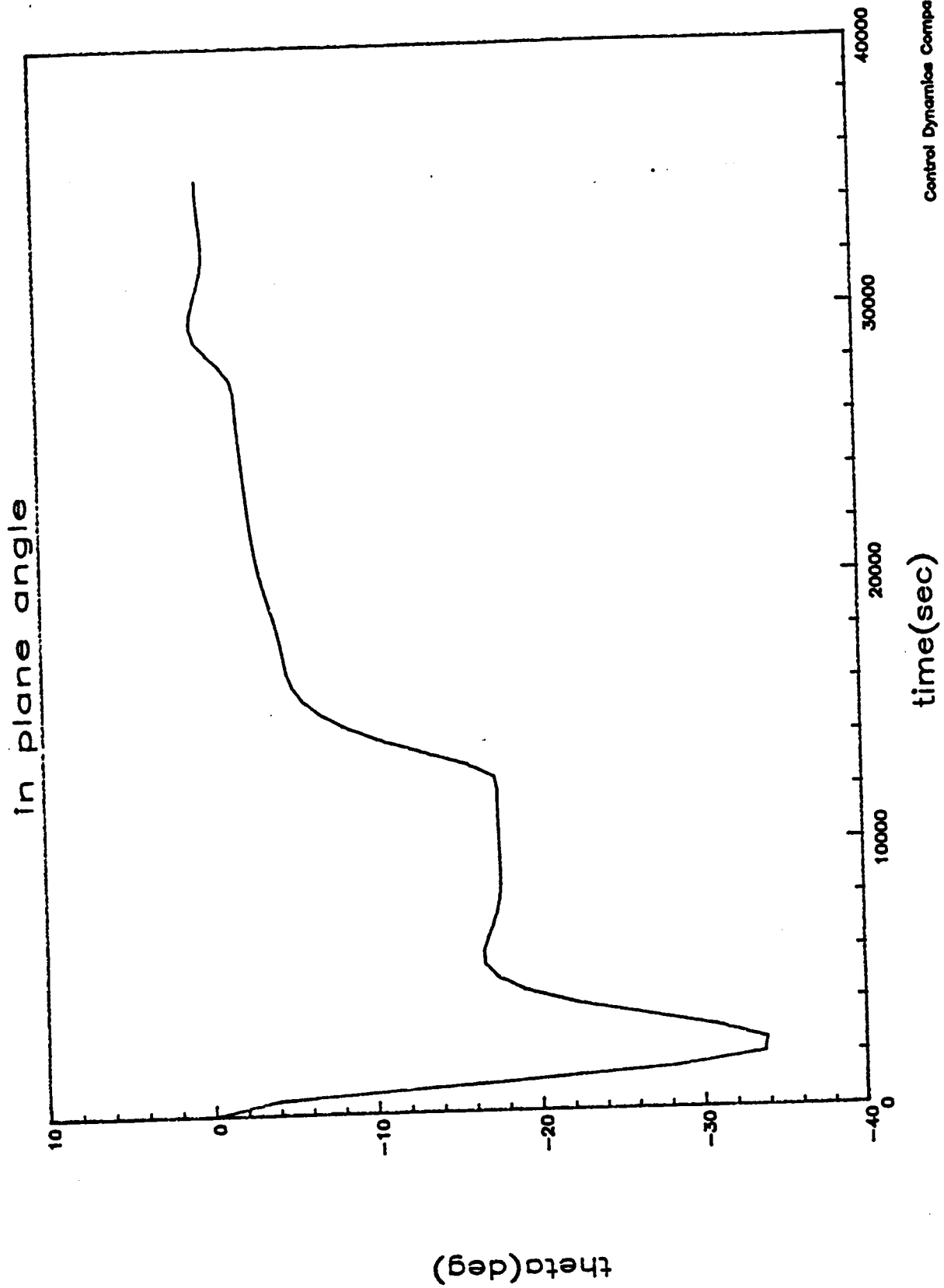




Control Dynamics Company

Figure 2.3.6-4 Tether Velocity vs Time (8 hr Deployment)

13:57:02 13-Jun-86



13:57:02 13-Jun-86

Figure 2.3.6-5 Tether In-Plane Angle vs Time (8 hr deployment)

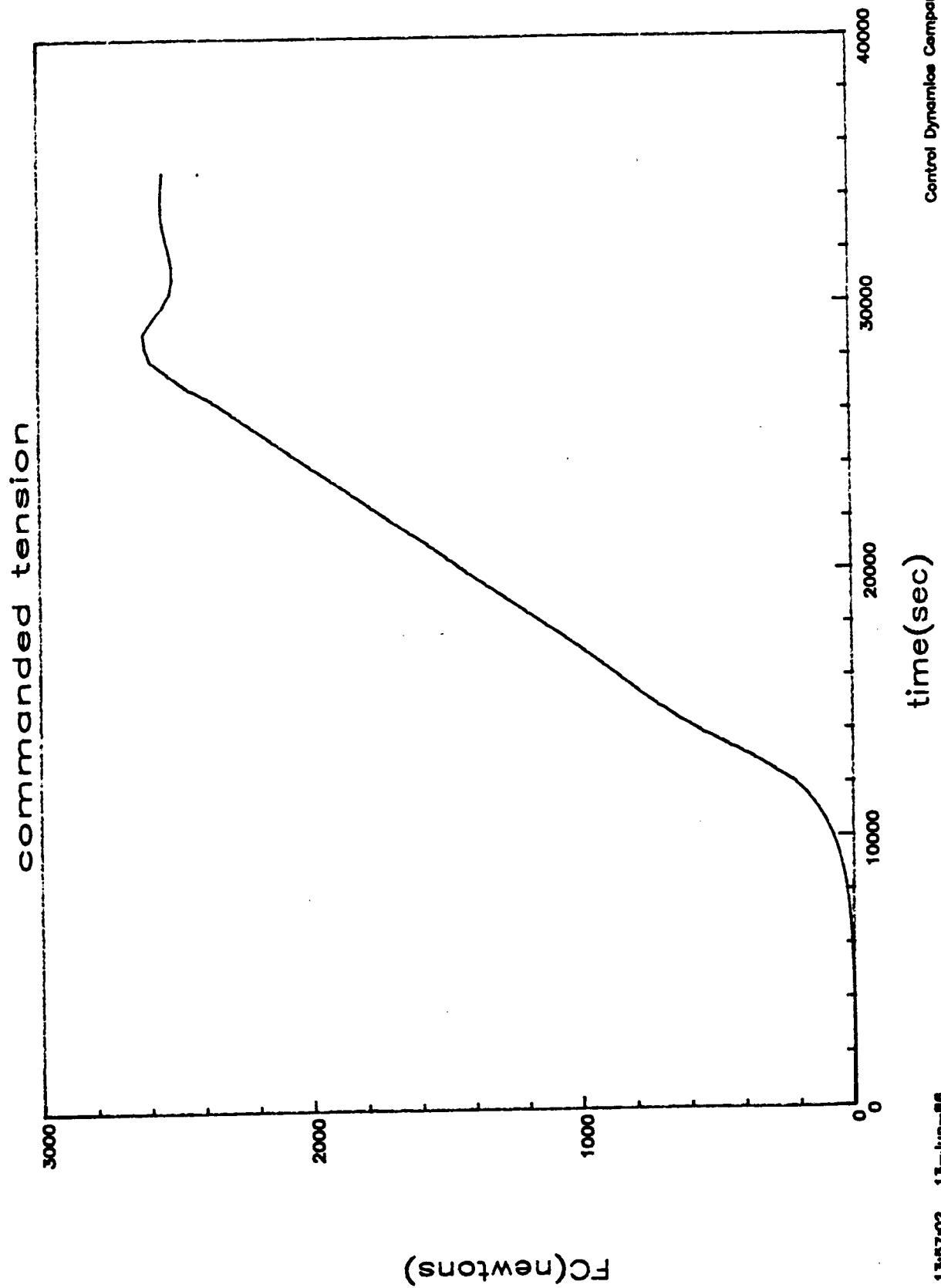
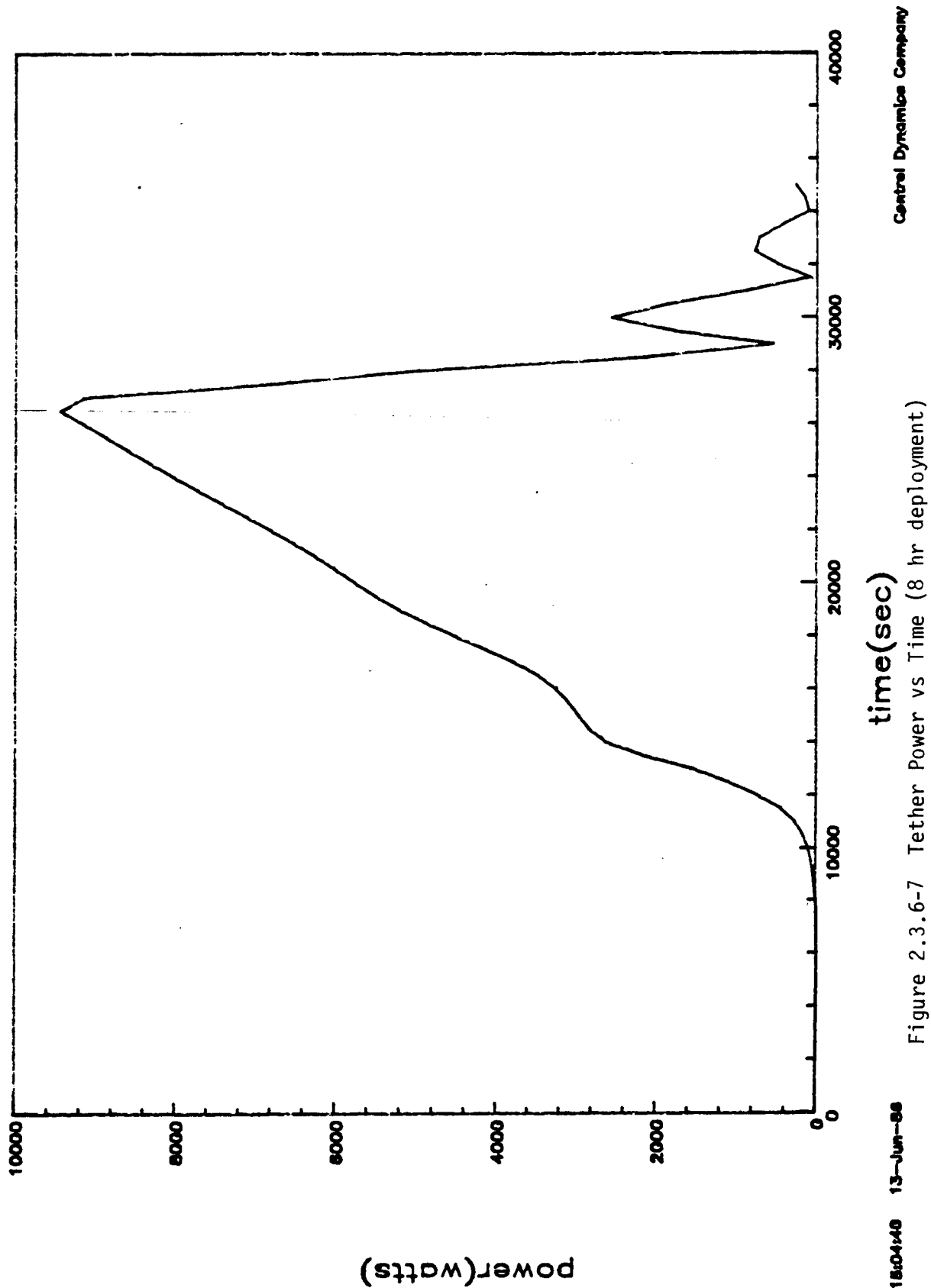


Figure 2.3.6-6 Tether Tension vs Time (8 hr deployment)

13:57:02 13-Jun-86



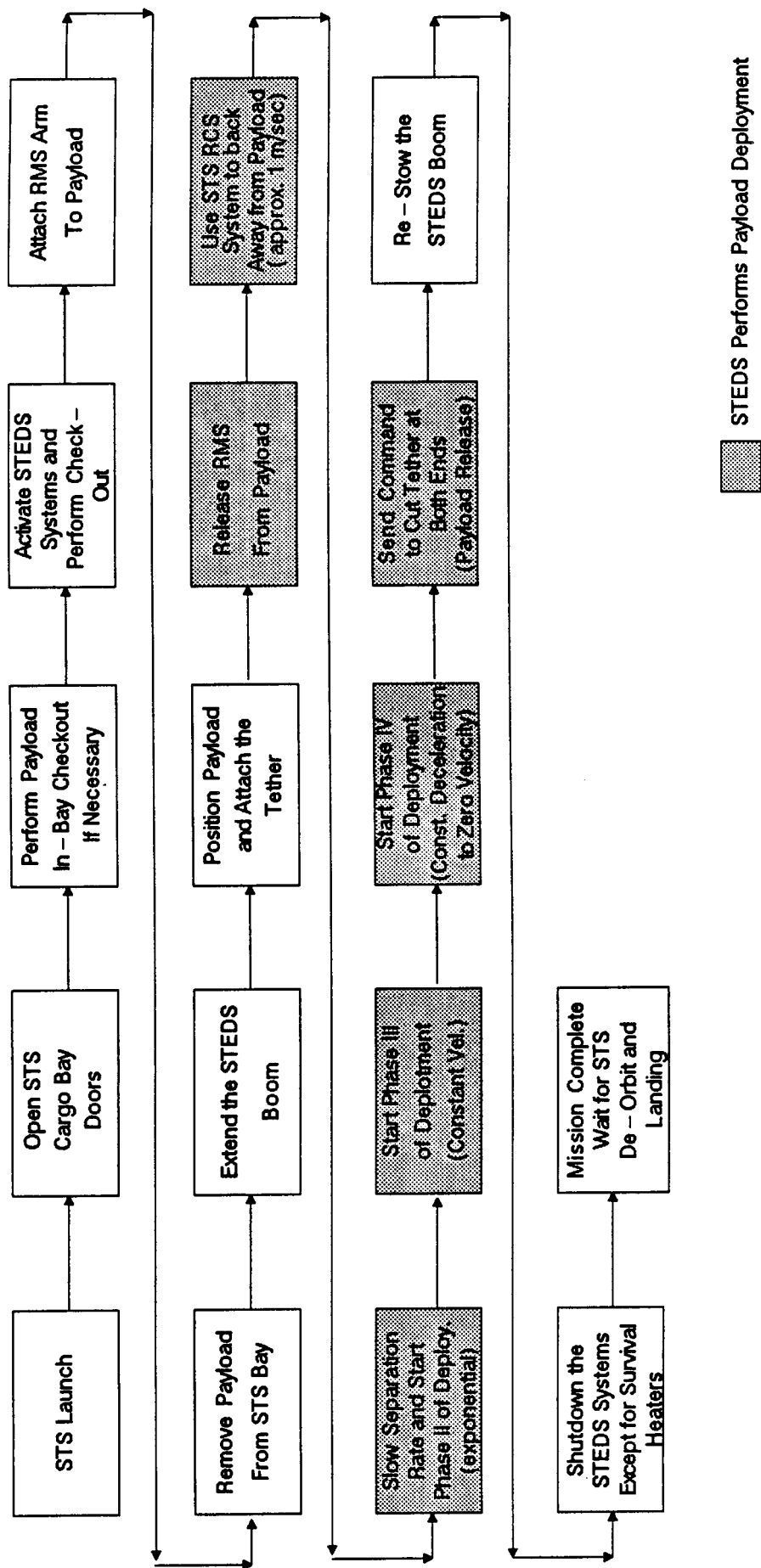
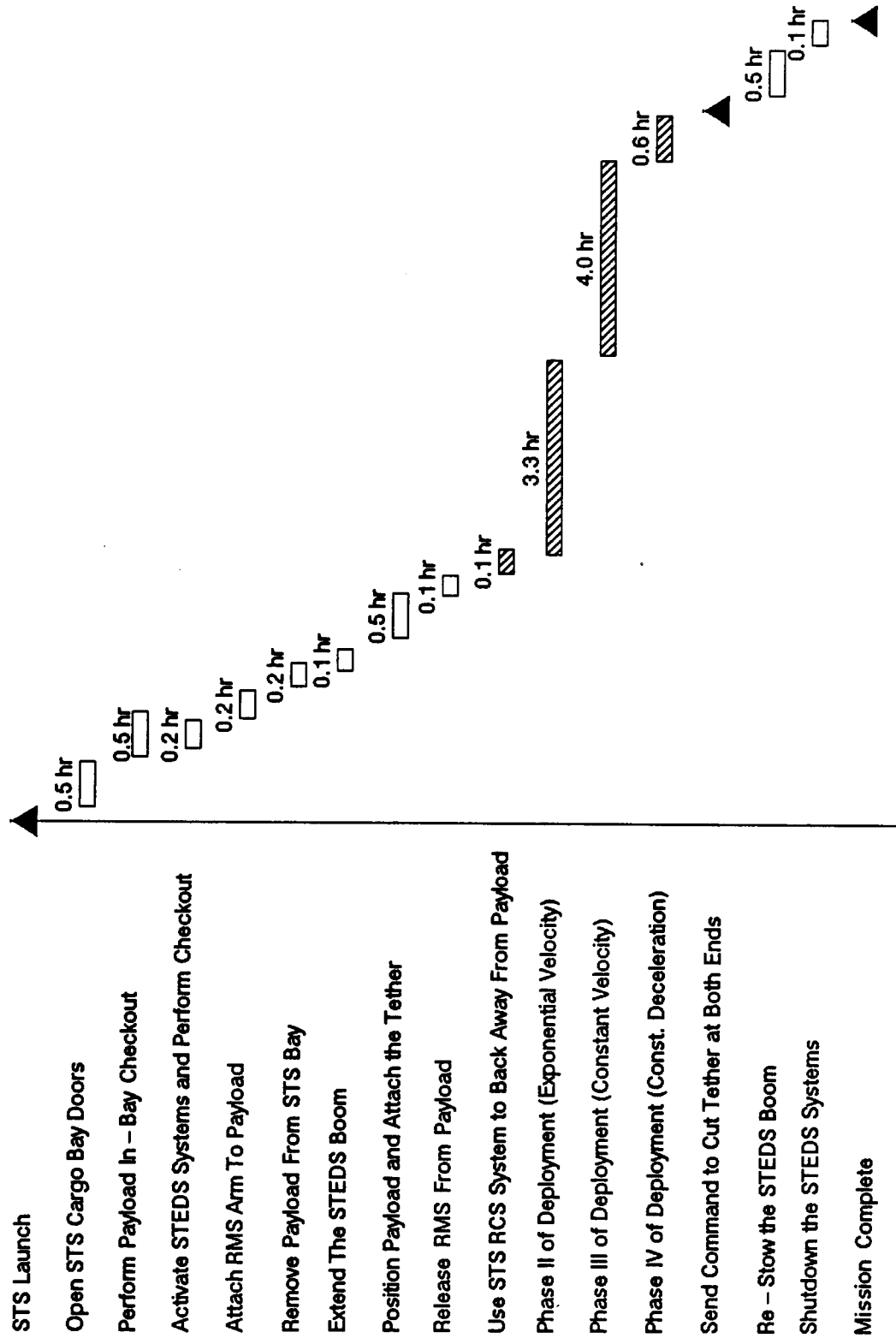


Figure 2.3.7 - 1 STEDS Operational Sequence

Figure 2.3.7 – 2 STEDS Deployment Timeline



confirmed the astronaut sends the command to release the tether terminal fitting and launch lock mechanisms. This allows the tether free movement along the tether guides.

The RMS now moves the payload out away from the bay to its maximum reach and releases the payload. The RMS arm is retracted and an STS RCS firing is initiated to back away from the payload as the tether plays out. This is the beginning of Phase I in the deployment cycle. The initial separation rate (about 1 m/sec) is maintained for only a few minutes at which time the tension is increased to start the second phase of the deployment.

The second phase is an exponential separation velocity profile. Its duration is dependent on the total deployment time selected for the particular payload. This phase is followed by a constant velocity phase which usually has the longest duration of the four phases.

The final phase of the deployment is the constant deceleration phase where the deployment velocity is brought to zero. At the end of this phase a command is sent by the astronaut to cut the tether at the STEDS. The tether will be automatically released at the payload when the payload tether adapted load cell senses the reduction in tension. If the load cell should fail a backup timer is used to release the tether after a set length of time.

At completion of the deployment the astronaut sends a command to the STEDS to restow the boom and the STEDS systems are powered down. The freon pumps and survival heaters remain powered to maintain required subsystem temperatures.

#### 2.3.8 STEDS COST ANALYSIS SUMMARY

A cost analysis for the STEDS was performed using the RCA PRICE cost modeling system and a Lotus-123 based LCC model. A summary of the results of this

## Final Report - Volume II - Study Results

analysis is presented in Table 2.3.8-1. Details of this cost effort are presented in the separate cost document accompanying the study report (DR-6 Sections 2-6 thru 2-10 and its Appendices).

Hardware Design and Development Cost	\$ 8,928,000
Hardware Production Cost	\$ 7,382,000
Operations and Support Cost	\$276,248,476*
Software Cost	\$ 2,102,500
	<hr/>
Total STEDS Cost	\$294,660,976

\*Note: STS Launch Costs are \$262,083,333

Table 2.3.8-1 STEDS Costs (Constant 1987 Dollars)



# SUMMARY TABLE - STEDS

PHYSICAL CHARACTERISTICS	QUANTITY ON DESCRIPTION
Mass	
Structure	o 927 kg (2044 lb)
Tether	o 418 kg (922 lb)
STS Attachment	o Normal keel and sill trunnions
OPERATIONAL CHARACTERISTICS	
Launch/Recovery	o STS cargo bay
Payload Attachment	o Accomplished on-orbit with RMS and deployable boom
Payload Release from Tether	o Automatic after STS end is severed by Astronaut command
Transfer Capability	o 10,000 kg payload from STS nominal altitude (300 km) to 600 km
Thermal Control	o High temperature quartz lamps o Interface with STS fluid loop for tether control system cooling
Tether control	o Generator and mechanical brake used in "tension only" control mode
SPECIAL TETHER BENEFITS	o No propellant contamination environment o Deployments can be accomplished in 8 hours or less
COSTS	o Table 2.3.8-1

3.0 CONCLUSIONS OF TETHER APPLICATIONS IN SPACE STUDY

3.1 TETHER TRANSPORTATION MISSIONS FROM SHUTTLE

- a) The design, development and test cost for the STEDS hardware is approximately one half of the cost of the MOMV, i.e. \$18M vs \$32M.
- b) The life cycle cost (LCC) of either the STEDS or the MOMV is so dominated by operations, particularly launch costs, that the total hardware procurement costs represent less than 10% of total LCC and is insignificant in terms of a cost differentiator between the two systems
- c) The STEDS, as the design is presently conceived, has a slight launch cost advantage relative to the MOMV primarily due to its shorter length which translates into LCC operational advantage over the MOMV. If total LCC is compared the STEDS has a 15% cost advantage over the MOMV or \$295M as opposed to \$348M, a \$53M cost differential. However, it must be noted that the cost differential indicated is probably within the error band of the relative costing numbers and its significance is diminished as a criterion for determining whether the STEDS or the MOMV should be developed as an alternative payload transportation system from the STS.
- d) Even if a 15% cost advantage could be realized using a tether deployment system it is doubtful that it could compete with conventional propulsion techniques when one considers the flexibility of conventional propulsion and the orbit insertion accuracies that could be achieved, and the risks associated with tether deployment.

- e) A tether deployer from the STS would be a viable contender for situations where a MOMV type propulsion stage could not be employed to transport a payload from the Shuttle standard orbit due to contamination or some other reasons requiring that the Shuttle insert the payload by direct ascent. However, the economic viability of developing a tether deployer for such cases would depend on the number of payloads that fit into this category.

### 3.2 TETHERED PLATFORM

- a) Tethering a platform to the Space Station will essentially eliminate the stationkeeping fuel required by a co-orbiting platform. The amount of fuel this represents depends upon the accuracy with which the co-orbiting platform orbital parameters can be established relative to the Space Station and the difference in ballistic coefficients between the platform and Space Station. If the orbital parameters can only be set to the accuracies obtainable by GPS then a "reasonable" amount of fuel could be saved which translates into meaningful cost savings. However, the fuel and hence cost savings are reduced if other techniques in addition to the GPS system (e.g. ranging relative to the shuttle, timed engine burns, etc.) are employed to more accurately establish the orbital parameters of the co-orbiting platform relative to the Space Station.
- b) Tethering the co-orbiting platform to the Space Station will adversely affect the micro-gravity environment on the platform. It is apparent that for tethers on the order of 10 km the "g" level on the platform will exceed those desired by most microgravity experiments. Shortening the length of the tether although reducing the "g" level on the platform will reduce the stability of the

tethered platform system since the tension in the tether will also be reduced. This can lead to safety problems if the length of the tether is significantly reduced from a nominal 10 km length.

- c) The tension loads applied to the Space Station structure will require that the truss structure be strengthened. The preliminary analyses indicated that the amount of strengthening required will result in a significant increase in the weight of the proposed Space Station structure. Increased production and transportation costs will result due to the increased structural weight. However, it should be noted that if there is a requirement that the Space Station accommodate tethered payloads including platforms then the cost for strengthening the Space Station truss structure should not be charged to the tethered platform.
- d) Due to the adverse effect of tethering on platform "g" level it is apparent that a tethered platform would primarily house astrodynamic or possibly earth pointing experiments as opposed to materials processing experiments. Although relatively precise pointing control accuracies can be achieved by the use of the KITE system, there is a viewing time problem with some astrodynamic payloads. The maximum viewing time that are expected on an inertial target is  $1/2$  orbit before a reacquisition must be initiated in order to avoid the tether wrapping around the platform. Many astrodynamic payloads require viewing times considerably in excess of  $1/2$  orbit in order to integrate sufficient light energy to form acceptable images. This requirement would result in the need to gimbal those payloads allowing them to remain inertially fixed during platform re-acquisition adding to the payload integration cost.
- e) Both the tethered and free flying platforms have virtually identical sensing systems if they are to achieve equally precise pointing performance. Although the free flying platform would require a

propulsion system, the tethered platform would also require a propulsion system to provide attitude stabilization in the event of a tether failure. It is also anticipated that there will be a cost equivalence between the KITE actuation system on the tethered platform and the momentum exchange actuation system aboard the free flyer. Additionally, the power, communication, and thermal control systems on a tethered versus free flying platform will also be equivalent. However, the tethered platform needs a reeling mechanism capable of both deployment and retrieval which is not required by the free-flying platform. A dual system will be necessary if micro-g conditions are to be maintained on the Space Station. The reeling mechanisms will increase the hardware acquisition costs of a tethered platform over the equivalent free-flyer by \$114M.

- f) Items b) thru e) need to be countered balanced against the possible fuel savings that could be realized as described in item a) and at present it seems that a tethered platform is then a reasonable economic choice.

### 3.3 COMMUNICATION TETHER

The results of this study indicate that using a fiber optic cable for communication between the tethered platform and Space Station is not cost effective until very high data rates, beyond those specified for the free flying platforms are realized. Even at elevated data rates it appears that there isn't a significant cost difference between a conventional communication system and a fiber optic tether. When one factors fiber optic development, programmatic and operational risk it does not appear that it is an economically viable alternative to the conventional approach.

3.4 POWER TETHER

The results of this study indicate that the power tether may be marginally cost competitive with a conventional solar panel power system. The power tether shows a cost benefit of \$832k, but given the high risks and many unknowns of developing this type system it is not possible to come to a definite conclusion about the economic viability of this system. This is due primarily to the inability to properly assess the amount and type of micrometeoroid protection required by the high voltage tether to prevent arcing from damaged insulation and the development and production costs for high voltage slip ring assemblies.

It should also be noted that the \$832K cost advantage identified for the power tether assumes that the tethered platform is treated as an attached payload. This treatment implies that the 10 kW of power needed by the tethered platform is supplied from the baseline Space Station power system without adding any supplemental solar panel capacity to the Space Station to compensate for the loss of the 10 kW power capacity that a free flying platform would add to the Space Station constellation. If an additional 10 kW of solar panel capacity would be added to the Space Station keeping the total power capacity of the constellation constant the power tether would be approximately \$10M more costly than the conventional solar panel power system.

It should also be noted that the \$832K cost advantage identified for the power tether assumes that the tethered platform is treated as an attached payload. This treatment implies that the 10 kW of power needed by the tethered platform is supplied from the baseline Space Station power system without adding any supplemental solar panel capacity to the Space Station to compensate for the loss of the 10

kW power capacity that a free flying platform would add to the Space Station Constellation. If an additional 10 kW of solar panel capacity would be added to the Space Station keeping the total power capacity at the constellation constant the electrodynamic power tether would be approximately \$10M more costly than the conventional solar panel power system.

3.5 CRAWLER SYSTEM

- a) The crawler system (i.e. lab) can be used as a variable "g" lab, however, unreasonably long tethers would be required to reach "g" levels in the order of  $10^{-2}$  a number quoted by the community interested in variable "g" experimentation.
- b) The design, development and build of the crawler system is high ( $\approx \$35M$ ) and an evaluation needs to be made whether the cost is worth the return.

4.0 RECOMMENDED FUTURE EFFORT

As a result of the studies performed, the data obtained and the conclusions drawn from that data the following tasks are recommended as a continuation to the efforts described in this report.

Crawler as a Variable "g" Lab and Mass Balancer

1. The Crawler concept has significant potential both as a variable gravity lab and mass balancer for the Space Station capable of placing the Space Station CM at a desired location within relatively broad bounds. The use of a Crawler as a variable "g" lab should be further investigated by performing the following:
  - (A) Detailed investigations of the experiment types that require variable "g" environment and the characteristics of these experiments.
  - (B) Group the experiments into reasonable payload compliments and derive the resource requirements for the Crawler if these experiments were mounted on it.
  - (C) Examine whether these experiments can reasonably be performed on the core Space Station by using the Crawler as a mass balancer placing the CM of the Space Station-tether combination at various points relative to the core Space Station.
  - (D) Refine the Crawler system design in accordance to the above generated requirements and update its cost. Also define the Crawler system design and cost that would only act as a mass balancer allowing the experiments to be performed on the core Space Station, and compare them with the variable "g" lab Crawler configuration and determine which concept is more cost effective in meeting experiment requirements.
2. The use of a Crawler to compensate for Space Station CM movements due to internal mass motions such as fluid transfers, and the docking of the STS and other elements that may be serviced by the Space Station should be investigated by performing the following tasks.
  - (A) Determine the maximum CM excursions at the Space Station due to internal mass motion and the docking of logistic/servicing elements.
  - (B) Define the Crawler system characteristics/requirements that will compensate for the expected Space Station CM motions.



(C) Design and develop the cost of a Crawler system that will compensate for the expected Space Station CM variations.

(D) Design, develop and cost a conventional type tether system with ballast weight that could compensate for the expected shuttle mass motions, compare those to the Crawler system and specify the tether configuration that would be most cost effective in compensating for Space Station CM motion.

(E) Determine the additional cost that would be incurred if the tether mass balancing system would simultaneously act as a variable "g" lab and determine whether such a concept is economically viable.

#### Investigation of SEDS Deployment Technique

The basic problem with the economic viability of the tether as a transportation device from the STS is its size and weight when compared to a conventional propulsion stage. The SEDS deployment technique holds the potential of significantly reducing the tether system size and weight, thereby making it more competitive with conventional propulsion techniques. The following tasks should be performed to establish the economic viability of the SEDS deployment technique.

A) Define the SEDS deployment sequence/technique and determine the requirements placed on the STS, particularly in terms of propellant consumption.

B) Determine the sensitivity of the SEDS deployment technique to various system errors and determine the sensitivity of orbit insertion accuracies to these errors.

C) Determine techniques/control system configuration that would reduce orbit insertion errors due to system error sources.

D) Design and cost a SEDS tether deployment system and determine its cost effectivity relative to conventional propulsion techniques.

#### Use of a Tether for Plasma Measurements

Simultaneous measurements of plasmas, atmospheric densities and other orbital parameters at varying altitudes from which gradients can be determined has been of interest to the scientific community for many years. A tether system containing various sensors deployed along its

length is uniquely suited and probably the only reasonable way to make such measurements in a cost effective manner. The following tasks should be performed to determine the configuration of a tether plasma measuring system.

- A) Determine the type of plasma/orbital parameter measurements that are of interest.
- B) Define the types of sensors available to make the required measurements.
- C) Determine the techniques by which such sensors could be mounted along the tether length and establish the tether plasma measurement system deployment sequence.
- D) Design and cost a tether plasma measurement system.

#### Further Investigations of Space Station Tethered Platforms

The results of the present study indicate that tethering a science platform to the Space Station has economic merit if the orbital parameters cannot be adjusted any better than the capabilities represented by the GPS system, and that the KITE system performs as projected. However, there are a number of areas that need further investigation to establish whether the economic advantage presently projected is in fact the case. These investigations are:

- A) Definition of the accuracies with which a co-orbiting platforms orbital parameters could be adjusted using other aids such as Space Station radars timed burns, etc., in addition to the GPS system, and define the hardware and operation cost of these additional aids.
- B) Design and cost of a KITE system that will achieve the desired platform pointing performance.
- C) Define the impact on the KITE system design if a power tether is used requiring that power be transferred across the KITE interface.
- D) Determine the additional payload integration hardware (particularly gimbaling systems and their associated component/electronics) that would be needed to allow payload viewing of a single source for indefinite time periods and develop costs for these systems. Compare these costs to the payload integration hardware needed for a free-flyer and determine the cost differential between the two approaches.

E) Determine the additional structural Space Station weight that would be required to accommodate a tethered platform and establish whether this additional weight and cost will be absorbed by the Space Station program.

F) Based on the above data, refine the determination of the economic viability of tethered vs. free flying platforms.

#### Dynamic Model Verification

Numerous dynamic models of varying degrees of complexity have been formulated to describe the behavior of tether systems. These models give varying results for the dynamic behavior of the same tether system and, at present, there is no good way of determining which descriptions adequately describe tether behavior. In addition the present tether modeling/simulation capability is better than the accuracy with which system and environmental parameters can be specified. It is therefore apparent that tether orbital flight experiments need to be formulated and flown that will verify tether dynamic behavior and yield data that will enable more accurate specification of system and environmental parameters.

It is recommended that the following tasks be performed to specify and fly a tether flight experiment that will result in the data needed to verify the results of tether dynamic simulation and enable accurate specification of system and environmental parameters.

A) Determine the system and environmental parameters that have "large" degrees of uncertainty and define the types of measurements needed to establish more accurate values.

B) Determine the technique by which tether dynamic behavior could be accurately established and define the types of measurements and measurement accuracies needed to perform this function.

C) Define the system configuration that will perform the desired measurement described in items "A" and "B".

D) Perform a preliminary design of the tether experiment system and determine the system cost including launch, launch vehicle, flight operations and data reduction. Using this data define a phase C/D program that will meet with budgetary constraints and still yield the data in a timely fashion.

E) Perform the detail design, fabrication and test of the tether experiment system.

## Final Report - Volume II - Study Results

F) Fly the tether experiment system, obtain/reduce the data and define tether dynamic behavior and system/environmental parameters.

G) Input the more accurate system and environmental parameters into the various dynamic models for tether systems and establish the degree of fidelity of each.